Exploring novel design applications of speed-modulated ironing within internal structures of 3D prints

Graduation report Tristan Lievestro

TU Delft

Mentor: Mehmet Ozdemir
Chair: Zjenja Doubrovski


Ultimaker 2+

Contents

Abstract

This report explores whether speed-modulated ironing (SMI) can be effectively used for enhancing mechanical properties of 3D prints and presents two design applications that illustrate the potential of this technique. SMI is a technique which utilizes the second nozzle of a dual nozzle 3D printer to precisely re-heat printed layers. The G-code for this nozzle is custom made within a Grasshopper script, allowing for precise control over its speed and location. 3-point bending and tensile tests were conducted on 3D printed PLA specimens ironed with various speeds to evaluate the impact of SMI on material bonding both within and between print layers. Increased bonding within the layers was achieved for tensile dog bones printed with transversal infill. An iron-speed of 3mm/s increased the ultimate tensile strength by 12%. Other infill orientations did not mechanically improve through ironing, suggesting limited benefits for inherently strong infill configurations. Increased interlayer bonding was achieved with 3-point bending specimen printed upright. An Iron-speed of 5mm/s increased the ultimate flexural strength with 87.8% and increased material stiffness by 45%. Through differential scanning calorimetry (DSC) it was found that ironed samples contain more crystalline regions compared to un-ironed samples, which explains the observed increase in material strength and stiffness on a material level. Two applications are presented to demonstrate the potential of speed-modulated ironing for strengthening 3D prints. First, a 3D-printed trombone mouthpiece was reinforced, providing a real-world example of the benefits of SMI. Second, a topology-optimized workflow is proposed that selectively irons the most structurally significant regions within a print, allowing designers to balance mechanical performance and print time. Overall, this report proposes a new method to effectively strengthen 3D prints through speed-modulated ironing, that only requires a dual-nozzle 3D printer and Grasshopper.

Figure 1: Ultimaker dual nozzle print head

Introduction

This report investigates novel applications of speed-modulated ironing to enhance mechanical properties of 3D prints. 3D printing, or fused deposition modelling (FDM) to be more precise, is a technique where three-dimensional objects are 'printed' by depositing melted material, typically plastic, layer by layer. Once deposited, the material quickly cools down, resulting in a solid model. FDM printing offers more design flexibility and material efficiency compared to most other traditional production methods. Initially developed for rapid prototyping, FDM printing has evolved into a versatile tool widely used across various industries and is increasingly becoming an addition to the toolkit of DIY enthusiasts at home (Cano-Vicent et al., 2021).

Although its added benefits for prototyping and small quantity production are evident, FDM printing is not without limitations. In terms of mechanical performance, 3D printed parts significantly underperform compared to parts made with traditional fabrication methods like injection moulding. This is due to the discontinuous nature of the process, the melted adjacent strings of filament cool rapidly, causing them to solidify before they are completely fused. This leaves voids between the strings of filament which prevents the material to achieve full mechanical properties (Coogan & Kazmer, 2017). Floor et al. (2015) found that specimens printed with PLA exhibit a reduction in stiffness to two-thirds and a halving of strength compared to injection-molded PLA specimen whilst the weight of the printed specimen only dropped 20%. Because of this, 3D printing still remains mostly a prototyping production method as manufacturers rather opt for durability for their products.

A lot of research has been done on print settings, materials, parameters and techniques that improve the mechanical properties of FDM printed parts. These range from experiments on slicer settings like infill patterns and layer heights to modification of the print material or the printer itself. One effective way to increase mechanical performance of 3D printed parts is extending the material's time above glass transition temperature. This can be achieved by increasing the nozzle temperature for example. Fusion between new and existing printed layers takes place before the extruded filament cools down below its glass transition temperature, and the longer it stays at a higher temperature than its glass transition temperature, the better the bond becomes (Syrlybayev, 2021). In terms of tensile strength higher nozzle tempera-

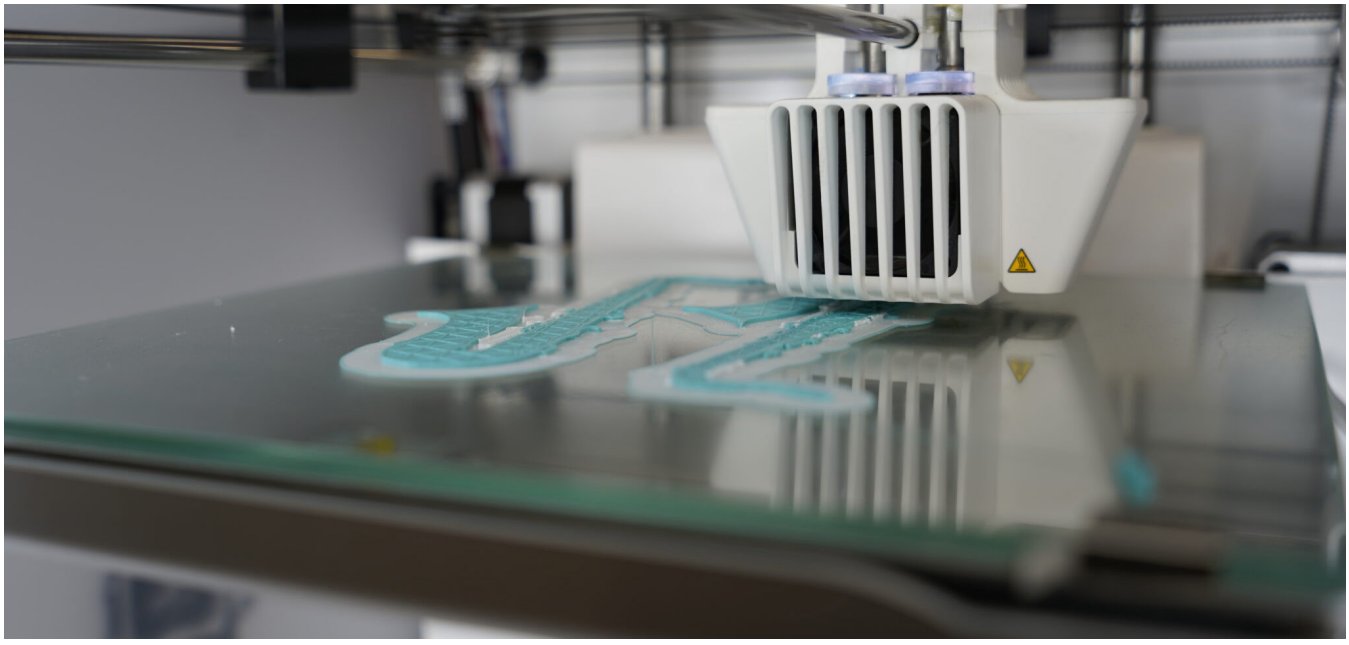

Figure 2: FDM printing

tures result in better mechanical performance. However, too high temperatures lead to degradation of the base polymer which quickly worsens the mechanical properties. Ning et al. (2016) observed that increasing the nozzle temperature to 240°C results in a more complete fusion of printed layers but also results in the formation of pores within the material, ultimately reducing tensile strength. High printing temperatures also causes the material to become less viscous, resulting in stringing and oozing of the filament when being printed, diminishing print quality.

However, increasing nozzle temperature is not the only method to improve layer adhesion. Multiple researchers have explored pre-processing extruded layers with heat through various techniques that avoid the drawbacks of excessive nozzle temperatures. Kishore et al. (2017) used an infrared lamp to pre-heat the extruded material and achieved an increase in average tensile strength in the z-direction of 81%. However, to prevent the plastic from overheating with this technique, an additional force convection cooling mechanism had to be developed. Another pre-processing method is pre-heating the deposited layers with lasers. With this technique a laser is attached to the printer head and its beam is aimed slightly in front of the print nozzle. Luo et al (2018) where able to improve the inter layer shear strength of PEEK with 45% and Ravi et al (2016) achieved a 50% increase in the strength of interlayer bonding. Although these both these pre-processing methods show clear improvement in enhancing mechanical properties of FDM printed parts, they require additional components and software to use.

To provide a strengthening solution that does not require any additional components or specific software, this report explores whether speed-modulated ironing could be used to enhance mechanical properties of 3D prints by applying heat through the second nozzle of a dual nozzle 3D printer. This would offer users a solution to enhance the mechanical performance of their 3D prints without having to modify their print-setup or spend additional costs on materials and components.

Speed-modulated ironing is performed with a dual nozzle FDM 3D printer. The first nozzle is used to print regularly, i.e. extruding material, such as PLA or PET, layer by layer following the shape of a model. The second nozzle however, is not loaded with a material. Instead, this nozzle is heated to a temperature well above printing temperature (300 degrees compared to 200) and used to iron over the freshly printed layer that was printed by the first nozzle. Depending on the material that is used, ironing can modify the properties of the material in several ways. For example, foaming filaments will expand when being ironed, whilst cork-fill material will change colour (figure 3). This report will primarily focus on regular plastic (PLA) and the effect of ironing on its arrangement of polymer strains and thus its mechanical properties. The strength of speed-modulated ironing is that both the position and the speed of this ironing nozzle can be controlled, allowing for local property variation and gradients. By adjusting the ironing speeds, the amount of heat being transferred into the material can be controlled. Previous research explored several design applications for this technique for the outer walls of 3D prints. This included applications regarding change of colour, translucency and roughness.

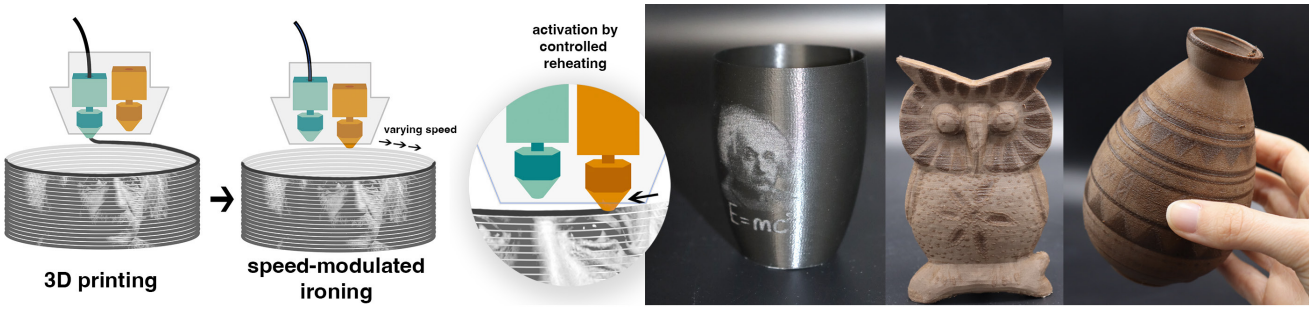

Figure 3: Speed-modulated Ironing (Ozdemir, 2024)

Alzyod et al. (2024) have investigated the effects of ironing, with regular slicing settings, on the mechanical performance of 3D prints. Significant enhancements in tensile, compressive and flexural strengths were found (25%-35% improvement). Although this indicates that ironing is of beneficial effect on the mechanical properties of 3D prints, the ironing was done over entire surfaces of prints with consistent speeds (>10mm/s). In this report, less of the surface will be covered by the ironing nozzle and with slower ironing speeds (<10mm/s). Alyzod's research focussed more on preserving mechanical performance when undergoing ironing. The ironing speeds investigated in Alyzod's paper are too fast to transfer enough heat to achieve polymer strain rearrangement in the 3D print and are more focussed on smoothening out the creases within the print.

In this report different methods for mechanical strengthening 3D prints using speed-modulated ironing are designed and investigated. The main focus of this report is the question whether speed-modulated ironing could be used to mechanically enhance 3D prints. Mechanically enhancing 3D prints through ironing could open several ways to strengthen 3D prints without having to adjust the infill direction, flowrate, print speeds or even provide extra strengthening solutions that regular slicer settings do not provide. The option to strengthen prints with ironing provides a solution for 3D printing without having to modify the printer and/or change material, making it an accessible technique for everyone who has access to a dual nozzle printer. Moreover, the ability to locally very material properties by changing ironing speeds opens all kinds of interesting strengthening possibilities and advantages over production methods like injection moulding. To examine the potential strengthening effects of ironing on 3D prints, tensile and 3-point bending tests were conducted. Horizontally oriented specimens were tested to assess within-layer strengthening, while vertically oriented specimens were used to evaluate interlayer strengthening. In these tests, parameters like iron nozzle speeds, offsets between ironing paths and ironed layer intervals were adjusted. Through an empirical iterative approach, different parameters were selected for further exploration, eventually leading to an overview of this techniques' strengthening possibilities. Two different demonstrators were designed and tested to illustrate the strength of using speed-modulated ironing to strengthen 3D prints.

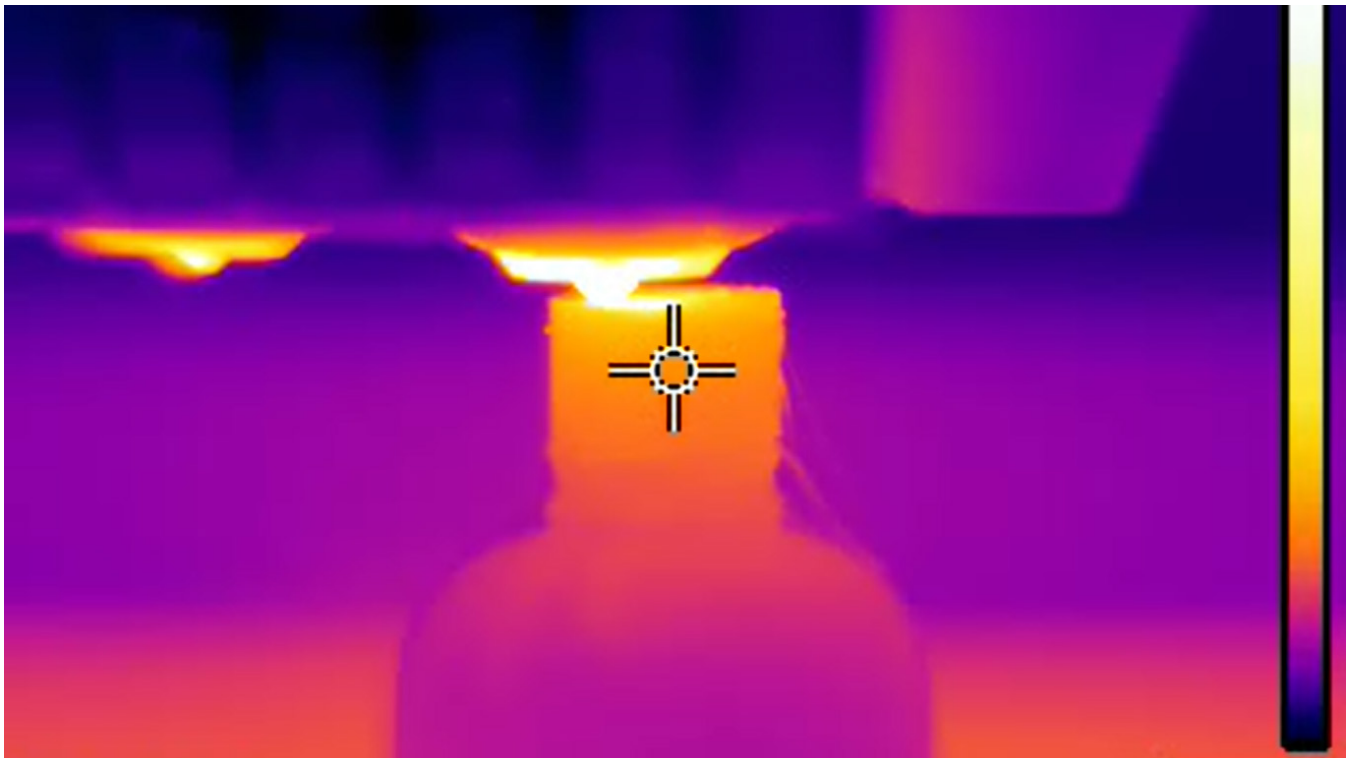

Figure 4: Ironing observed with thermal camera

Related work

This report aims to extend this knowledge about speed-modulated ironing and investigate possibilities of this technique for strengthening the internal structures of 3D prints. The literature review for this study is organized into three sections

- Strengthening techniques for 3D printing
- Ironing in 3D printing
- Using ironing to strengthen 3D prints

Strengthening techniques for 3D printing

A lot of research has been conducted on parameters that influence the mechanical properties of 3D prints, ranging from studies on isotropy to studies that investigate the influence of different print settings on layer adhesion. As mentioned in the introduction, 3D printed parts have worse mechanical performance compared to parts that are fabricated with traditional production methods like injection moulding. Ahn, Montero, Odell, Roundy, and Wright (2002) found that for ABS, the printed specimen achieved 65 to 72% of strength of the injection moulded specimen and in compressive tests 80 to 90%. Floor et al. (2018) found that specimens printed with PLA exhibit a reduction in stiffness to two-thirds and a halving of strength compared to injection-moulded PLA specimen whilst the weight of the printed specimen only dropped 20%.

The mechanical performance of 3D prints, especially with sub-optimal infill configurations, is largely dependent on layer adhesion. Enhancing layer adhesion can be done with 3 different general approaches: Heating approaches, chemical approaches and mechanical approaches (Masania, 2022). As transferring heat is the working principle behind speed-modulated ironing, several heating approaches will be investigated further in this chapter. The most obvious heating method is increasing the nozzle temperature as this is a basic setting in all slicer software. Floor et al. (2018) has done extensive research into regular print settings, like nozzle temperature, and their effect on mechanical strengths. Five parameters were ranked on their influence on mechanical strength as follows: Fill density, print speed, layer height, orientation and nozzle temperature. In this 'related work' section the parameters that are most likely to affect speed-modulated ironing in some way are explored further with special focus on the different heating techniques.

Strengthening strategies with regular print settings

Whilst exploring different papers regarding regular print parameters like layer height, infill orientation and print orientation it becomes apparent that there is a lot of discrepancy between the findings. For example, the literature is divided whether a larger layer height is stronger compared to a smaller layer height. Jatti et al. (2019) found that with a larger layer thickness the ultimate tensile strength (UTS) of the specimen decreases. Similar results were found by Randriguez-Panes et al. (2018) and Coogan et al. (2016). Conversely, Torres et al. (In Press) found that smaller layer thicknesses had worse mechanical performance. When looking at print orientation, results in the literature differ whether printing on the side or flat is stronger. However, a wide variety of studies indicate that tensile bars printed upright perform the weakest (Floor, 2018). In terms of infill orientation the results vary whether longitudinal infill (lines in 0°) or diagonal infill (45°), with respect to the tensile/compression direction, is strongest. Tymrak, Kreiger, and Pearce (2014) even found that linear was slightly stronger for PLA, but diagonal for ABS.

Sun et al. (2020) have researched the effects several orientations of in-plane isotropy on the strength and toughness of 3D prints. In-plane isotropy means that the paths or structure of each layer is uniform, but the orientation of these layers with respect to each other can vary. They concluded that a Bouligand structure with a rotational angle of 15 degrees increases the strength and toughness with 12% (Figure 5). They also highlighted that a transversal infill with no rotation at all was the weakest possible infill. Due to the poor ductile properties high stress and low strength will

lead to earlier fracture formation at layers with transversal paths. To investigate whether Ironing could improve strength and toughness, this type of infill would be a good starting point to try to enhance.

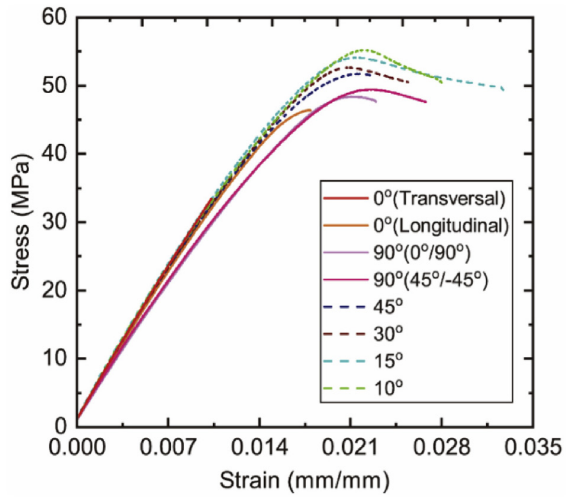

Figure 5: Stress/Strain curve of mulitple infill configurations

Heating strategies using regular print settings

One method for enhancing layer adhesion that solely utilizes regular slicer settings is increasing nozzle and bed temperatures (Thumsorn et al., 2022). When melted semi-crystalline polymers such as PLA cool down, the amorphous part of the polymer chain segments can form crystals. This is called crystallization and happens when the materials' temperature is above glass transition temperature and below melting temperature. These crystal parts of the polymer form a rigid structure and make the material stronger and stiffer. In general, elongating this time window in which these structures can be formed, improves the mechanical properties of the 3D print. However, heating the material too much leads to degradation of the material. For PLA, this phenomenon starts to occur from 240°C (Behzadnasab, 2016). Increasing nozzle temperature to 240°C contributes to a more complete merge of the printed layers, but more pores are generated inside the specimens, leading to the decrease in tensile properties (Ning et al., 2016). The findings on the effect of high print temperatures on the ductility of printed parts differ within the literature. Behzadnasab, et at. (2016) have found that with increasing temperatures, not only the tensile strength, but also the elastic modulus of the printed parts increases. Conversely, Guessasma et al. (2019) found the elastic modules to be lower as temperature increases, due to the lower degree of crystallinity through high cooling rates.

Heating strategies that require additional components

Other, more advanced, ways to improve layer adhesion is to facilitate crystallization right between the two printed layers. This is called trans-layer crystallization. Yao et al. (2024) have developed a technique to preheat a printed layer with a laser before printing a new layer. This preheating causes the material to melt precisely at the interface which allows the crystals to form at the right location. With this technique they significantly increased the crystallization level of the polymer and improved interlaminar strength. They demonstrated 20% increase in tensile strength and 10-20% increase in bending strength for PEEK and CF-PEEK. However, the usage of lasers proved to be a difficult strengthening technique to standardize since different materials respond differently to the lasers' heat. Sabyrov et al (2020), found that with this technique different colour filament performed differently, with darker material absorbing more energy compared to lighter materials.

Kishore et al. (2017) investigated a similar principle, but instead of lasers used an infrared heat source to preheat the deposited layer for optimal bonding. This proved to be very effective in improving interlayer strength, especially at slow print speeds (Figure 6). Although an increase of twice the fracture energy was achieved, it proved difficult to preheat the extruded layer consistently to glass transition temperature without overheating it. An additional force convection cooling mechanism had to be developed to ensure a consistent start temperature of the filament, eliminating the risk of the plastic overheating. With this extra cooling system in place the average tensile strength in the z-direction was increased by 81%.

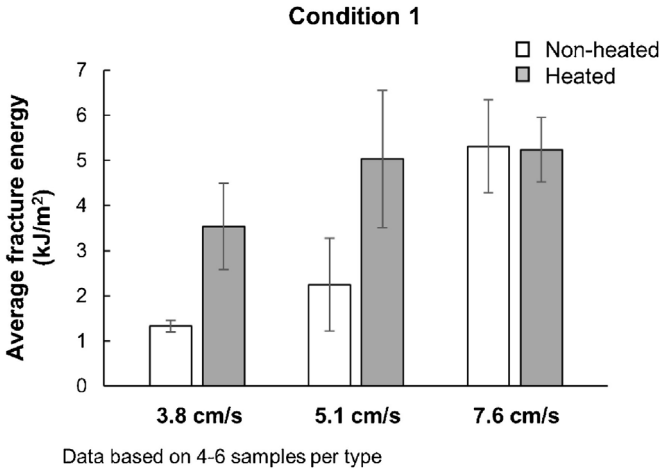

Figure 6: The effect of infrared heat on the fracture energy of samples printed with different speeds (Kishore, 2017).

Strengthening strategies that modify material

Thumsorn et al. (2022) have investigated enhancing material properties with different kinds of fillers. Although improvement of properties like toughness were achieved, the fillers caused worse layer adhesion because of faster solidification due to the additives. In this report several materials are investigated that have some sort of additives (Foaming PLA, Silk PLA) and it is therefore important to note that unexpected results could be due to non-optimal settings for these additives and their solidification times. 3D Matter (2015a/b) have discovered that there is quite a significant variance in strength and stiffness for different PLA and ABS manufacturers. 10 to 36 MPa for PLA and 40 to 70 MPa for ABS. Moreover, they also found a variation of strength between different colours of the same material from the same manufacturer, with a maximum increase of 9% between purple and grey. This is important to remember when comparing results of different materials.

Ironing in 3D printing

Ironing for smoothening

Although ironing 3D prints for mechanical enhancement is a novel approach, the technique itself has been around for quite some time. It is a feature that most slicers have incorporated in their software. Usually ironing is used to smoothen out the top layer of a 3D print. The heated nozzle brushes over the top layer which flattens protrusions whilst simultaneously extruding a reduced amount of material to fill gaps and creases (Butt et al., 2022). Alzyod et al. (2023) have investigated 3 different iron parameters and their influence on surface roughness: Path speed, Ironing spacing and Flow rate. The spacing between the ironing lines turned out to have the biggest influence on the surface roughness. Smaller spacing causes more overlap of ironed lines, smoothening the surface better.

In an attempt to make the surface layer applicable for fused filament fabrication for printing electronic circuits, Neuhaus et al. (2024) have tested multiple iron settings to achieve smoother surface finishes. For PLA they achieved a mean surface roughness reduction of 83.7 to 92.9 % with ironing. This is comparable with post processing the 3D prints with 1200-grit sandpaper. Montalti et al. (2024) have experimented with different sizes and shapes of tips to iron with. Compared to classic ironing performed with the extruder tip, this method allowed for higher movement speed, greater spacing between passes, shorter work time, and better surface finish.

Ironing for modifying material properties

Improving surface smoothness with ironing has been studied thoroughly. Aside from improving smoothness, Butt et al. (2022) have found that ironing significantly increases the hardness of prints as well with approximately 8.2%. These papers all investigated settings that only allowed for an entire layer to be ironed, with the same ironing settings. By separating the printing and ironing from one to two nozzles, local ironing with variable settings can be achieved (Ozdemir et al., 2024). This is interesting for materials that change properties when being exposed to heat, such as corkfill PLA, woodfill PLA or foaming PLA. Ozdemir and Doubrovski (2023) proposed an approach to locally modify material properties by including different print parameters in the design space. By doing so they could locally modify material properties of a 3D print whilst only using one material. Ozdemir et al. (2024), have done research on these 'programmable' materials and how they change visual properties whilst being exposed to different temperatures. This result-

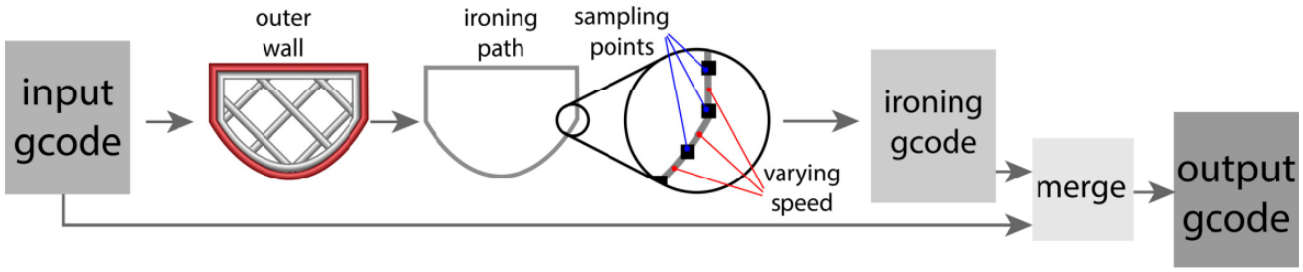

Figure 7: Ironing GCode workflow (Ozdemir, 2024)

ed in data that could be used for projecting images onto 3D prints. To achieve this a script was made in Rhino/Grasshopper that used this data to generate custom G-CODE for the ironing nozzle (Figure 7). This script is the foundation of the script used for the research in this report (Appendix 3).

Using ironing to strengthen 3D prints

Previous efforts to use ironing for structural strengthening in 3D prints are limited. Sardinha et al. (2020) examined impact of ironing on the interlaminar strength (ILS) of 3D prints and compared it with un-ironed samples. They found that, although ironing influenced the thermal behaviour of deposited layers, it was not effective in enhancing ILS of parts due to the generation of geometric irregularities. However, other techniques that smoothen 3D prints such as 3D Chemically Melting Finishing (3D-CMF) do show significant improvements in both bending and tensile tests (Takagishi & Umezu, 2017). This creates an argument that if the geometric irregularities of ironing can be eliminated or reduced, it could potentially be used to mechanically strengthen 3D prints.

Alyzod et al. (2024) have achieved significant improvements in mechanical performance of 3D printed parts due to ironing. Ironing caused a noteworthy increase in ultimate tensile strength (UTS) of 29%. Similarly, the compressive strength exhibited substantial growth of 25% and flexural strength increased 35%. The ironing examined in this study was done at consistent and high speeds (>10mm/s) and covered the entire surface of the print.

Understanding Speed-modulated ironing for strengthening 3D prints

Looking at previous research conducted on heating methods for strengthening 3D prints, there is a good reason to assume that ironing could have a beneficial effect on a print's mechanical performance. This raises the question of whether applying heat through a nozzle could produce the same, better, or worse effects compared to heating printed layers with lasers or infrared light as described in 'related work'. Whilst the concept of re-heating the material is similar, the way it is applied is completely different, including all kinds of new parameters in the research domain. To narrow the scope of the research, the focus is on two main questions:

- Can ironing be used to strengthen interlayer bonding?
- What effect does ironing have on the tensile and stiffness properties of 3D-printed parts?

Aside from these main two questions regarding the plausibility of this technique, other questions arise on how speed-modulated ironing can be effectively used for mechanical enhancement. What are optimal ironing speeds to improve tensile and flexural strengths? How does ironing influence material performance of different print orientations? Where and to what extent should ironing be applied to achieve optimal results? What are suitable use-cases for this technique? These questions focus more on the actual use of the technique.

Experiment

In order to answer these questions a series of experiments was conducted. These include tensile tests and three-point bending tests. The specimen tested where standardized ISO dog bones for the tensile tests and strips for the 3-point bending tests. Several different ironing approaches are explored and tested for their mechanical impact. These approaches include different ironing speeds, print orientations and ironing paths. In order to have full control over the ironing nozzle, i.e. its movement, positioning, heat, etc. a grasshopper script was used to generate the ironing nozzles G-code (Appendix 3)

In general, there are two different ways in which a print can fail. The print can break perpendicular or parallel to the printed layers. Usually, a 3D print performs stronger when a load is applied perpendicular to the print layers, but this heavily depends on the direction of infill. To assess the effect of speed-modulated ironing on these two different failure-types, the conducted tests are divided into two main categories.

- Within-layer strengthening
- Interlayer strengthening

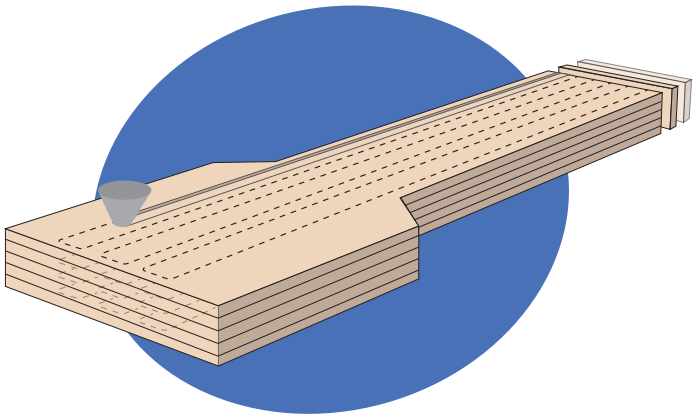

Within-layer strengthening

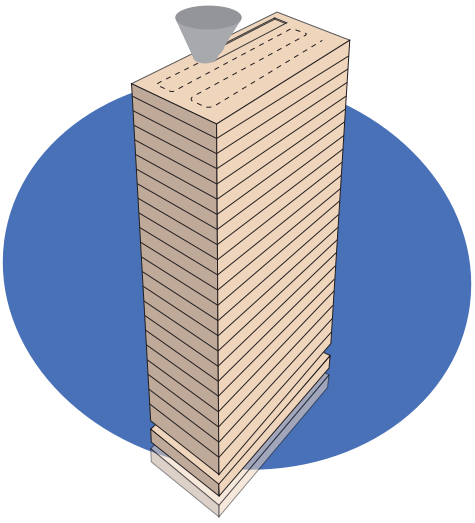

Interlayer strengthening

Within-layer strengthening

With the horizontally-oriented specimen for the within-layers strengthening tests, the ironing was done transversal to the print direction (In parallel to the layers), evaluating the effect of ironing within the layers. This effect of ironing within the XY-plane is heavily influenced by the choice of infill direction. Aside from a potentially improved layer adhesion, the effects of a different isotropy or a different material configuration due to the smearing of the ironing nozzle, could also be of influence on the mechanical results. To investigate the ironing's effect on tensile strength and stiffness, tensile tests were conducted with these samples. The main parameter was the speed of the ironing.

Interlayer strengthening

Conversely, with the vertically-oriented specimen for the interlayer strengthening the focus was solely on improving the layer adhesion between the vertically stacked printed lines. Interlayer bonding is something that is difficult to improve within regular slicing settings as simple tweaks like changing infill direction have no effect. Both 3-point bending and tensile tests were conducted with these samples as printing tensile samples upright proved to be difficult and unreliable.

Material

For this research, the main material of interest was Polyactic Acid (PLA). Previous conducted research regarding speed-modulated ironing focussed predominately on visual and haptic characteristics of the outer layers of 3D prints. Since regular PLA hardly shows any visual change when being ironed this material is often neglected in these studies. However, PLA is the most common material for everyday use of 3D printing. If standard PLA can be modified to improve the mechanical properties of a 3D print, ironing could become a widely applicable solution for mechanical issues in 3D printing, without the need for alternative materials.

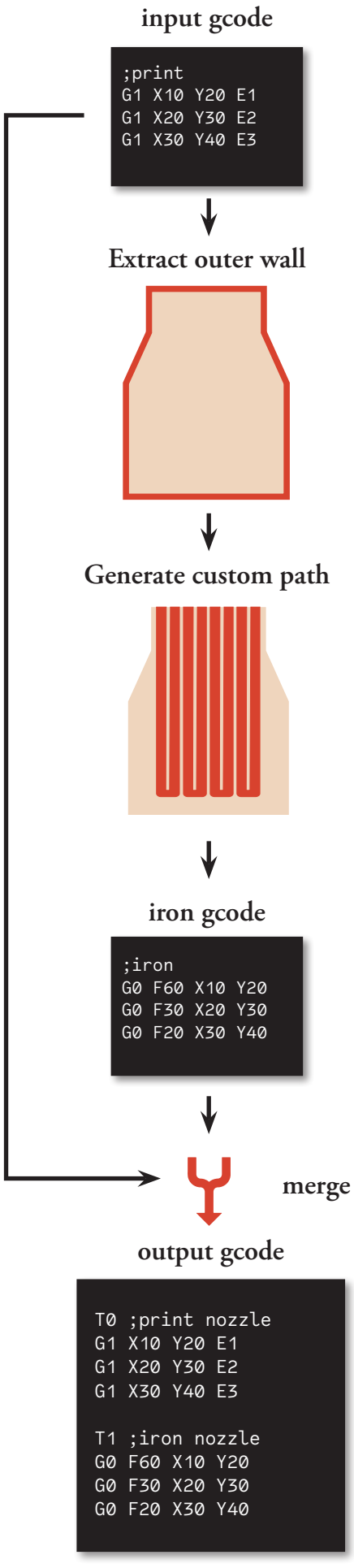

Figure 8: Ironing GCode workflow

Within-layer strengthening

Within-layer strengthening

As described in 'speed-modulated ironing for strengthening 3D prints' the main parameter for this print orientation was the speed of the ironing nozzle. However, this was not the only parameter tested. In total 6 different parameters are tested with this research. These include:

- Amount of ironed lines
- Interval between ironed layers
- Materials
  - Regular PLA
  - Silk PLA
  - Foaming PLA
- Z-offset
- Ironing speed
- Infill orientation

The results for these can be found in Appendix 1 & 7.

Ironing Speed

As the name "speed-modulated ironing" suggests, one of the key strengths of this new technique is the ability to control the velocity of the ironing nozzle. With slower ironing speeds, more heat can be transferred to the material. As described in 'related work' there is a temperature window in which the polymer strains can reorganize and form crystals resulting in stronger material properties, whilst too much heat will destroy the material. To assess which speeds positively enhance the mechanical properties a batch of dog bone specimen was made, printed with regular PLA and ironed with various speeds. These specimen were tensile tested and stress/strain data was retrieved and analysed.

Methodology

The specimen oriented flat on the print bed were tensile tested in multiple configurations. An ISO 527-2 standard model was printed with 3 different infill orientations. Parallel infill lines, oriented perpendicular to the pulling direction, longitudinal infill and 45/-45 degrees infill which is the standard Cura infill. The printed dog bones consisted solely of infill lines as outer walls and skin layers could result in unwanted noise in the data. For the exact print settings of this dog bone see Appendix 2. Within Rhino/Grasshopper a pattern was generated for the ironing nozzle. This pattern consists of several lines in the longitudinal direction of the pulling direction across the entire dog bone. The script was made in such a way that the number of lines and the interval on which layers would be ironed could be controlled. For exact explanation of the grasshopper script please see Appendix 3.

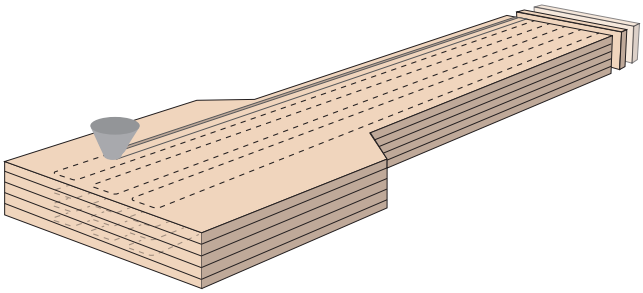

Figure 9: Ironing nozzle follows a pattern generated with Grasshopper

To keep the samples organized and identifiable a code was given that indicated how many lines were ironed per layer and what was the interval of ironed layers. For example, a sample that was ironed every other layer with 6 lines was given the code: E2L-6L.

Specimen

In this test a total of 23 samples were tested. 17 ironed samples with varying iron speeds, ranging from 15 to 1mm/s and 6 un-ironed samples. 3 un-ironed samples were the regular dog bones with transversal infill (Appendix 2), and the other 3 were made with longitudinal infill. This was done to create a sort of visual domain and see how the samples with different ironings speeds stack up to the weakest (transversal) and strongest (longitudinal) infill (Torrado & Roberson, 2016b). All the ironed samples were ironed every other layer with 8 lines. The spacing between the lines was 1.35mm. With the ironing nozzle being 1mm wide this means that there is a slight area of 0.35mm which is not ironed between the ironed lines.

Type	Name	Ironspeed	Sample amount
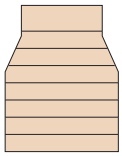	unenforced (transversal)	-	3x
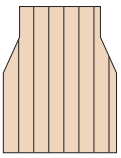	unenforced (longitudinal)	-	2x
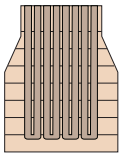	E2L-8L	15mm/s	3x
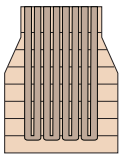	E2L-8L	10mm/s	3x
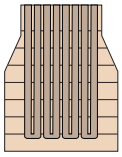	E2L-8L	7mm/s	3x
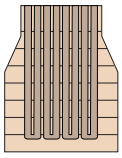	E2L-8L	5mm/s	3x
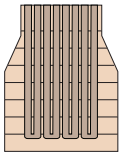	E2L-8L	3mm/s	3x
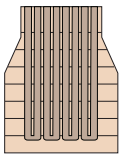	E2L-8L	1mm/s	3x

Figure 10: Regular PLA dog bone being ironed with a speed of 3mm/s

Tensile test

The research was conducted on the Zwick Z010, a tensile machine that was loaded with 10kN. All the samples were weighed and measured before being tested. This is important to discover any inconsistencies with the printed samples and necessary to calculate the stress and strain. The pulling speed was set at 1mm/min, which made the tensile data quite precise. Since the samples are quite brittle and have a small plastic region when tested, this low pulling speed helped to get as much insights about their deformation as possible.

Figure 11: Zwick Z010 tensile test setup

Ironing Speed Results

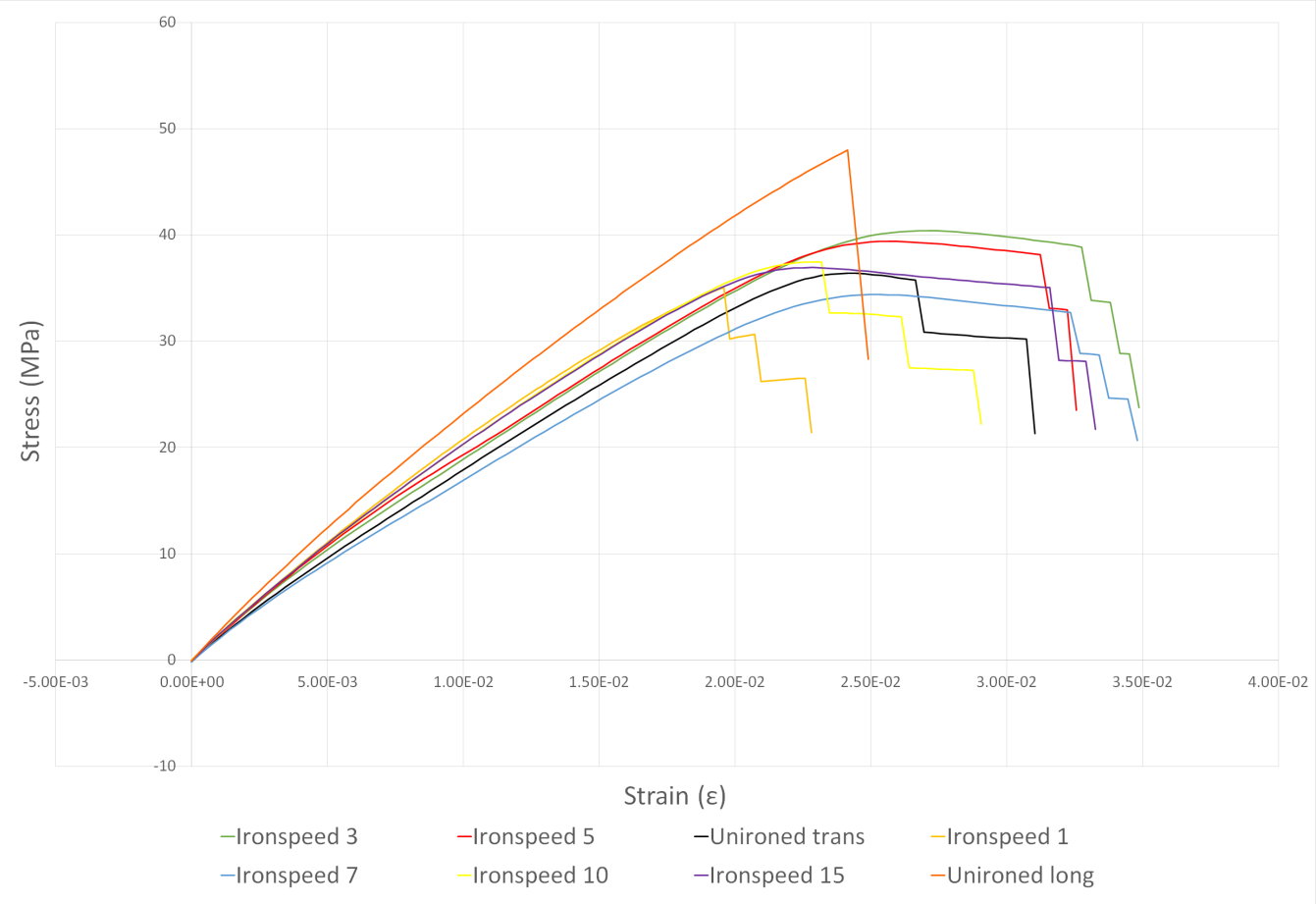

Figure 12: Stress strain curve regular PLA: Varying iron speeds from 15mm/s to 1mm/s (Averages)

Strength

In this graph (figure 12) the averages of the 23 samples are plotted. As could be expected, the un-ironed longitudinal samples had the highest peak stress. With iron-speeds 3 and 5, a clear improvement in both strain and stress was measured compared to the un-ironed transversal samples. The 3mm/s iron speed samples showed an increase in peak stress of around 12%.

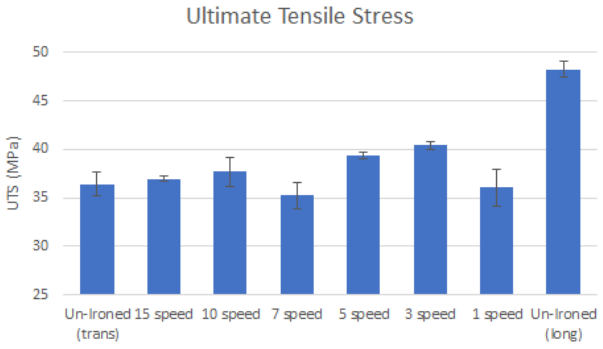

Figure 13: Ultimate tensile stress

Looking at the average ultimate tensile stresses of the samples no clear pattern can be retrieved (figure 13). This is mostly due to iron speed 7, which performed worse than the un-ironed transversal samples. Although this could potentially be due to an error whilst making the samples, it could also showcase that multiple properties are of influence and are influenced with ironing. If we would exclude iron speed 7, it is possible to recognize a pattern. The slower the ironing, the more heat is being transferred to the material, the stronger the samples. This is true up until iron speed 1, which deformed the samples in such a way that they broke before being able to plastically deform.

Elongation

When looking at elongation (figure 14) it can be concluded that ironing helps with making the samples more ductile. However, a clear pattern to estimate what iron-speed improves the ductility the most is hard to retrieve. An interesting outlier is the iron speed of 10mm/s, which was measured to be a lot more brittle compared to the other samples.

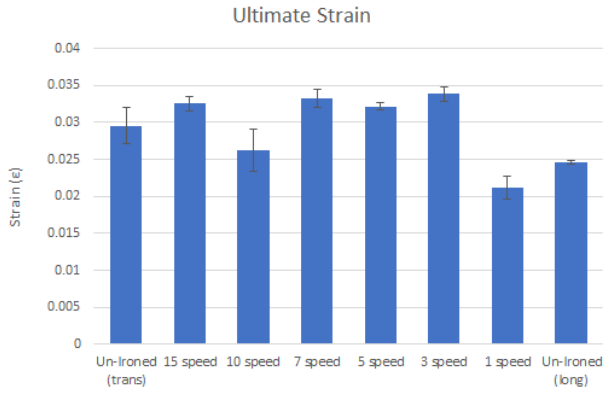

Figure 14: Maximum strain

Stiffness

Looking at the specimen's stiffness there is a slight increase with 15mm/s and 10mm/s iron-speeds, 7mm/s again performs worse, after which the stiffness increases for 5mm/s up until 1mm/s (figure 15).

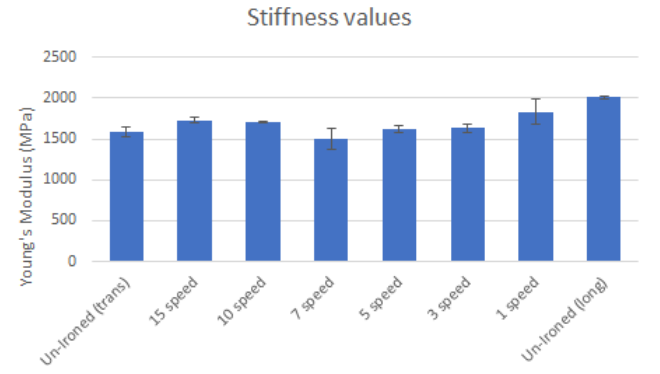

Figure 15: Stiffness values

Alternating line infill (-45°/45°)

To determine the added value of speed-modulated ironing, the optimal ironing speed identified in the ironing speed test (3mm/s) was applied to samples with infill lines alternating at -45° and 45° relative to the pulling direction (Default CURA infill). This type of isotropic infill is strong in multiple directions. This test was conducted to see whether an overall strong 3D print that uses alternating line infill could be strengthened even more in a specific direction. This would showcase a mechanical strengthening solution for designers to use without having to compromise on general strength of parts.

Alternating line infill (-45°/45°) results

As can be seen in figure 16, the ironing negatively influenced both the stress and strain of the specimen. This test was done to get quick sense of a order of magnitude of the influence of ironing on this type of infill. As these initial results did not show promising improvement further printing and testing of samples was abandoned to save time. The sparsity of the tested samples makes it impossible to draw scientific rigorous conclusions on this data. For further research multiple iron speeds should be tested with this type of infill as well. For now, we can assume that the strength of speed-modulated ironing lies with strengthening 3D prints that have a weak infill direction, not with strengthening already strong isotropic

Type	Name	Ironspeed	Sample amount
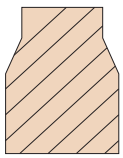	unenforced (**-45°/45°**)	-	1x
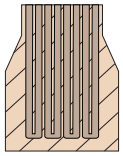	E2L-8L	3mm/s	3x

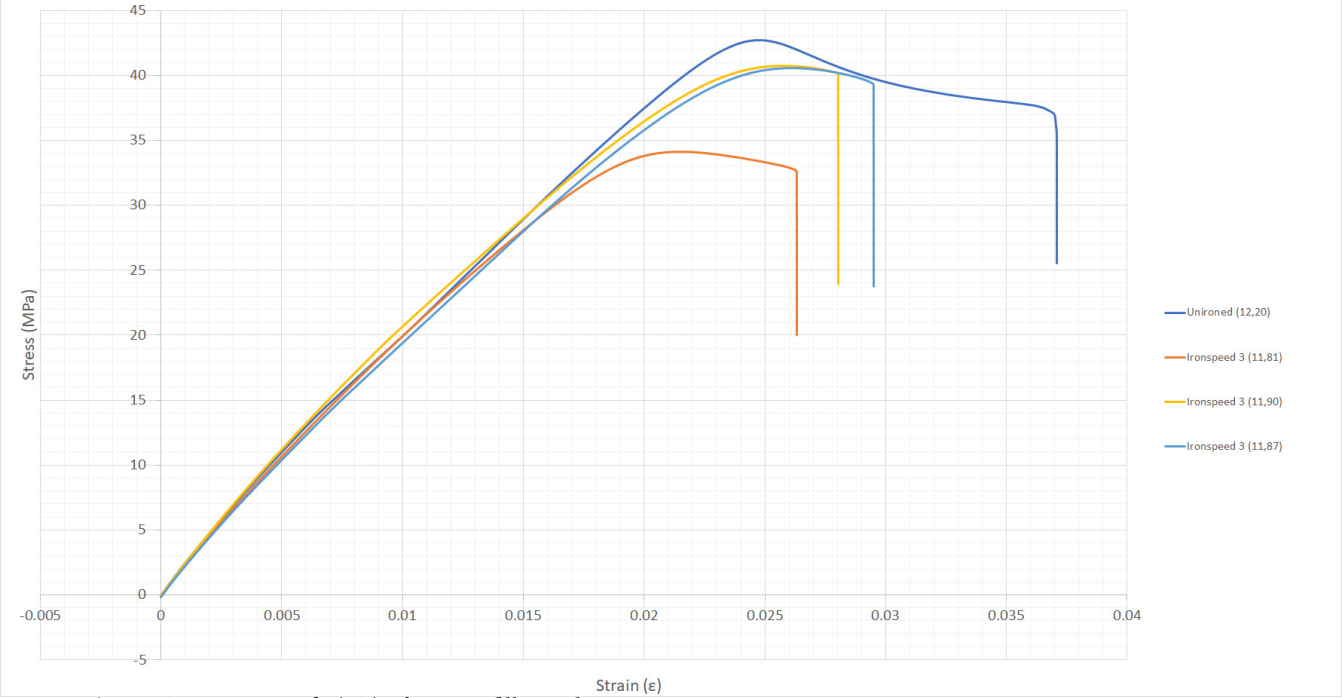

Figure 16: Stress/Strain curve of -45/45 degrees infill samples ironed with 3mm/s

Interlayer strengthening

Interlayer Strengthening

To assess what influence ironing could have on flexural/tensile strength, stiffness and interlayer bonding of vertically-oriented 3D prints, 3-point bending tests and tensile tests were conducted. The test specimen used for this test were printed upright which meant that the print needed to be ironed every layer to maintain structural consistency. Similar to the speed test conducted on the horizontally-oriented 3D prints, the ironing speed was the parameter independent variable. With the specimen printed upright, the results of both tests are directly influenced by the bonding of the layers. However, due to the excessive heat being transferred every layer, the specimen deformed geometrically. This led to the inclusion of another parameter within the 3-point bending test, which is the offset from the outer wall of the print to the ironing lines. The goal of this test was to increase interlayer bonding, flexural strength and stiffness, without jeopardizing the appearance of the 3D print.

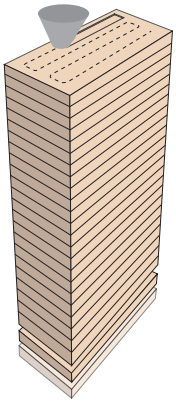

Figure 17: Ironing pattern of vertically-oriented samples

3-Point bending tests

3-Point bending flexural tests provide values for the stiffness, flexural strain and flexural stress of the 3D printed samples. The upper anvil directly presses on the print perpendicular to the print direction (figure 18). Because of this, the interlayer adhesion of the print will be of significant influence for the observed strengthening of the test samples.

Methodology

For these tests, a specimen that is accordance with ISO 178 is used. This specimen is a simple strip with a length of 80mm, a width of 10mm and a height of 4mm. The test was conducted on a Zwick Roell Z010. The specimens were printed with concentric infill and jerk and acceleration settings were changed to match the Z-Direction tensile test specimens (Appendix 8). Since the 3 point bending specimens are significantly shorter than the tensile specimens it was easier to iron every layer without causing too many irregularities. The specimen stood upright quite firmly and no additional support was needed to prevent the specimen from moving. Because of this print consistency, the choice was made to retrieve the stress/strain curve from this data as well. For this, specific formulas were needed to compensate for the irregular stresses within the specimen.

Flexural Stress *Flexural Strain*

$$\sigma_f = \frac{3FL}{2bd^2} \qquad \epsilon_f = \frac{6Dd}{L^2}$$

- σ_f • Modulus of Rupture, the stress required to fracture the sample (MPa)
- ϵ_f • Strain in the outer surface (mm/mm)
- F • Load at a given point on the load deflection curve (N)
- L • Support span (mm)
- b • Width of test beam (mm)
- d • Depth or thickness of tested beam (mm)
- D • Maximum deflection of the center of the beam (mm)

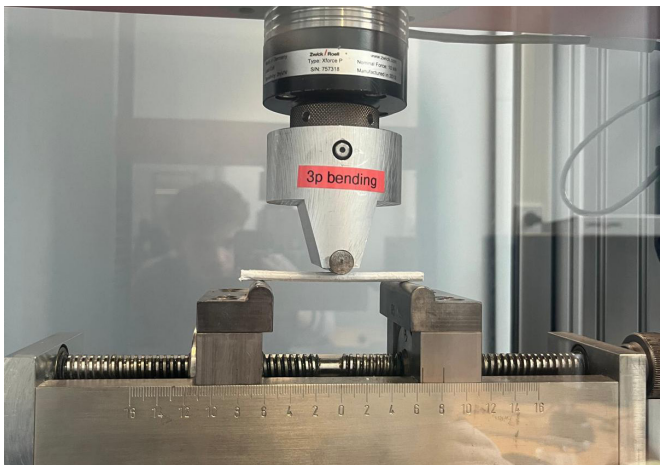

Figure 18: 3-point bending setup

Type	Name	Ironspeed	Sample amount
	unenforced	-	3x
	unenforced (210°C)	-	3x
	5mm/s	5mm/s	3x
	3mm/s	3mm/s	3x

3-Point bending Results

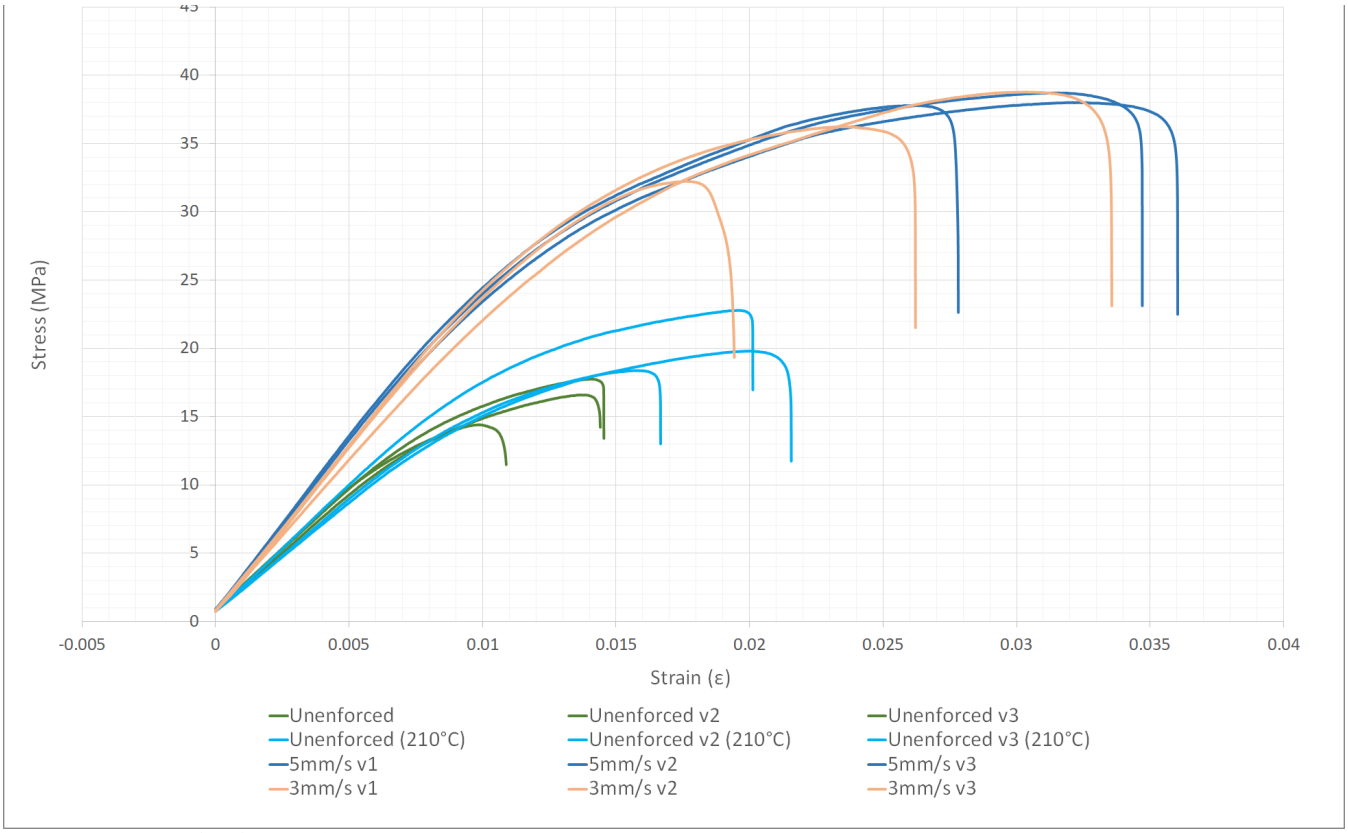

Figure 19: 3-point bending results

As can be seen in graph (figure 19) the samples that were ironed (EF), both the 5mm/s and 3mm/s exhibited significantly more flexural strength and strain resistance compared to the un-ironed samples (UF). Upon inspection of the cross section the unenforced samples turned out to be under extruded (Figure 21). This is quite interesting since the ironed samples, which use the same G-code , do not show any signs of under extrusion. This could be due to the printing nozzle leaking some filament when being retracted and the ironing nozzle smearing the filament over the surface, filling the gaps and creases by doing so. To make a fair comparison, other un-ironed samples where printed with an increased nozzle temperature of 210°C instead of 200°C. Looking at their weights, these samples are similar to the ironed samples and they did not show any signs of under extrusion. For the remainder of this paragraph the ironed samples are compared to these improved samples.

Strengthening values

The average peak flexural strength showed an increase of 17,8MPa for 5mm/s iron speed and 15,4MPa for 3mm/s iron speed. This is an increase of 87,8% and 75,9% respectively. The flexural strain of the ironed samples increased significantly as well, although quite inconsistent. This inconsistency in strain at break could be due to material irregularities, like gaps and creases, inflicted by the printing process. The stiffness of the ironed samples also increased significantly compared to the un-ironed samples. The average young's modulus increased 755,1MPa for 5mm/s and 633,6MPa for 3mm/s which is an increase of 45% and 37,7% respectively.

Close-up of fractures

The fractures of the samples were examined closely with a microscopic camera (figure 21). Upon closer inspection a clear improvement in the material's blending can be seen, as the printed lines are almost vanished completely. However, the ironing also led to small pores within the filament that are not present in the un-ironed samples. This could be evidence of the material deteriorating because of too much heat.

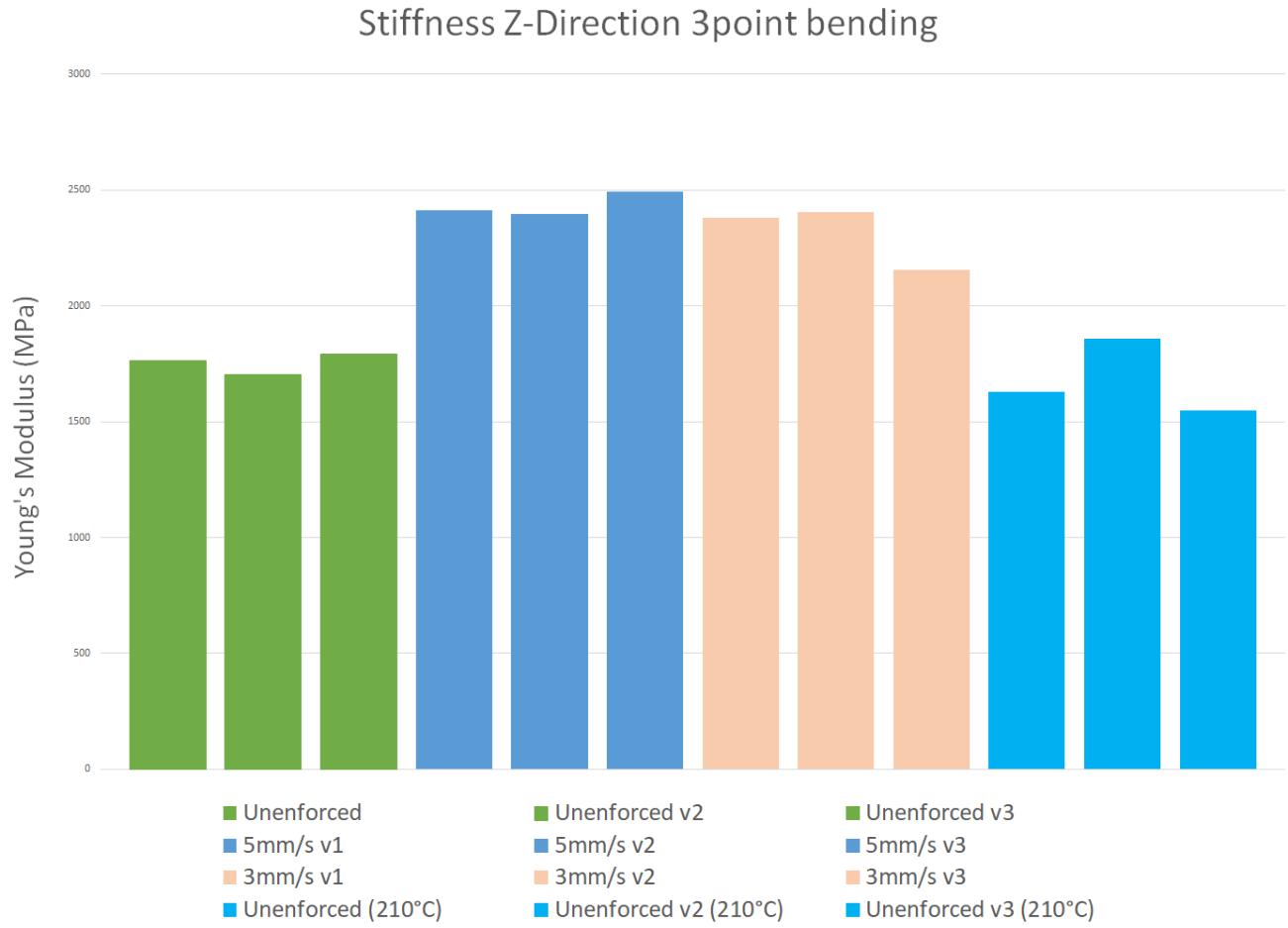

Figure 20: Stiffness values of vertically-oriented samples

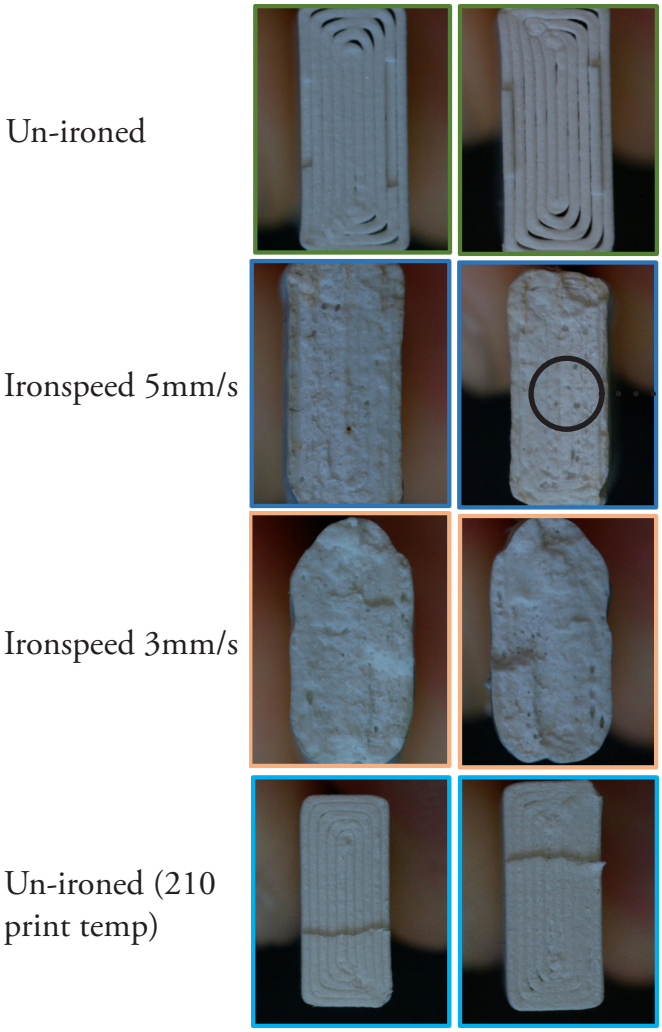

Figure 21: Close-ups of fractured Cross-sections

Geometrical distortion

Another interesting finding was that the specimen that was ironed with a speed of 3mm/s initially had a steeper Standard Force/Standard travel curve compared to the 5mm/s specimen. In other words, more force was needed to achieve the same amount of travel. However, due to the stress/strain curved being normalized with the specimen's cross section area this does not show in the flexural stress/strain curve as the cross-section area is distorted in such a way that the width and height were not representative of the actual area. This arises the question whether the achieved stiffness was due to the geometry being distorted into a more oval shape, or that layer adhesion was improved through transferred heat inflicted by ironing.

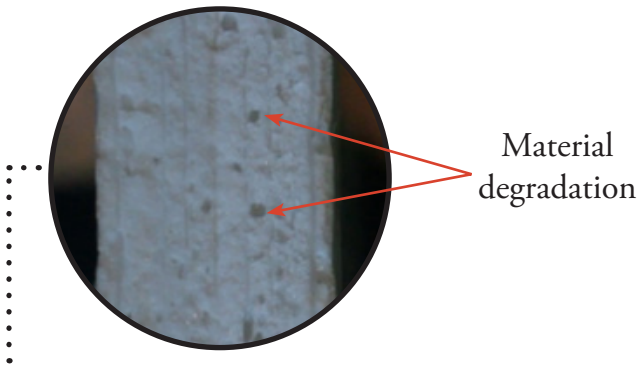

Offset

An additional experiment was set up, testing two iron patterns with different offsets from the outer layer of the test specimen. The aim of this experiment was to eliminate the distortion of the outer geometry which could have affected the increase in the specimen's mechanical performance. Aside from its possible impact on the 3point-bending test results, the distortion of the geometry is in general undesirable and insights on appropriate offsets for ironing would help for future usage of speed-modulated ironing within internal context of 3D prints.

Specimen

For this experiment two different offsets are tested, one of 0.4mm and the other 0.8mm (figure 22). The first being the exact nozzle radius, meaning that it will perfectly cover the outer edge of the 3D printed specimen when ironing. The other 0.8, which leaves an outer edge of 0.4mm unironed. To maintain a spacing of roughly 1mm between the ironing paths the number of lines had to be reduced for this specimen.

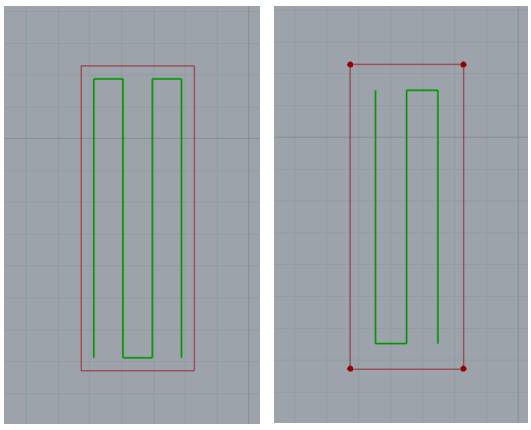

Figure 22: 0.4mm offset (Left), 0.8mm offset (Right)

Type	Name	Ironspeed	Sample amount
	unenforced (210°C)	-	3x
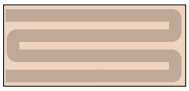	5mm/s	5mm/s	3x
	5mm/s 0.4mm	5mm/s	1x
	5mm/s 0.8mm	5mm/s	3x

Offset Results (ironspeed 5mm/s)

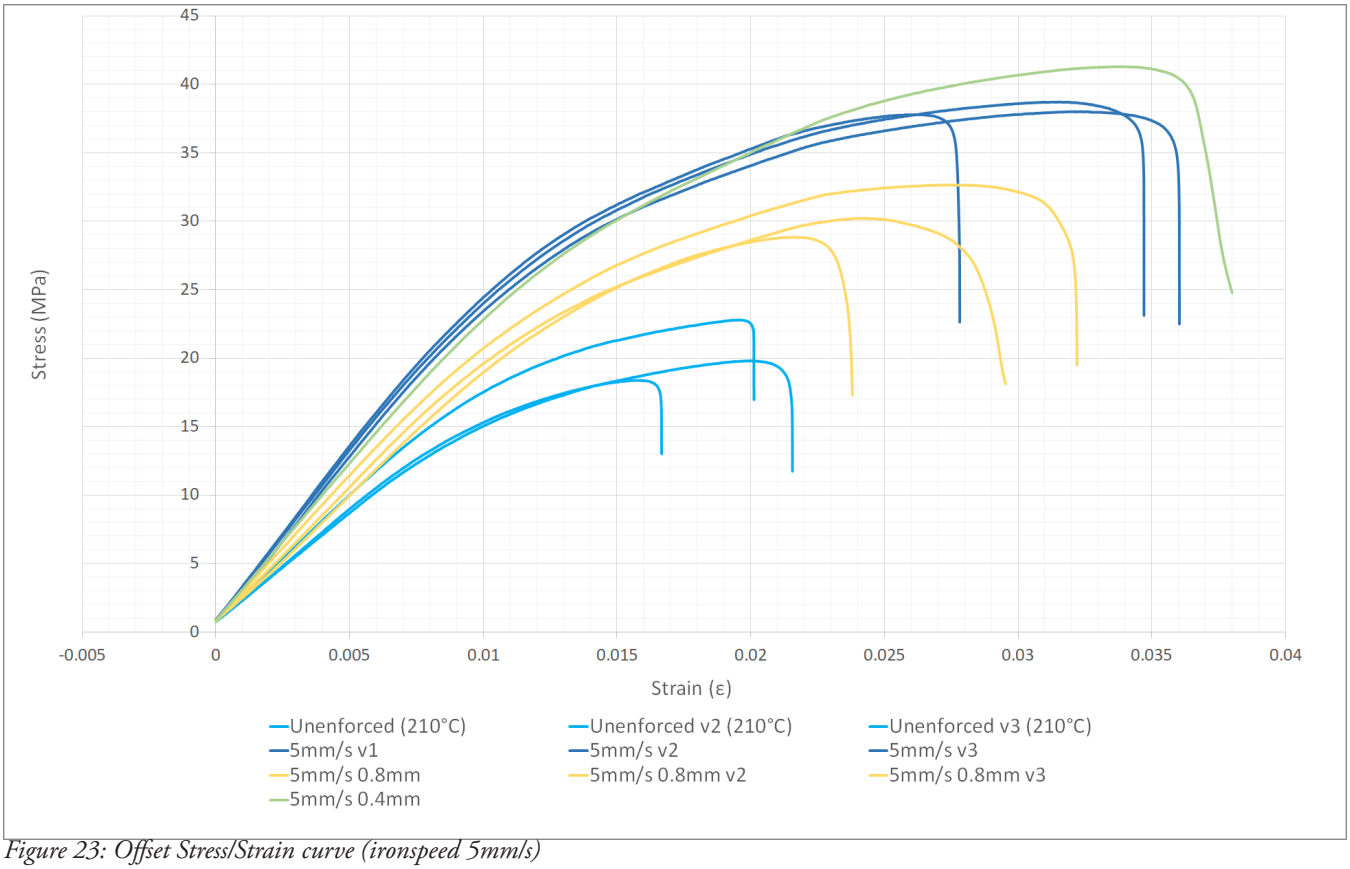

Figure 23: Offset Stress/Strain curve (ironspeed 5mm/s)

Type	Name	Ironspeed	Sample amount
	unenforced (210°C)	-	3x
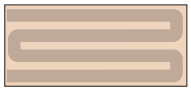	3mm/s	5mm/s	3x
	3mm/s 0.4mm	5mm/s	1x
	3mm/s 0.8mm	5mm/s	3x

Offset Results (ironspeed 3mm/s)

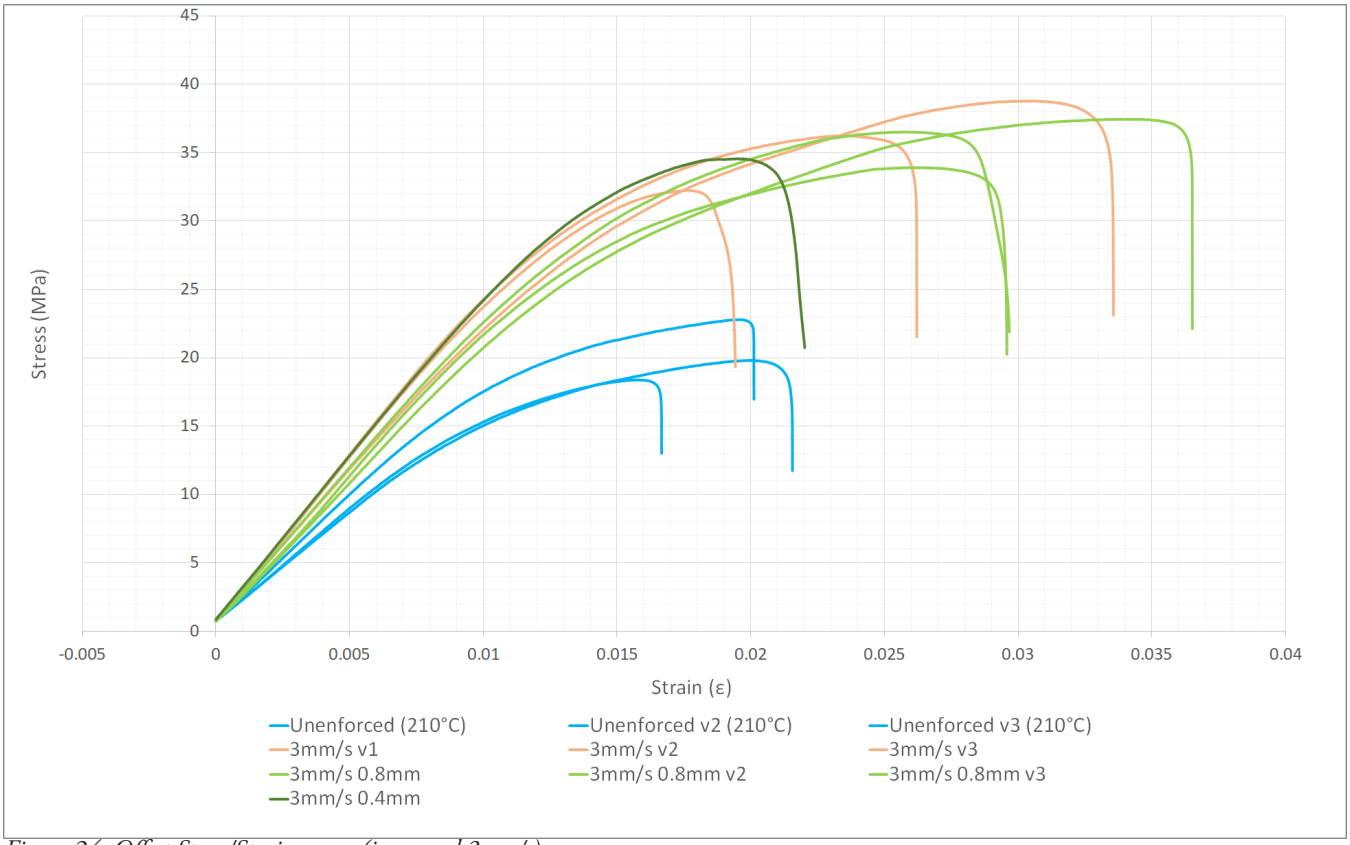

Figure 24: Offset Stress/Strain curve (ironspeed 3mm/s)

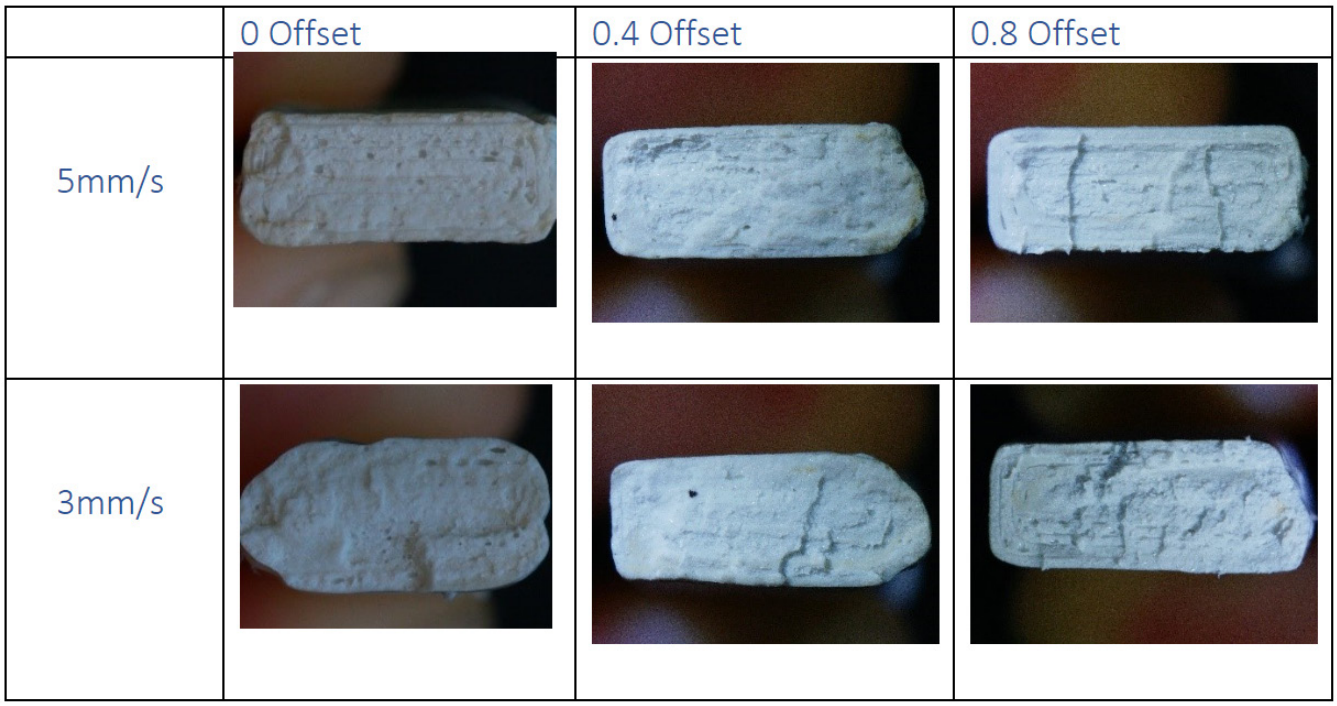

Figure 25: Close-up Cross-section images of samples without and with offset

When examining both graphs (figure 23/24)it becomes apparent that ironing with an offset still significantly improves ultimate flexural strength and stiffness values. The 3mm/s samples performed more or less similar to the samples ironed without an offset. This rejects the plausibility of the distorted geometry being the leading cause for the material enhancement. Due to the small sample size it is not possible to make claims on whether ironing with an offset performs worse or better than ironing without an offset.

Close-up of fractures

When examining the cross-sectional areas of the fractured samples, improvements in the preservation of the outer geometry can be observed (figure 25). The outer walls of the samples ironed with an offset of 0.8 mm show no visual signs of ironing, resulting in a visual appearance closer to that of a non-ironed specimen, as can be seen in Figure 26/27. The glossiness of the samples, inflected by the re-melting of the plastic, decreases as the offset increases.

Small deformations remain

Although visual improvements are made, the starting point of the ironing path still deforms the geomtery of the specimen. This is due to a combination of the printing nozzle oozing a small amount of filament during retraction and landing and the ironing nozzle transferring excessive heat when retracting and landing as well. For future usage of speed-modulated ironing the ironing process should be initiated on the inside of a 3D print, minimizing its impact on the visible outer geometry.

Figure 26: Effect of offset on outer surface of samples ironed with 3mm/s. (from left to right) No offset, 0.4mm offset, 0.8mm offset, Un-ironed

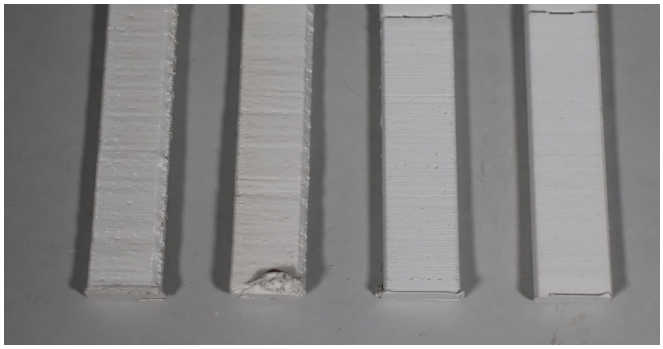

Figure 27: Effect of offset on outer surface of samples ironed with 5mm/s. (from left to right) No offset, 0.4mm offset, 0.8mm offset, Un-ironed

Z-Direction tensile tests

Printing the ISO (527-2) model upright and iron every layer proved to be quite a challenge. Printing such a high specimen and switching between iron and print nozzle every layer caused a lot of print irregularities. Since the specimen are tested in the Z-direction, one incorrect layer could significantly influence the results of the test. In contrast to the script used for generating the G-code for the 3-point bending samples, the script that was used to generate the ironing G-code for these specimen did not have a Z-retraction built in. This means that the ironing nozzle approaches the model at the exact height it will also iron, resulting in the nozzle bumping into the model and causing print irregularities. Moreover, after having ironed a layer, the ironing nozzle moved away from the print at the same height as well, resulting in severe stringing as the material sticks to the heated nozzle.

Figure 28: Severe stringing of vertical printed dogbone

After several iterations the a cura profile was made that together with a 5mm/s iron-speed, resulted in specimen that were able to be tensile tested.

Figure 29: Ironing vertical specimen proved to be difficult. Un-ironed (left), Ironed (middle, right)

Z-direction tensilte tests result

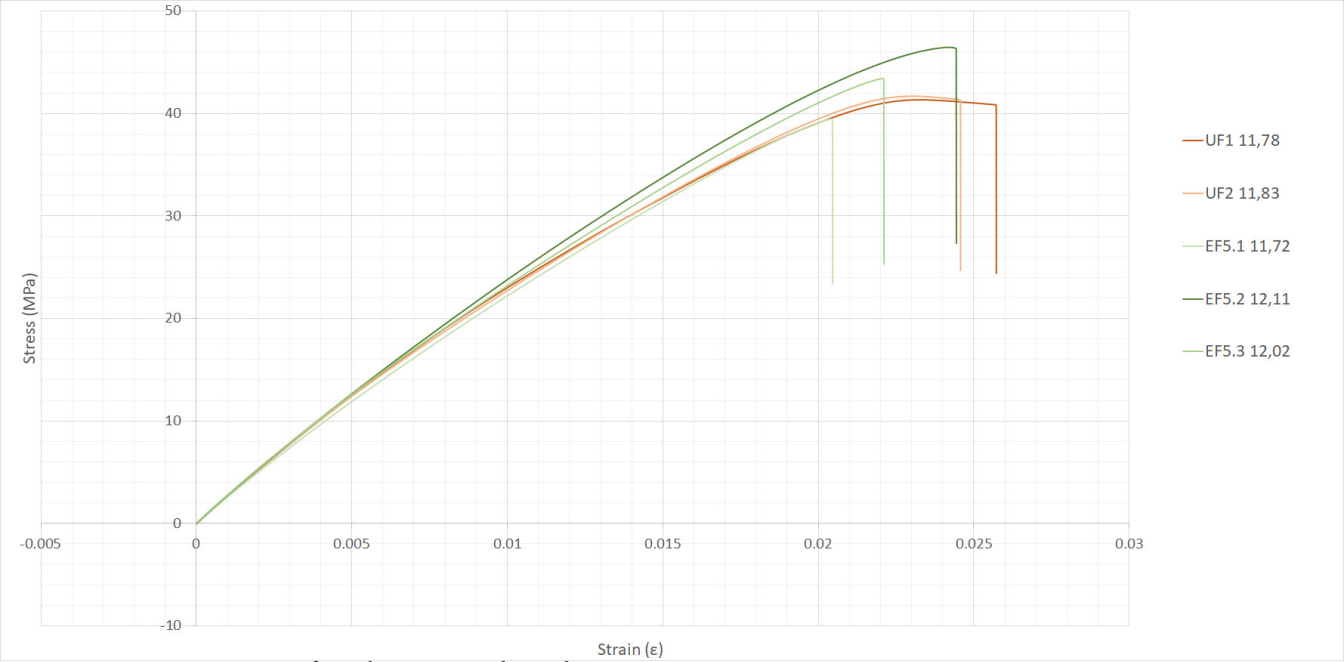

Figure 30: Stress/Strain curve of tensile test, vertical samples

The ultimate tensile strength (UTS) of some of the ironed samples increased. The second sample's UTS (EF5.2) was the highest amongst the three with 46.5MPa, which is an increase of 11.9% compared to the average of the un-ironed samples. Looking at the slope of the stress/strain curves it can be concluded that the ironed samples also became a bit stiffer. Looking at the cross section of the broken samples it is clear to see that the heat facilitated extra material blending between the layer's interfaces. Unlike the un-ironed samples, the ironed samples did not break precisely between two printed layers.

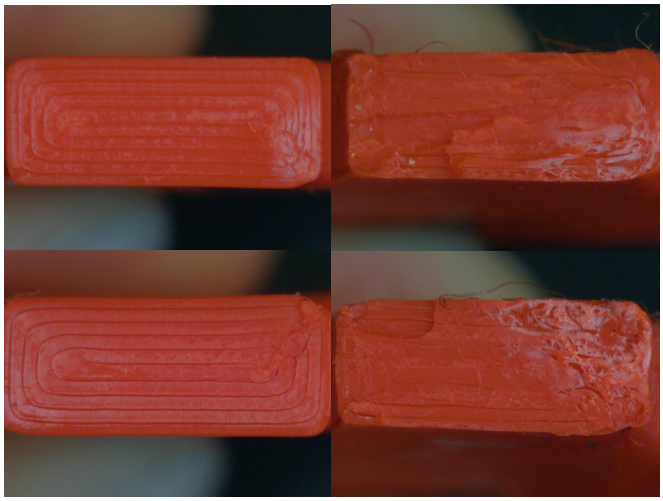

Figure 31: Close-ups of fractured cross-sections. Material degradation (pores) visible with ironed sample (right).

Although visually the ironed specimen seems to have a better layer adhesion than its un-ironed counterparts, the results are way less significant than with the 3-point bending specimen. Looking more closely at the cross section of the broken samples, the ironed samples seem to have some form of polymer degradation on one corner. This could be because the ironing nozzle starts ironing at one corner consistently and since the ironing nozzle does not retract in the z-direction more heat is being transferred on that specific location. This could be the reason why the ironed samples broke prematurely and had worse strain compared to the un-ironed samples.

Ironing on material level

Ironing on material level

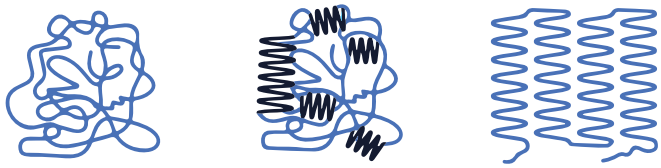

Figure 32: Polymer chain configurations

PLA, which is studied in this research, is a semi-crystalline polymer, meaning that a part of its polymer strains are organized in a crystalline manner whilst the remaining strains are unorganized or better said – amorphous (Figure 32). The percentage of crystallinity says a lot about the mechanical behaviour of the polymer. A higher degree of crystallinity corresponds with increased stiffness, brittleness and stronger internal bonds, whilst a low percentage of crystallinity makes the material easier to deform. For FDM-printing, low-crystalline polymers are therefore easier to process and are the most widely used for everyday printing. Typical crystallinity percentages of PLA used for FDM printing lie between 1 and 2% after being extruded, with printed pristine PLA having a crystallinity percentage of 1.45% (Coppola et al., 2018)(Agaliotis et al., 2022).

When examining the results of the 3-point bending tests, the question arises whether the observed increase in material strength and stiffness is solely due to improved layer bonding or also influenced by a higher percentage of crystallinity. To answer this question the samples where tested with Differential Scanning Calorimeter (DSC).

Method

DSC is a thermoanalytical technique in which the difference in the amount of heat required to increase the temperature of a sample and reference is measured as a function of temperature (Freire, 2003). Aside from determining thermal properties of a material, a DSC showcases at what temperatures particular phase transitions, like glass transition temperature (Tg), melting (Tm) or cold-crystallization (Tc), occur (Figure 33). To determine the crystallization percentages of ironed vs un-ironed PLA samples, the energy required to break down the crystals within the material (Melting, ΔHm), is compared with the energy required to melt PLA if it were 100% crystalline ($\Delta Hm°$) according to the following formula.

$$\% \text{ Crystallinity} = [\Delta Hm - \Delta Hc] / \Delta Hm° \cdot 100\%$$

ΔHc is the energy of the crystallization that occurs within the material because of the applied heat during the test. To determine the crystallinity percentage of the material before it was exposed to this heat, this additional cold-crystallization energy (ΔHc) has to be subtracted from the melting energy (ΔHm), leaving only the energy that is required to break down the already present crystals. The amount of energy in J/g can be found by integrating the areas under the cold-crystallization and melting peaks of the DSC curve (IMAGE). The value of $\Delta Hm°$ for PLA is 93 J/g (Coppola et al., 2018).

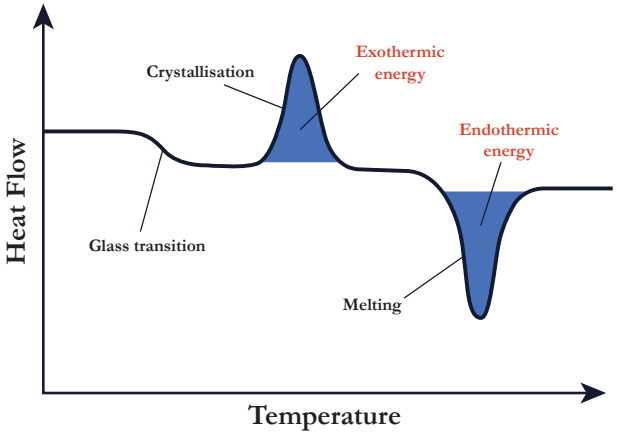

Figure 33: DSC curve

Test

For this test the TA DSC 2500 was used to analyse the thermal properties of two different samples that have the same configuration as the samples used in the 3-point bending tests. One sample was ironed with a speed of 3mm/s and an offset of 0.4mm and the other was not ironed. Due to the contamination of the samples used in the 3-point bending tests new ones had to be print-

ed for this test. This, in combination with other filament being used, makes the results of the DSC not directly comparable with the observed mechanical alterations from the 3-point bending tests. However, it does demonstrate what happens to the samples on a material level when undergoing ironing.

For this test the following parameters were selected.

Test type:	Heat-cool-heat
Initial temperature:	25 °C
Max temperature:	200 °C
Heating rate:	10 °C/min

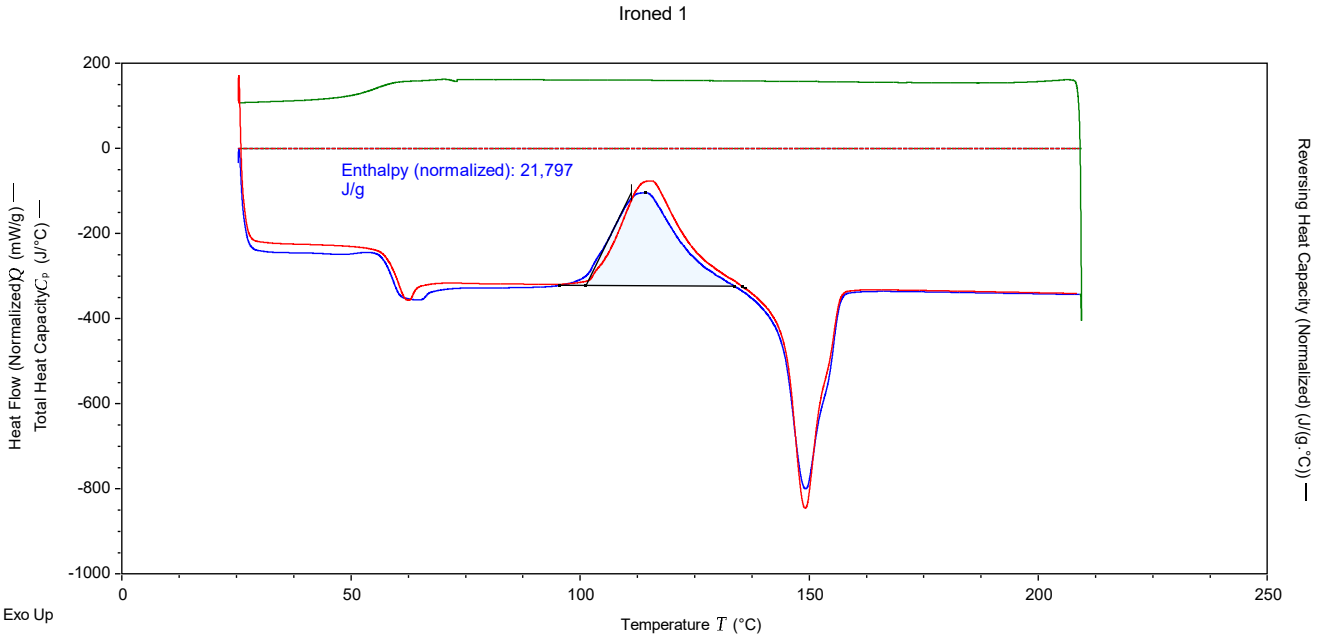

Figure 34: DSC curve ironed sample (cold crystallization enthalpy)

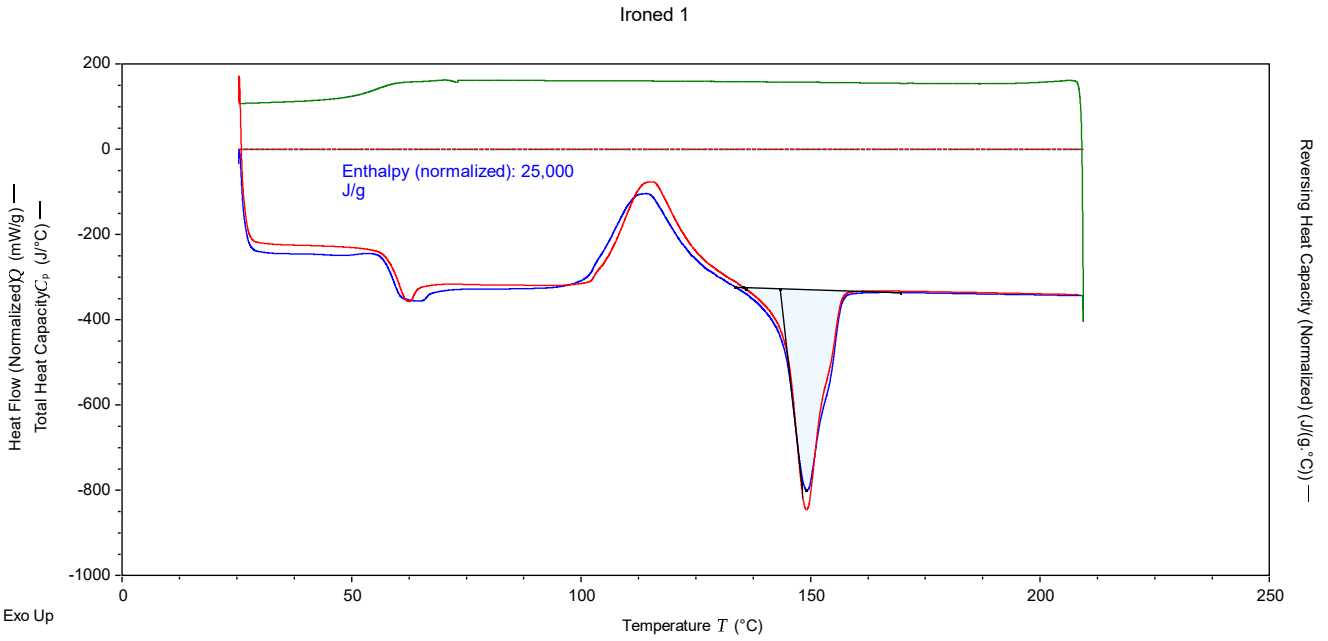

Figure 35: DSC curve ironed sample (Melting enthalpy)

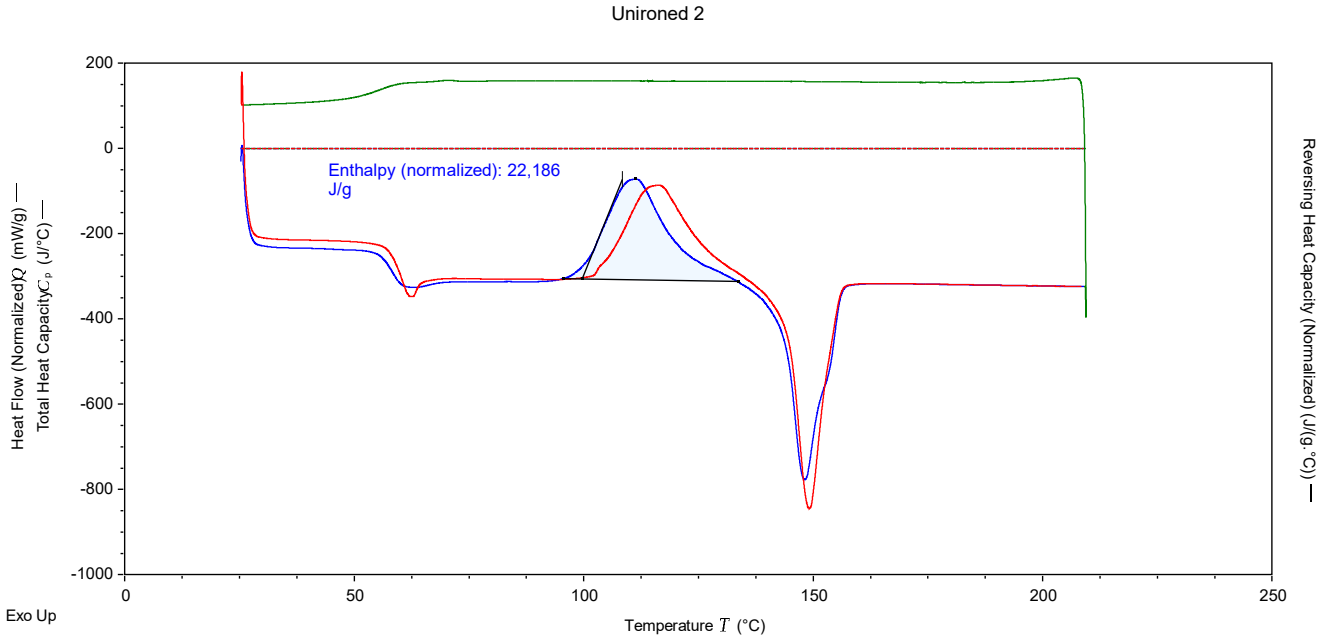

Figure 36: DSC curve un-ironed sample (cold crystallization enthalpy)

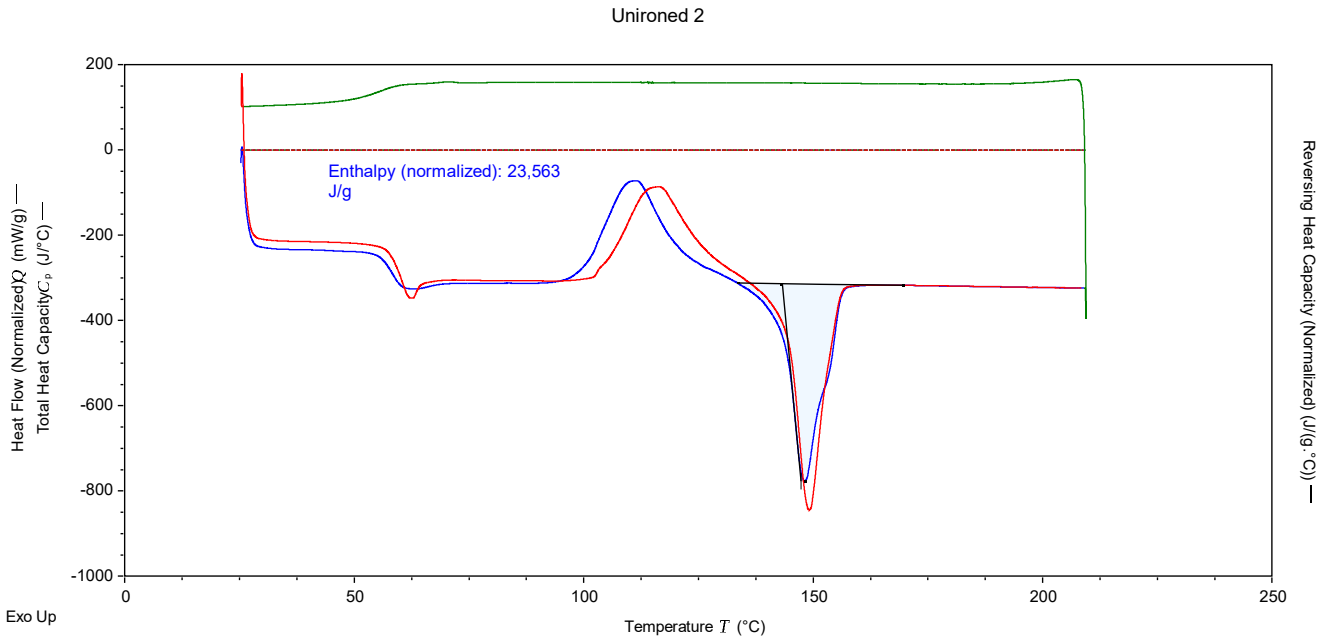

Figure 37: DSC curve un-ironed sample (Melting enthalpy)

Amorphous unironed

When examining the DSC curves of the ironed and un-ironed samples a clear difference in cold-crystallization temperature (Tc) can be observed between the first (blue) and second (red) heating cycle of the un-ironed samples. This illustrates that the initial structural state of the un-ironed sample, which depends on the thermal history such as cooling rates and/or processing conditions, contained more amorphous regions compared to the material's inherent structural state (Figure 36/37). These regions were free to move and form crystals at lower temperatures, resulting in an earlier peak.

Crystalline ironed

With the ironed sample, the cold-crystallization peak of the first heating cycle aligned with the second heating cycle (Figure 34/35). This suggests that ironing eliminated the processing effects of FDM printing and caused the sample to demonstrate similar thermal properties to that of the material's inherent structural state. This finding suggests that the ironed sample has a higher degree of crystallinity compared to its un-ironed counterpart, as it requires higher temperature for cold-crystallization to occur.

Crystallinity calculations

To verify this, the enthalpies of the cold-crystallization and melting peaks of both samples were found by integrating the area's under the peaks and calculating the crystallinity percentage.

- % Crystallinity Un-ironed = 1,67%
- % Crystallinity Ironed = 4,22%

As expected, the crystallinity percentage of the un-ironed sample is close to the percentages found for PLA in the literature; 1,45% (Agaliotis et al., 2022). The Ironed sample however, showed an increase of 2,55%. This seems like a marginal difference, but for this low-crystalline polymer this more than doubles the amount of crystal regions, which is likely to have significantly contributed to the observed mechanical modifications of the ironed samples.

Discussion

The results of the conducted research on speed-modulated ironing for strengthening 3D prints show promising directions for further exploration. Since the aim of this research was of a more explorative nature, the tests were not conducted with scientifically rigorous sample sizes. Therefore, factual claims on the effect of speed-modulated on mechanical performance cannot be made. However, the test data and observations are examined carefully with this data scarcity in mind and some preliminary conclusions can definitely be drawn from it. Especially since multiple specimens with the same configuration showed repeatable behaviour throughout the tests. These conclusions could help with focusing successive research on this topic.

Looking at the ironing performance on vertically-oriented 3D prints the iron-speed test showed some promising results. Comparing the results with other reports on tensile testing of 3D printed dog bones, the achieved improvements on mechanical performance were comparable to changing infill types and directions. For example, Sun et al. (2020) changed the dog bones' infill direction from transversal to longitudinal and improved the peak stress with 10MPa. This makes the 5MPa improvement by ironing with 3mm/s iron speed quite significant. A collection of multiple comparable papers are highlighted in APPENDIX 4. Although the details of these conducted tests (e.g. material choice, size of dog bone, tensile test speed, etc.) differ, the results are all within the same ballpark. When examining the ultimate tensile strength, young's modulus and maximum strain charts, no clear pattern can be recognized. This emerges the probability that multiple parameters are influenced by the ironing process and influence the mechanical performance of the ironed parts.

In order to estimate the added value that speed-modulated ironing can bring on vertically-oriented 3D prints, the most optimal iron-speed (3mm/s) retrieved from the speed-test was tested on dog bones with alternating 45/-45 degrees infill. This type of infill is strong in multiple directions. If ironing would improve the mechanical performance of a part with this type of infill in a specific direction, the added benefit would be evident. This would allow a designer to improve a parts strength in a certain direction, without having to compromise on strength in another direction. However, the ironed samples performed worse. For horizontally-oriented 3D prints the strength of speed-modulated ironing lies therefore with mechanically enhancing specific print designs that are limited in their choice of infill.

"For horizontally-oriented 3D prints the strength of speed-modulated ironing lies therefore with mechanically enhancing specific print designs that are limited in their choice of infill."

In terms of added value, the effect of speed-modulated ironing on vertically-oriented 3D prints is significant. As explained in the introduction and related work, other methods that enhance layer adhesion all have their own limitations. Some require modifications on the printer, others effect the entirety of the print, etc. Within slicer software, the two main parameters that are of influence on vertical mechanical properties are nozzle temperatures and layer height. With speed-modulated ironing, both the stiffness and ultimate tensile strength of parts can be increased locally with no modifications needed for the printer and without compromising on print quality. Looking at the fracture cross-section of the tested specimen clear improvement on material blending is observable. A downside of this technique is that it is prone to overheating and degrading the material. In order for this technique to become widely applicable clear insights should be gathered on the effect of heat on the material.

"With speed-modulated ironing, both the stiffness and ultimate tensile strength of parts can be increased locally with no modifications needed for the printer and without compromising on print quality."

Ironing proved to be most useful in enhancing layer adhesion and improving interlayer strength and stiffness. Together with the dimensional flexibility that FDM printing offers, this opens up an abundance of possible use cases where ironing could be the solution for mechanical performance issues. In the next chapter, several of these possible use cases are highlighted and tested. However, mechanical solutions is not the only use for speed-modulated ironing. Throughout the research several applications for speed-modulated ironing that influenced visual and haptic properties within 3D context arose. For further research these would be interesting to explore.

"Ironing proved to be most useful in enhancing layer adhesion and improving interlayer strength and stiffness. Together with the dimensional flexibility that FDM printing offers, this opens up an abundance of possible use cases where ironing could be the solution for mechanical performance issues."

Applications

Based on the findings of the conducted experiments two use cases are designed to demonstrate the strengths and possibilities of speed-modulated ironing. These applications are made to bridge the gap between the conducted research and the future possibilities of this technique, demonstrating strengthening of functional prints and showcasing a technique that generates time-efficient ironing patterns for optimal mechanical performance.

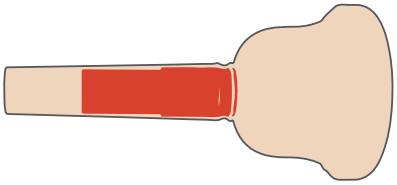

Strengthening a 3D printed Trombone mouthpiece

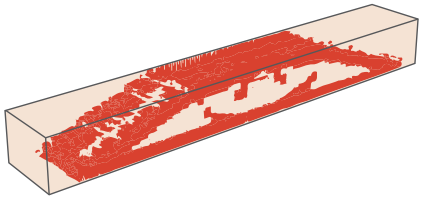

Topology optimized ironing

Strengthening a 3D printed trombone mouthpiece

Strengthening a 3D printed trombone mouthpiece

The results of the 3-point bending test demonstrated significant increase in interlayer bonding and flexural strength through ironing. To demonstrate this techniques' strengthening capabilities in a real-life scenario a trombone mouthpiece was selected for ironing. A trombone mouthpiece is a perfect example of a 3D print that is mechanically constrained by its print orientation as the smoothness of the mouthpiece is crucial for both the player's comfort and the quality of the sound. This means that the mouthpiece should be printed upright, which is the weakest orientation for withstanding the forces acting on the print. The point where the mouthpiece is placed into the horn becomes a mechanically critical area, as it relies solely on interlayer strength. This is a perfect example of a 3D print that could benefit from the extra stiffness and flexural strength at a specific location. Ironing could provide a solution that strengthens the design without needing to modify the printer and increasing the print time too much. Since the quality of the print, i.e. no cracks, bumps, etc. is important for the sound of a mouthpiece, strengthening a mouthpiece with ironing whilst maintaining structural integrity would be a nice challenge to demonstrate the potential of the technique.

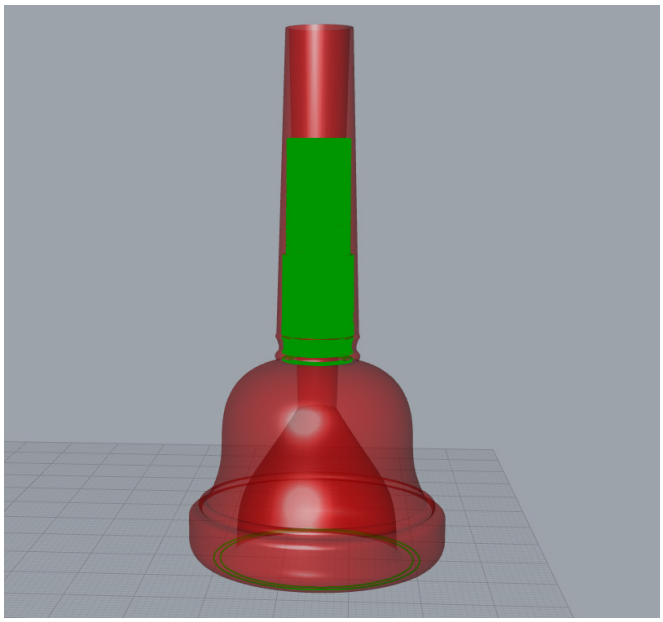

Figure 38: Ironing pattern for the trombone mouthpiece

Method

An ironing pattern was added where the trombone mouthpiece makes contact with the lead-pipe of the trombone (figure 38). To make sure there are no print inconsistencies on the outside of the mouthpiece the ironing pattern maintained an offset of 0.8mm from the outer and inner surfaces. Two ironing lines were made where the pipe was broad enough to maintain a 0.8mm offset with the outer surface and a 1mm offset between the two lines. The ironing speed were set at 5mm/s and 3mm/s, based on the results of the Z-direction 3-point bending tests.

Figure 39: Flexural test trombone mouthpiece setup

Test setup

The test setup uses the same configuration to that of a 3-point bending test, only the mouthpiece is fixed in a tube which is positioned on one side of the upper anvil (figure 39). This asymmetry of the test setup could affect the precise force values. However, since the aim of this test is to simply compare the different ironing configurations this setup is still sufficient.

Results

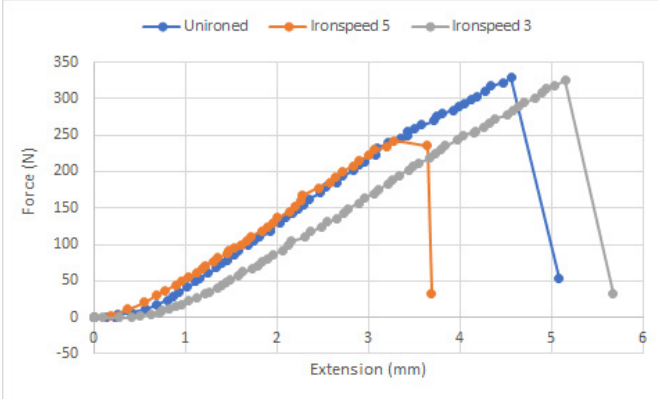

Figure 40: Force/Extension graph trombone mouthpiece

When examining this force/extension graph it becomes clear that the ironing did not positively influence the mechanical strength of the trombone mouthpiece (figure 40). The sample ironed with a speed of 5mm/s followed the same trajectory of the un-ironed sample but broke of prematurely. A potential cause of this could be a print inconsistency due to the discontinuous nature of the ironing process. The mouthpiece ironed with a speed of 3mm/s demonstrated a comparable force resistance to that of the un-ironed mouthpiece, but looked to be less stiff. However, because the test setup was not entirely rigid, the samples were able to move slightly, which makes it difficult to draw conclusions about their stiffness.

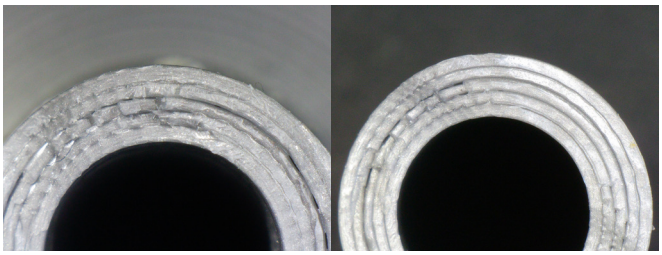

Figure 41: Cross-section Un-ironed mouthpiece

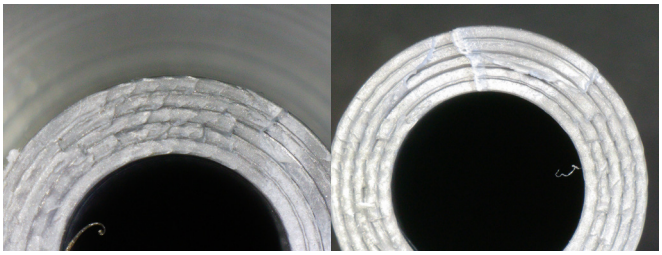

Figure 42: Cross-section mouthpiece ironed w/ 5mm/s

Figure 43: Cross-section mouthpiece ironed w/ 3mm/s

Cross-sections

Looking at the cross-sections of the fractured mouthpieces hardly any visual change can be seen between the un-ironed sample and the sample ironed with an ironing speed of 5mm/s (figure 42). The ironing paths only passed the printed surface one or two times, based on the thickness of the area. It is likely that the observed improvement of blending of the material with the Z-directions 3-point bending tests was mostly caused by the ironing nozzle going over the surface and heating the area multiple times. Since those 3-point bending samples had a smaller surface area, the entire layer heated up when being ironed, even when not directly covered by the ironing nozzle.

When examining the cross section of the 3mm/s sample some improvement can be seen in terms of blended layers (figure 43). However, comparing these cross sections with those of the Z-direction 3-point bending tests the effect is quite marginal. Where the Z-direction samples showed signs of material degradation due to the exposure of heat, the material of the mouthpiece sample looks completely unscathed.

Insufficient Ironing

Based on the force/extension data in combination with the cross section images it can be concluded that the ironing configuration was not suitable for this use case. The question arises whether the ironing speed should be lowered even further, or more ironing paths would facilitate improved layer blending. Another set of mouthpieces were printed with increased ironing paths, 3 paths instead of 1 & 2 and two different ironing speeds; 3mm/s and 2mm/s. To maintain spacing between the ironing lines and the outer wall of the 3D print this meant that the ironing lines overlapped.

Results additional path/Slower iron speed

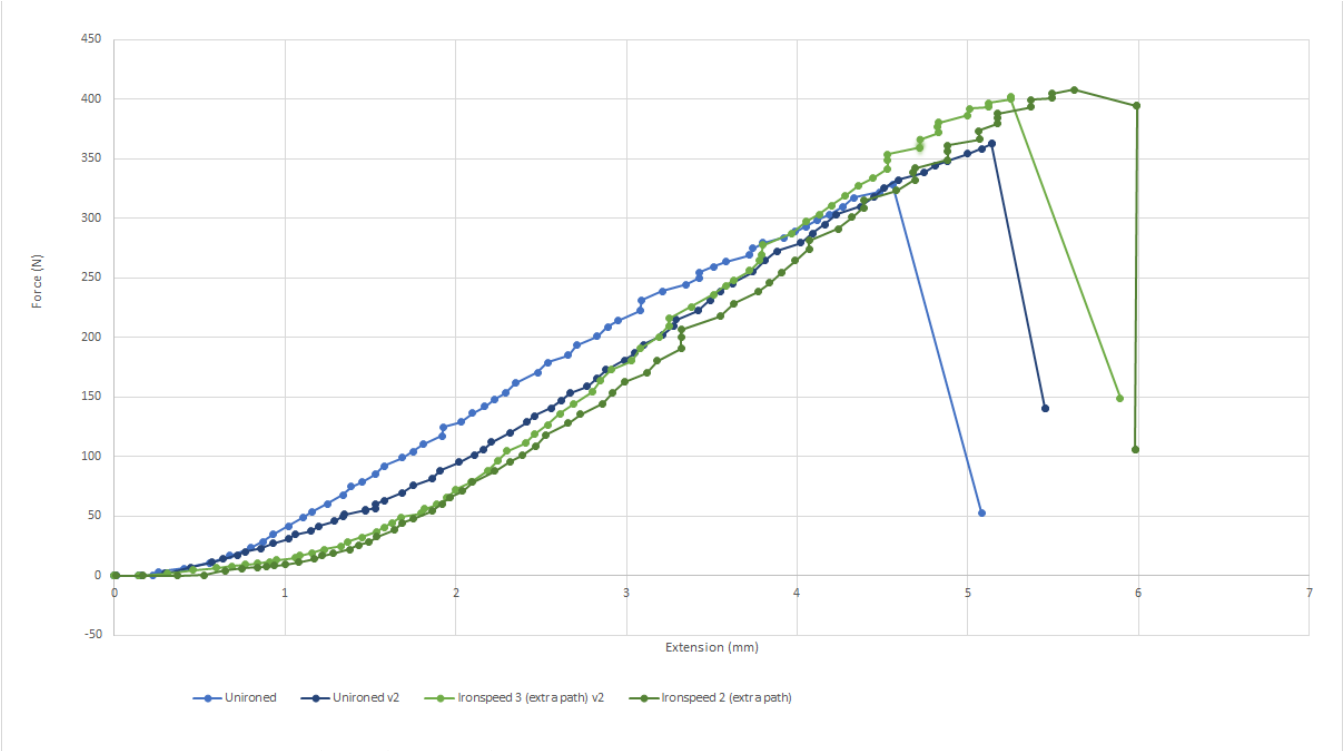

Figure 44: Force/Extension graph trombone mouthpiece

Strength

Clear improvements in terms of force resistance are made with these two ironing configurations. The sample ironed with a speed of 3mm/s showed an increase in ultimate flexural force of 57N, which is an increase of 16,5% compared to the un-ironed sample. The sample ironed with a speed of 2mm/s showed an increase of 62,5N which is an improvement of the ultimate flexural force of 18,1% compared to the un-ironed sample.

Cross-sections

Examination of the fracture cross-sections revealed a noticeable increase in layer adhesion. The print lines of the 3mm/s sample were hardly visible. However, it still fractured between two different print layers, indicating that, although improved, the interlayer area is still the weakest region of the 3D print. The 2 mm/s ironed sample did not show any signs of print lines and its fracture surface extended across multiple printed layers, indicating improved layer blending.

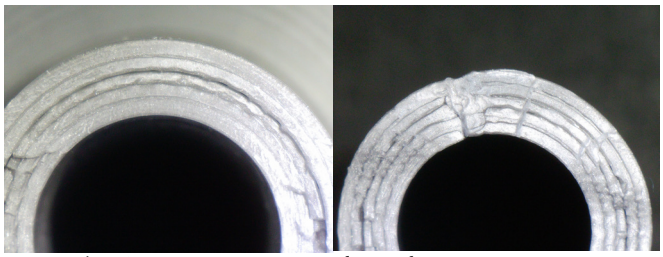

Figure 45: Cross-section Un-ironed mouthpiece

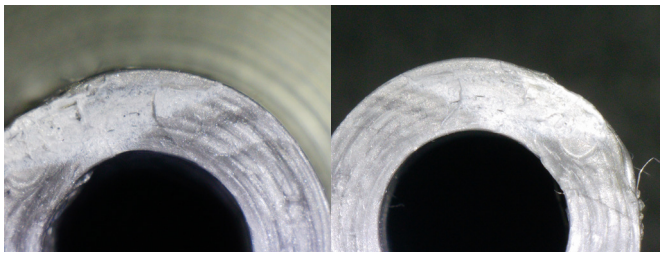

Figure 46: Cross-section mouthpiece ironed w/ 3mm/s + extra path

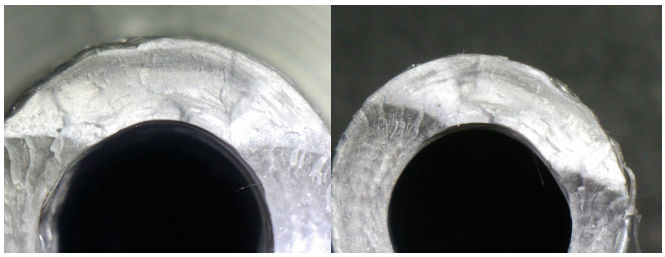

Figure 47: Cross-section mouthpiece ironed w/ 2mm/s + extra path

Topology Optimized Ironing

Topology Optimized Ironing

Ironing is a time consuming practice. For switching the nozzles the printer head needs to travel to a specific leaver located at the edge of the print domain. After having travelled back and forth the ironing itself takes a significant time as well, of course depending on the iron speeds and paths. When every layer is opted to be ironed this practice usually takes more than double the time compared to un-ironed prints. To reduce the extra time inflicted by ironing and still significantly strengthen 3D prints for a specific use case, a topology optimization algorithm was used to determine where the 3D printed part should be ironed. Topology optimization is a mathematical method that optimizes material layout within a given design space, for a given set of loads, boundary conditions and constrains. Through finite element analysis this method determines where within the given domain (the 3D model) material is needed to achieve optimal strength and stiffness. Usually topology optimization is used to make parts lighter, by removing all material that does not contribute to the parts' mechanical performance. However, for speed-modulated ironing the aim is to strengthen the areas within the part that do. By doing so, the amount of ironing and therefore iron time can be reduced whilst maintaining similar levels of mechanical enhancement.

Method

To incorporate topology optimization within the iron grasshopper script the plug-in tOpos was used. The boundary conditions are determined by the STL file of the model that can be exported from Cura. The load and constrains are added in manually within Rhino/Grasshopper. The plug-in asks for a fraction value as input. This value is the target volume that the algorithm is looking to achieve. For this research a fraction value of 0.2 was used, meaning that 80% of the volume will be removed. For this speed-modulated context, the fraction value determines the amount of ironing and thus the amount of iron time. After running, the tOpos plug-in gives a list of density values which belong to specific points within the boundary condition volume as output. These points can remapped to a grid of points that are structured for ironing paths. By remapping these points the density values are mapped to this grid as well, which makes it possible to remap the density values to iron speeds. By doing so the areas within the model that have high density values now get ironed with slower speeds, allowing for more heat transfer from the nozzle into the material (Figure 51).

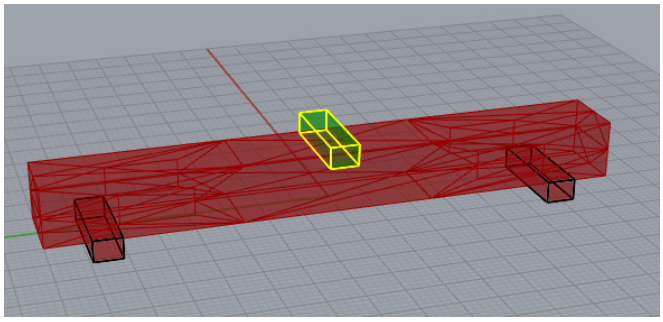

Figure 48: TopOpt boundary conditions: One applied force, two supports

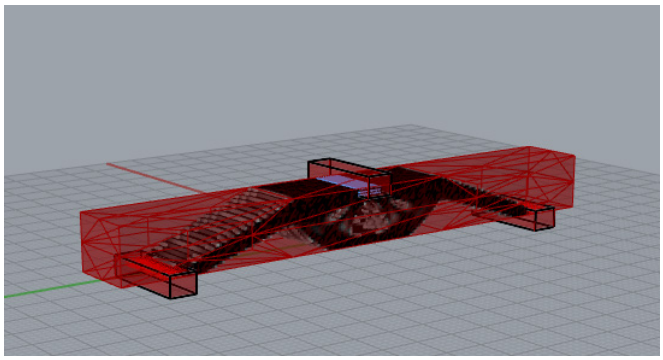

Figure 49: Topology optimized shape

Speed visualization

To visualize the difference in ironing speeds the areas that correspond with slow iron speeds were given a bright colour, whilst the fastest were given black (figure 50). By doing so the topology optimized shape can be clearly seen within the ironing paths.

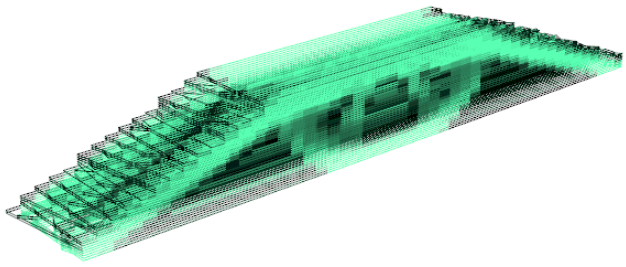

Figure 50: Ironing speeds heat map

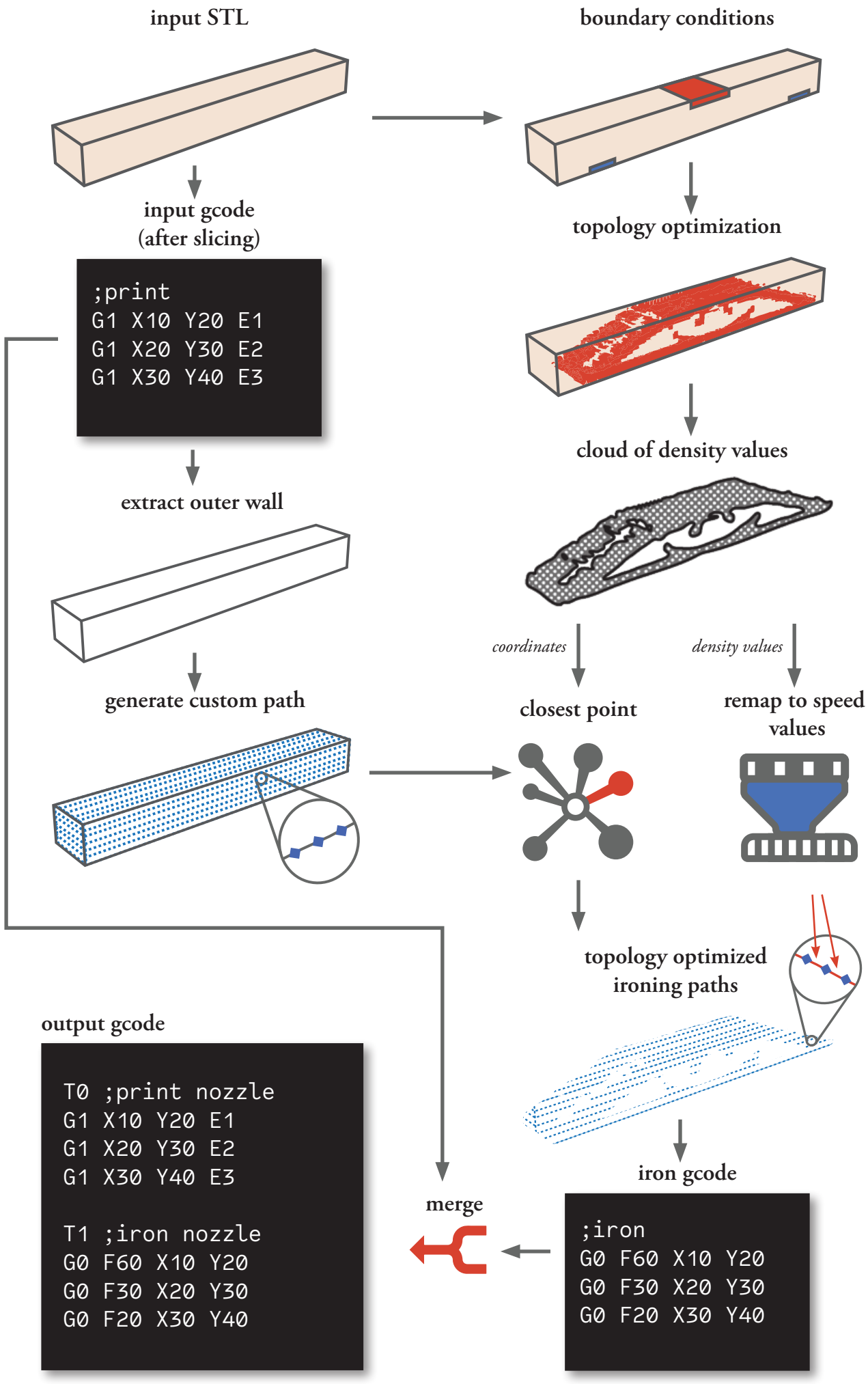

Figure 51: Topology Optimization Grasshopper workflow

To get a sense whether this topology optimized ironing actually improved mechanical performance a 3-point bending test was conducted. Instead of the regular 3-point bending specimen dimensions the model was made twice as thick (8mm instead of 4mm) to allow for topology optimized structures to take shape (Figure 52). The boundary conditions that were used as input for the tOpos plug-in were the same as the actual 3-point bending test setup, making sure the optimized shape is specific for this type of test. Aside from two different types of iron-layer intervals (Every layer, every other layer) both longitudinal and transversal infill were included in the samples.

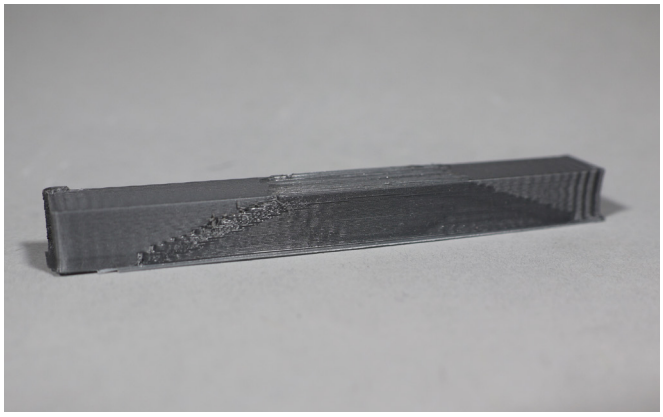

Figure 52: Topology Optimized 3-point bending sample

Results

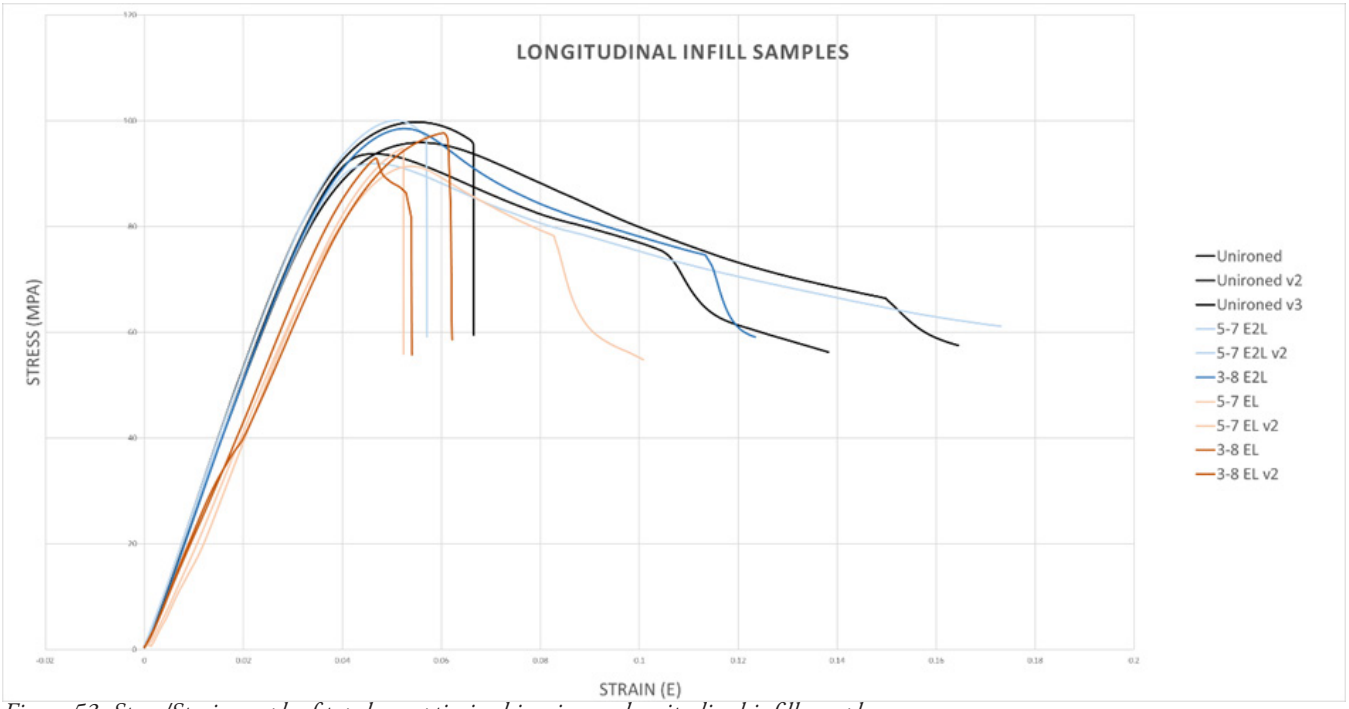

Figure 53: Stress/Strain graph of topology optimized ironing on longitudinal infill samples

Mechanical properties

Looking at the results of the samples with longitudinal infill no substantial change in mechanical performance can be retrieved. The samples all demonstrate a similar peak strength. The ironing did slightly effect the stiffness of the samples negatively with the samples being ironed the most (slowest speed and every layer) showing an average decrease in Young's Modulus of 16,2% compared to the un-ironed samples (figure 54). Another interesting observation is that, during the 3-point bending test, half of the samples fractured, while the other half underwent plastic deformation without breaking. This difference in ductility is present in all different configurations of the samples, ironed and non-ironed, demonstrating that the ironing is not the driving factor for this phenomenon. Since the longitudinal infill is perpendicular to the bending direction, this type of infill is expected to demonstrate much greater stiffness and resistance to flexural stress compared to the transversal infill samples. With this already quite optimal construction of the sample, it is therefore not unexpected that the ironing does not posi-

tively influence the mechanical performance of the samples. However, the ironing does not negatively degrade the samples' mechanical properties notably as well. This suggests that, when applied with appropriate settings, ironing is relatively harmless to the overall mechanical performance, even in the inherently strong regions of a 3D print. This highlights the technique's flexibility and potential ease of use.

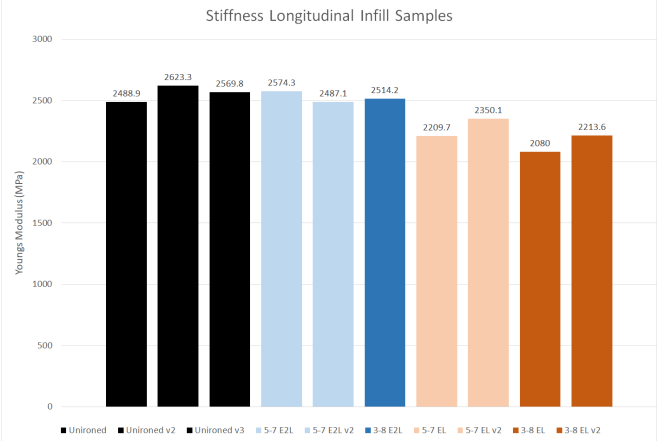

Figure 54: Stiffness of topology optimized samples with longitudinal infill.

Transversal Infill

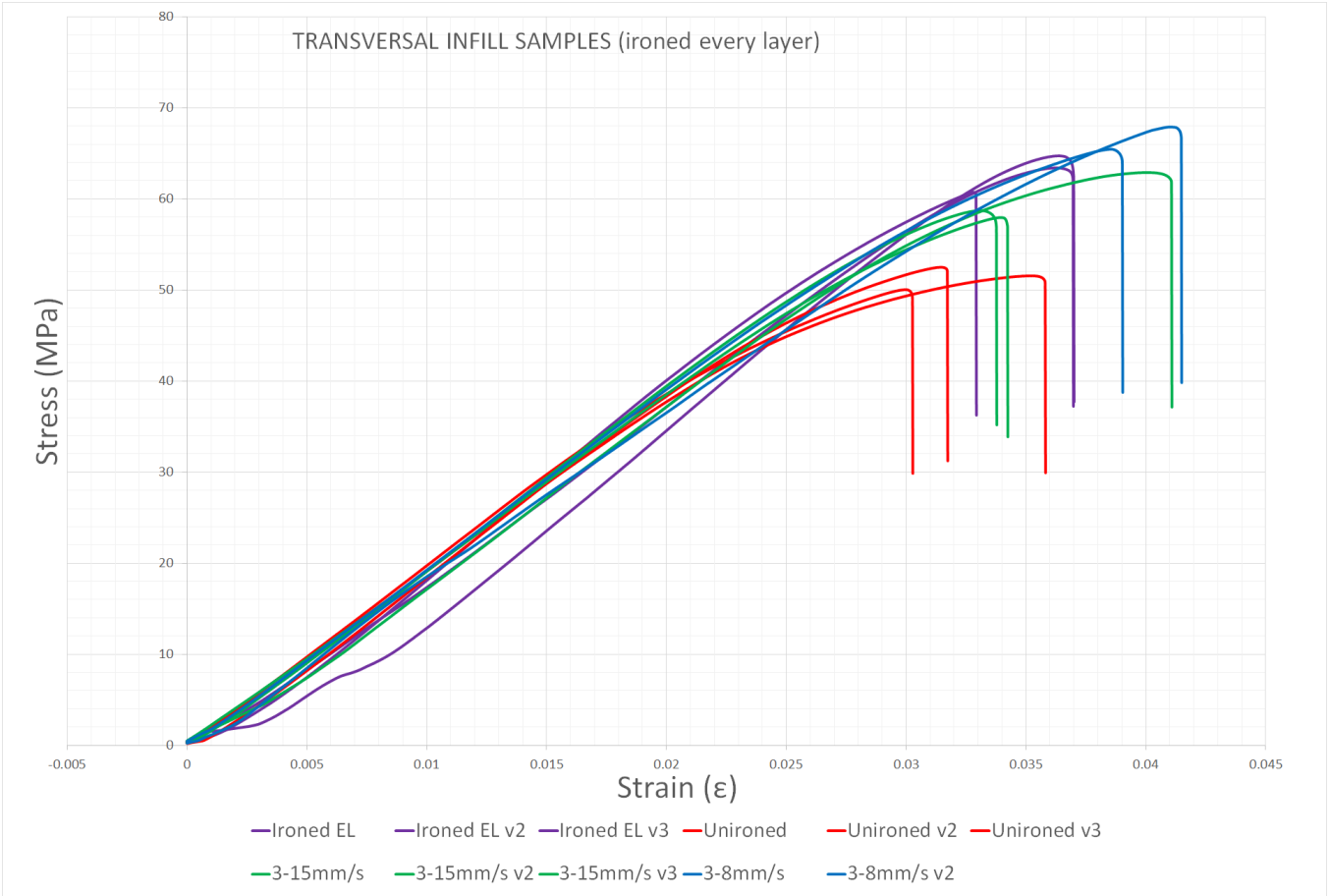

Figure 55: Stress/Strain graph of topology optimized ironing on transversal infill samples (Ironed every layer)

Strength

In contrast to the samples with longitudinal infill, topology optimized ironing is of significant influence on the mechanical properties of transversal infill samples (figure 55). All ironed samples showed an increase in material toughness compared to the un-ironed samples. The samples ironed with an iron speed domain of 3-15mm/s and 3-8mm/s demonstrated an average increase in ultimate flexural strength of 8,5MPa (16.5%) and 15,3MPa (29.8%), respectively. The latter even outperformed the samples that were ironed across the entire surface with a speed of 3mm/s, which showed an average increase of 11,6MPa (22.6%). This indicates that possibly, some form of material degradation occurred within those samples, due to the exposure of too much heat.

Stiffness

In terms of stiffness, almost all the curves follow the exact same linear trajectory within the elastic region (Figure 55). This indicates that topology optimized ironing hardly influenced the stiffness of the samples. One sample that was ironed every layer deviates from the other curves. This sample was slightly deformed due to excessive ironing, which caused the anvil of the 3-point bending machine to make contact with the sample a fraction later compared to the other samples. This sample however, does demonstrate a steeper curve within the elastic region, indicating increased material stiffness. It is possible that due to a potential process error, this specific sample may have received excess heat.

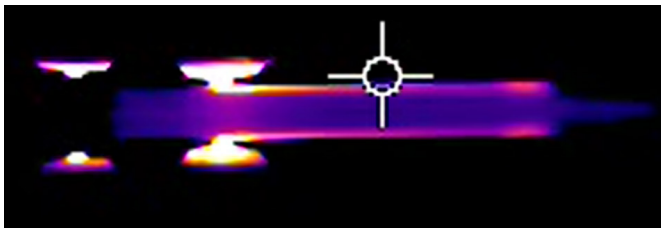

Figure 56: Sample ironed w/ speed domain 3-8mm/s

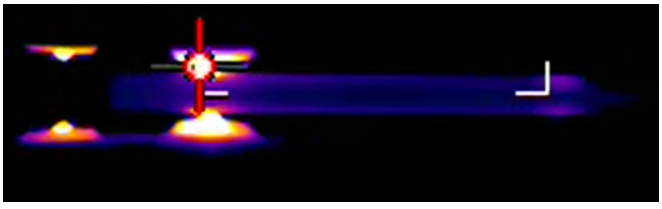

Figure 57: Sample ironed w/ speed domain 3-15mm/s

Thermal observations

When examining the two different iron speed domains with a thermal camera, it becomes apparent that the 3-8mm/s speed domain significantly transfers more heat compared to the 3-15mm/s speed domain (figure 56/57). As the thermal camera is set in such a way it does not show anything below 60°C (Glass transition temperature of PLA), only the parts were polymer chain rearrangement can take place are visible. With the 3-15mm/s sample, almost no heat is being transferred as the nozzle travels from right to left. This means that only the topology optimized structure within the sample is ironed thoroughly. When comparing the mechanical properties of the 3-15mm/s samples with the samples that are fully ironed, the 3-15mm/s samples only perform 6.1% less in terms of ultimate flexural strength. This indicates that selective ironing through topology optimization works to some extent. However, the samples with a 3-8mm/s iron speed domain outperformed the 3-15mm/s samples, indicating that it is not solely the topology optimized shape that contributes to the part's mechanical performance.

Print time efficiency

When comparing these percentages it becomes clear that topology optimized ironing is a valuable method to enhance material properties whilst preventing excessive print time (figure 58). With a significant shorter print time, 70 minutes compared to 173 minutes, the ultimate flexural strength of the topology optimized sample, ironed with speed domain 3-15, achieved an increase of 16.5% compared to 22.6% of the sample which was ironed across the entire surface. With the non-ironed samples only taking 25 minutes to print, this reduction of iron time is quite desirable. For this test the maximum travel speed was set at 15mm/s. This shortened the print time with 10 minutes compared to the samples ironed with an iron-speed domain of 3-8mm/s (70 minutes instead of 80). The script was made in such a way that the density values of the topology optimization were linearly mapped to the iron speed domain. Setting the travel speed, e.g. where the

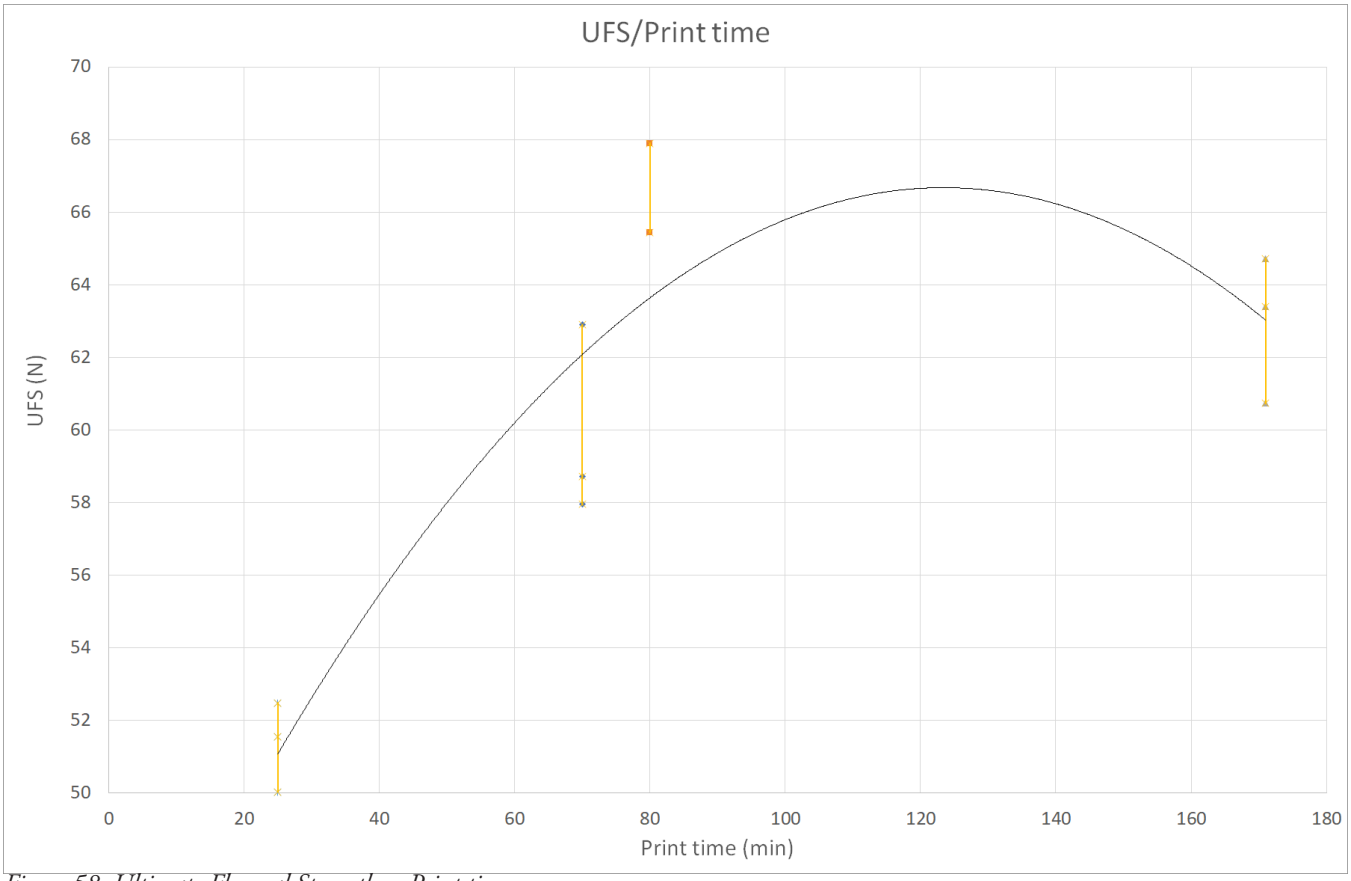

Figure 58: Ultimate Flexural Strength vs Print time curve

density values are zero, to an extremely large value would also significantly increase the iron speeds where slow ironing is desired. For further iteration the script should be modified to extract the null values and assign the iron speeds domain to the remainder of the density values, assigning a fixed travel speed to all null values. By doing so the travel speed can be increased without affecting the other iron speeds, significantly reducing additional print time.

Sample orientation

The ironing did not influence the stiffness of the samples. This is quite surprising when looking at the Z-direction 3-point bending results, as those samples showcased a large increase in material stiffness. Those samples differ in size and print orientation compared to these 3-point bending tests, the observed increase in material stiffness is therefore probably a combination of these factors with ironing. When comparing these results with the Iron Speed test performed on horizontally oriented dog bones, they both show insignificant improvement in the stiffness of the samples. It could indicate that the print and iron orientation is the determining factor that influences material stiffness and that vertically-oriented 3D prints that are 3-point bended perpendicular to their print direction only demonstrate this increase in stiffness. To strengthen this hypothesis the topology optimized sample should printed upright and tested.

Discussion

The un-ironed samples with the transversal infill samples differ from the un-ironed samples from the longitudinal infill samples. This is because the transversal infill samples were printed with different PLA on the Ultimaker s5 instead of the Ultimaker s7 which was used for the longitudinal infill. Originally, the transversal infill samples were also printed on the s7, but in an attempt to even out the sample sizes, the newly gathered data was completely different and incoherent (with respect to the earlier gathered data). So much so, that it was decided to completely re-run the test, to make sure no unintended parameters were of influence on the results. The original data can be found in Appendix 8.

Conclusion

This research has highlighted the potential of speed-modulated ironing for enhancing mechanical properties of 3D printed parts. With horizontally-oriented 3D prints, optimal ironing speeds, such as 3 mm/s, showed increased ductility and an increase in ultimate tensile stress of 12% for specimen with transversal infill, compared to un-ironed transversal specimens. Slower ironing speeds allowed more heat transfer, strengthening the material up to a point, but speeds as slow as 1 mm/s caused deformation and premature failure. Additionally, ironing slightly negatively influenced the mechanical properties of specimen with alternating -45°/45° infill, suggesting limited benefit in already strong configurations. These findings suggest that speed-modulated ironing for strengthening within the layer is best suited for enhancing weak infill configurations.

With 3-point bending tests performed on vertically-oriented 3D prints, significant enhancements in flexural strength, strain, and stiffness of 3D-printed PLA specimens were found. Ironing speeds of 5 mm/s and 3 mm/s increased peak flexural strength by 87.8% and 75.9%, respectively, compared to un-ironed samples. Similarly, Young's modulus increased by 45% and 37.7%, highlighting a significant improvement in material stiffness. Examining the cross section of the fractured specimen revealed improved material blending, with printed lines nearly or completely vanished. However, small pores were observed in the ironed samples, possibly indicating material degradation from excessive heat. Additionally, the outer geometries of the ironed samples were deformed significantly. This led to an additional experiment using ironing patterns with an offset (0.4 mm and 0.8 mm) which notably reduced the amount of deformation. With these samples similar mechanical improvements were found, confirming that the earlier observed mechanical improvements were not due to geometry distortion caused by ironing but rather improved material properties.

Through differential scanning calorimetry (DSC) it was found that ironing has a positive effect on the amount of crystallized regions within 3D prints. 3-point bending samples ironed with 3mm/s had a crystallinity percentage of 4,22%, which was 2,55% higher than un-ironed samples. As higher crystallinity percentages correspond with increased material properties like strength and stiffness, this test explains the increase in material properties on a material level, observed in this report.

The initial results of the mechanical tests of the 3D printed trombone mouthpiece were not in line with the expectations based on the results of the 3-point bending tests. With comparable ironing configurations as with the 3-point bending tests, e.g. offsets, speeds, etc., the mouthpieces performed similar or worse, compared to their un-ironed counterparts. Through close examination of the fractures, it was concluded that insufficient heat was applied, as the fractured surface of the ironed sample did not show any signs of improved layer blending. The cause of this was the surface area of the mouthpiece being larger. Due to the nozzle travelling further, it took longer to iron adjacent lines which probably led to insufficient heat exposure and limited the potential benefit of ironing in this context. Another ironing path was added, resulting in more heat being transferred to the layers, which improved the flexural strength with 16.5%. This test highlighted not only the importance of considering the size of the surface area which has to be ironed, but also the effect of transferred heat of adjacent ironing lines.

Using topology optimization to determine where ironing is of most structural benefit proved an effective technique to achieve mechanical improvement whilst restraining additional print time. The topology-optimized ironed samples demonstrated significant improvements compared to the un-ironed samples, achieving ultimate flexural strength and strain values nearly comparable to samples ironed across the entire surface with transversal infill (16.5% compared to 22.6% for

UFS), while reducing print time from 172 minutes to 70 minutes. The stiffness values of the samples remained unchanged, suggesting that the observed stiffness improvements in the 3-point bending tests on vertically-oriented 3D prints probably depended on print orientation and load direction. Overall, this test highlighted the efficiency and effectiveness of topology-optimized ironing in balancing print time and mechanical performance.

Overall, speed-modulated ironing proved to be an effective, easy-to-use method for enhancing 3D prints' mechanical properties without any modifications to the material or printer. Ironing significantly strengthened prints within-layer for sub-optimal infill configurations and increased interlayer strength for all configurations. By using clever topology optimization algorithms in combination with the flexibility of an ironing nozzle that can be velocity-controlled, strengthening can be done selectively, significantly reducing additional print time. With valuable insights gathered on the effect of ironing speeds and ironing offsets, a designer could safely use the designed grasshopper script to generate ironing G-code that does not reduce the visual quality of a print. This makes speed-modulated ironing a valuable option for mechanically enhancing various prints for everyone that owns a dual-nozzle 3D printer and has access to Rhino/Grasshopper.

References

Agaliotis, E. M., Ake-Concha, B. D., May-Pat, A. (2022). Tensile Behavior of 3D Printed Polylactic Acid (PLA) Based Composites Reinforced with Natural Fiber. Polymers, 14(19), 3976. https://doi.org/10.3390/polym14193976

Alzyod, H., Takacs, J., & Ficzere, P. (2023). Improving surface smoothness in FDM parts through ironing post-processing. Journal Of Reinforced Plastics And Composites, 43(11–12), 671–681. https://doi.org/10.1177/07316844231173059

Alzyod, H., & Ficzere, P. (2024). Ironing process optimization for enhanced properties in material extrusion technology using Box–Behnken Design. Scientific Reports, 14(1). https://doi.org/10.1038/s41598-024-52827-5

Butt, J., Bhaskar, R., & Mohaghegh, V. (2022). Investigating the Effects of Ironing Parameters on the Dimensional Accuracy, Surface Roughness, and Hardness of FFF-Printed Thermoplastics. Journal Of Composites Science, 6(5), 121. https://doi.org/10.3390/jcs6050121

Cano-Vicent, A., Tambuwala, M. M., Hassan, S. S., Barh, D., Aljabali, A. A., Birkett, M., Arjunan, A., & Serrano-Aroca, Á. (2021). Fused deposition modelling: Current status, methodology, applications and future prospects. Additive Manufacturing, 47, 102378. https://doi.org/10.1016/j.addma.2021.102378

Coogan, T. J., & Kazmer, D. O. (2017). Bond and part strength in fused deposition modeling. Rapid Prototyping Journal, 23(2), 414–422. https://doi.org/10.1108/rpj-03-2016-0050

Coppola, B., Cappetti, N., Di Maio, L., Scarfato, P., & Incarnato, L. (2018). 3D Printing of PLA/clay Nanocomposites: Influence of Printing Temperature on Printed Samples Properties. Materials, 11(10), 1947. https://doi.org/10.3390/ma11101947

Floor, J., Van Deursen, B., & Tempelman, E. (2018). Tensile strength of 3D printed materials: Review and reassessment of test parameters. Materials Testing, 60(7–8), 679–686. https://doi.org/10.3139/120.111203

Freire, E. (2003). Differential scanning calorimetry. Humana Press eBooks, 191–218. https://doi.org/10.1385/0-89603-301-5:191

Grasso, M., Azzouz, L., Ruiz-Hincapie, P., Zarrelli, M., & Ren, G. (2018). Effect of temperature on the mechanical properties of 3D-printed PLA tensile specimens. Rapid Prototyping Journal, 24(8), 1337–1346. https://doi.org/10.1108/rpj-04-2017-0055

Guessasma, S., Belhabib, S., & Nouri, H. (2019). Thermal cycling, microstructure and tensile performance of PLA-PHA polymer printed using fused deposition modelling technique. Rapid Prototyping Journal, 26(1), 122–133. https://doi.org/10.1108/rpj-06-2019-0151

Kishore, V.; Ajinjeru, C.; Nycz, A.; Post, B.; Lindahl, J.; Kunc, V.; Duty, C. Infrared preheating to improve interlayer strength of big area additive manufacturing (BAAM) components. Addit. Manuf. 2017, 14, 7–12.

Luo, M.; Tian, X.; Zhu, W.; Li, D. Controllable interlayer shear strength and crystallinity of PEEK components by laser-assisted material extrusion. J. Mater. Res. 2018, 33, 1632.

Masania, K. (2022). Lecture 2: Fused-Filament Presentation. AE4ASM521: Additive Manufacturing

Montalti, A., Galiè, G., Pignatelli, E., & Liverani, A. (2024). Enhancing surface roughness of material extrusion additive manufacturing components via an innovative ironing process. Virtual And Physical Prototyping, 19(1). https://doi.org/10.1080/17452759.2024.2401929

Neuhaus, B., Idris, M. K., Naderi, P., El-Hajj, Y., & Grau, G. (2024). Low-Roughness 3D Printed Surfaces by Ironing for the Integration with Printed Electronics. Advanced Engineering Materials. https://doi.org/10.1002/adem.202301711

Ning, F., Cong, W., Hu, Y., & Wang, H. (2016). Additive manufacturing of carbon fiber-reinforced plastic composites using fused deposition modeling: Effects of process parameters on tensile properties. Journal Of Composite Materials, 51(4), 451–462. https://doi.org/10.1177/0021998316646169

Ravi, A.K.; Deshpande, A.; Hsu, K.H. An in-process laser localized pre-deposition heating approach to inter-layer bond strengthening in extrusion based polymer additive manufacturing. J. Manuf. Process. 2016, 24, 179–185.

Ozdemir, M., & Doubrovski, Z. (2023). Xpandables: Single-filament Multi-property 3D Printing by Programmable Foaming. TU Delft. https://doi.org/10.1145/3544549.3585731

Pawar, A., Ausias, G., Corre, Y., Grohens, Y., & Férec, J. (2022). Mastering the density of 3D printed thermoplastic elastomer foam structures with controlled temperature. Additive Manufacturing, 58, 103066. https://doi.org/10.1016/j.addma.2022.103066

Pernica, J., Sustr, M., Dostal, P., Brabec, M., & Dobrocky, D. (2021a). Tensile Testing of 3D Printed Materials Made by Different Temperature. MANUFACTURING TECHNOLOGY, 21(3), 398–404. https://doi.org/10.21062/mft.2021.039

Sabyrov, N.; Abilgaziyev, A.; Ali, M.H. Enhancing interlayer bonding strength of FDM 3D printing technology by diode laser-assisted system. Int. J. Adv. Manuf. Technol. 2020, 108, 603–611.

Sardinha, M., Vicente, C. M., Frutuoso, N., Leite, M., Ribeiro, R., & Reis, L. (2020). Effect of the ironing process on ABS parts produced by FDM. Material Design & Processing Communications, 3(2). https://doi.org/10.1002/mdp2.151

Sun, Y., Tian, W., Zhang, T., Chen, P., & Li, M. (2020). Strength and toughness enhancement in 3d printing via bioinspired tool path. Materials & Design, 185, 108239. https://doi.org/10.1016/j.matdes.2019.108239

Syrlybayev, D., Zharylkassyn, B., Seisekulova, A., Akhmetov, M., Perveen, A., & Talamona, D. (2021). Optimisation of Strength Properties of FDM Printed Parts—A Critical Review. Polymers, 13(10), 1587. https://doi.org/10.3390/polym13101587

Takagishi, K., & Umezu, S. (2017). Development of the Improving Process for the 3D Printed Structure. Scientific Reports, 7(1). https://doi.org/10.1038/srep39852

Thumsorn, S., Prasong, W., Kurose, T., Ishigami, A., Kobayashi, Y., & Ito, H. (2022). Rheological Behavior and Dynamic Mechanical Properties for Interpretation of Layer Adhesion in FDM 3D Printing. Polymers, 14(13), 2721. https://doi.org/10.3390/polym14132721

Torrado, A. R., & Roberson, D. A. (2016b). Failure Analysis and Anisotropy Evaluation of 3D-Printed Tensile Test Specimens of Different Geometries and Print Raster Patterns. Journal Of Failure Analysis And Prevention, 16(1), 154–164. https://doi.org/10.1007/s11668-016-0067-4

Torres, J., Cole, M., Owji, A., DeMastry, Z., & Gordon, A. P. (In Press). An
Approach for Mechanical Property Optimization of Fused Deposition
Modeling with Polylactic Acid via Design of Experiments. Rapid
Prototyping Journal.

Tymrak, B. M., Kreiger, M., & Pearce, J. M. (2014). Mechanical properties of components fabricated with open-source 3-D printers under realistic environmental conditions. Materials and Design, 58, 242–246. http://doi.org/10.1016/j.matdes.2014.02.038

Yao, J., Duongthipthewa, A., Xu, X., Liu, M., Xiong, Y., & Zhou, L. (2024). Interlayer bonding improvement of PEEK and CF-PEEK composites with laser-assisted fused deposition modeling. Composites Communications, 45, 101819. https://doi.org/10.1016/j.coco.2024.101819

Appendices

Appendices

Appendix 1

Strengthening test

After initial experimentation with speed-modulated ironing the question raised whether the technique could positively influence the mechanical strength of a 3D print. A test was developed to get a quick feel for the possibilities of ironing with regards to strengthening a print. This test involved a tensile test to failure with multiple 3D printed dog bones, some of which were mechanically modified by ironing. This modification was done by an ironing nozzle that made strands perpendicular to the print direction on several layers of the print. These strands were made by 'dragging' the heated ironing nozzle through the freshly printed layer. Almost like plowing a field. Several samples were made this way. One batch of samples that were ironed every 2 layers and one batch that were ironed every 3 layers. These were coded the following way 'Enforced (E2L-6L) and (E3L-6L). 6L stands for the number of ironed lines. The tensile test was performed with a 500N loaded tensile test machine and a pulling speed of 5mm/s.

Results

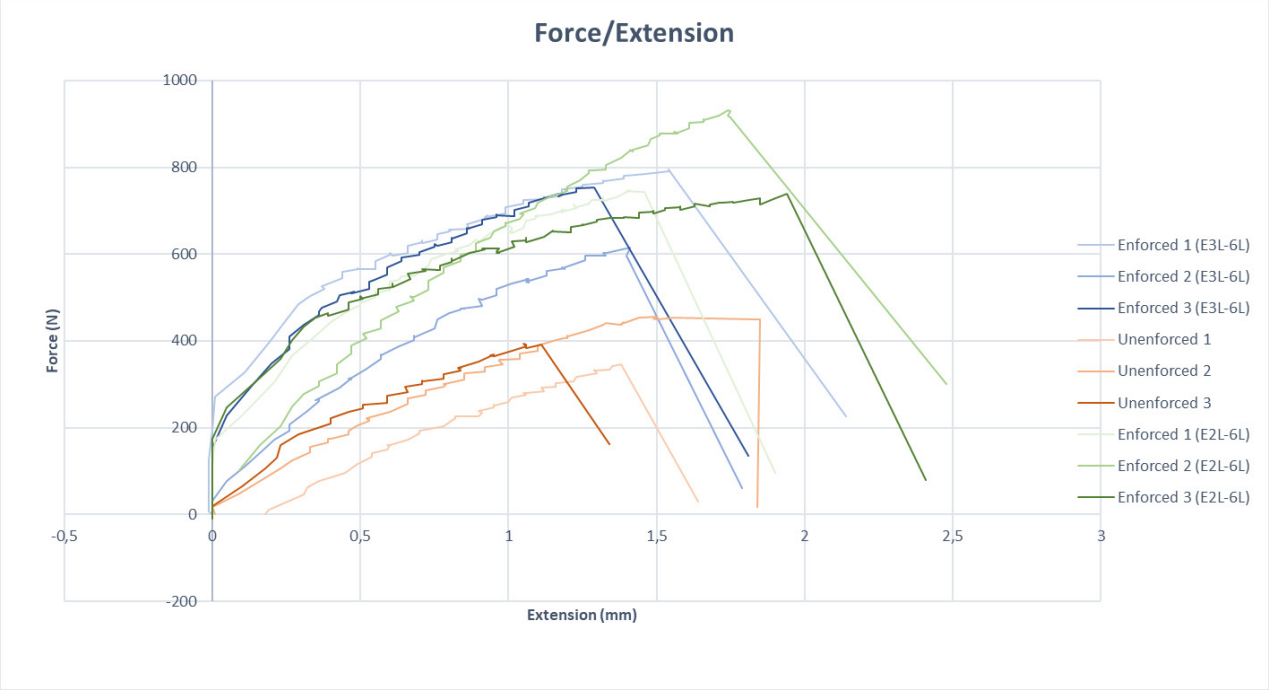

As can be seen from this graph the initial results looked very promising. Both the blue and green lines were dog bones that were enforced with ironing. The maximum load that these samples could withstand was significantly higher than the unenforced samples. In the most extreme samples, the enforced sample could withstand even three times the amount of force compared to the weakest sample. For the amount of extension, no significant benefit can be deducted from these results. Upon initial inspection it looks like the elasticity of the 3D prints remains unchanged. This can also be seen on the tested samples. All the samples, both enforced and unenforced, show a clean break line. Meaning that the materials brittleness has not noticeably changed.

Discussion

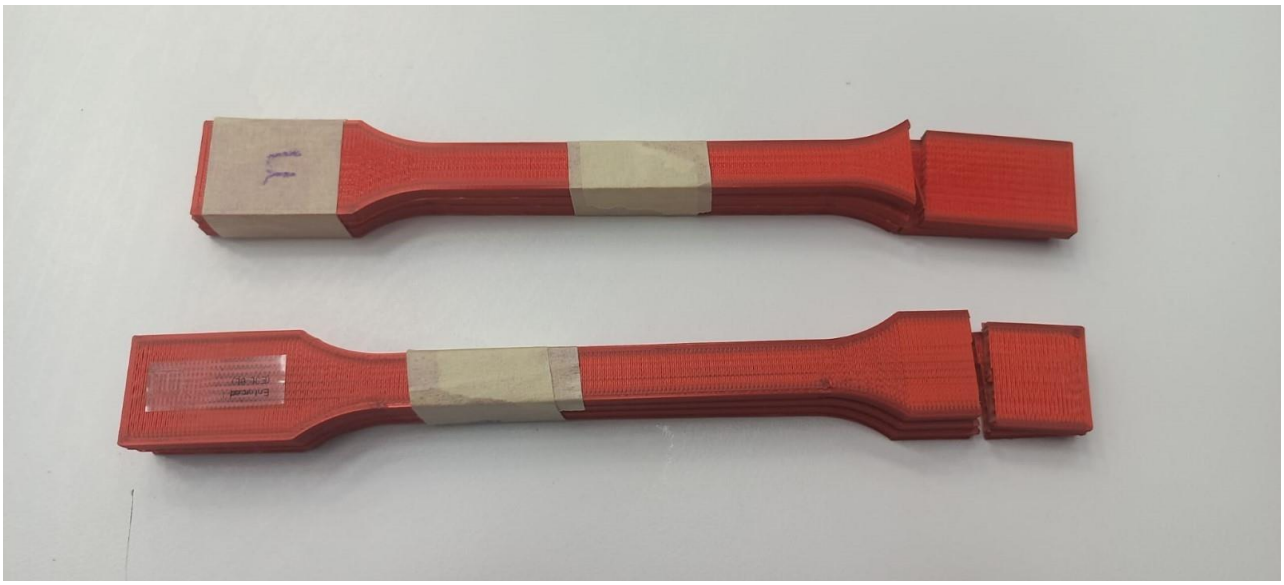

One interesting find is that all enforced samples broke in the same place and all unenforced samples broke in the same place. All the unenforced samples broke exactly where the dog bone's thickest part starts to become slimmer. Since this is the place where the outer edge makes the sharpest corner, it could be argued that this is the weakest part of the dog bone, especially since the part is printed in parallel with the tensile bench clamps. However, the enforced samples all broke were the dog bone makes contact with the tensile bench clamps. It could be that by tightening the clamps the print becomes weaker at that point. This would mean that the results of the test could be heavily influenced by the amount of force with which the clamps are tightened. Since the unenforced samples did not break at this same spot, it could be argued that the strengthening effect of ironing could be even greater than showcased in this graph. For future tests, the place where the dog bone is clamped should be enforced to make sure the clamping has no effect on the sample.

Appendix 2

The standard dog bone

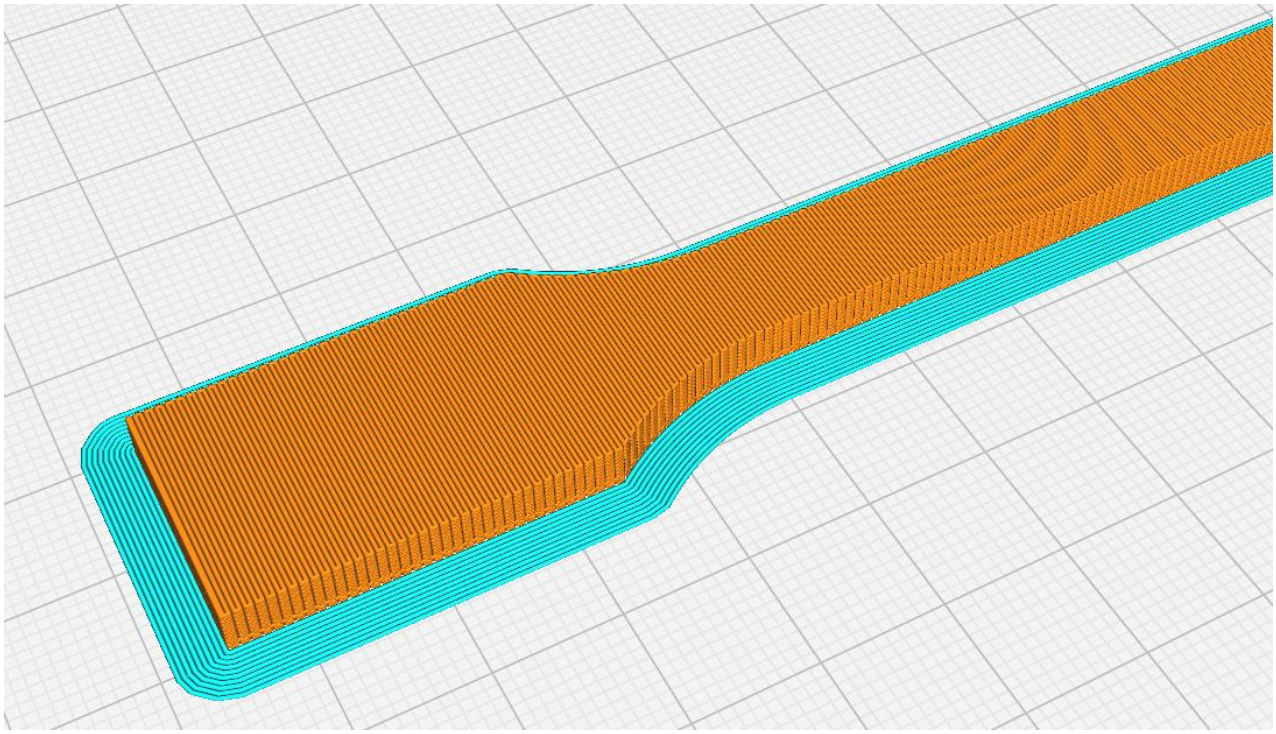

This dog bone was designed to validate whether ironing could mechanically enhance 3D prints. The bone is printed in such a way that its lines are perpendicular to the pulling direction. This is the weakest direction for this specific test. By making the bone in such a way we hope to see clear improvement due to ironing, which is done perpendicular to the print direction. The first ironed samples showed signs of under extrusion near the thicker ends of the dog bone. To solve this issue the infill flow was heightened from 95% to 105%. Although this solved the issue, we later discovered that the under extrusion was probably due to the print nozzle wait temperature being too low. Because of this, every layer that followed an ironing layer started with under extrusion due to the material being too cold. For the last batch of prints (regular PLA) the print temperature wait temperature was heightened from 175 to 190 degrees.

Appendix 3

In order to experiment with multiple iron settings and layouts a Grasshopper script was made that could generate G-CODE based on a certain pattern of points. As previously mentioned, the foundation of this script was made by Anonymous et al. The script starts with a G-CODE file as an input. From this G-CODE, a C# script can extract the points from either the OUTER-WALLS, SKIN or INFILL layers. Since the dog bone for the tensile tests consisted solely out of infill the script was set to extract the infill points.

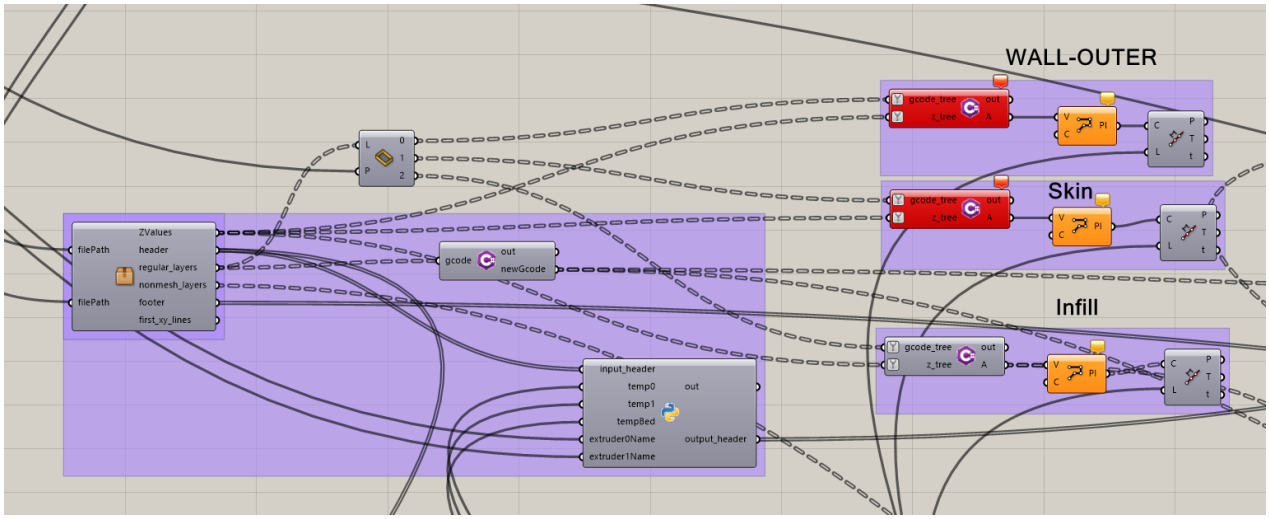

From these points the outer most points on the first layer (Z=0.02) are extracted to create a domain for the ironing lines. Between these points lines are created that can be divided with the divide curve component. The resulted points can then be weaved with a 1001 pattern to create the following shape.

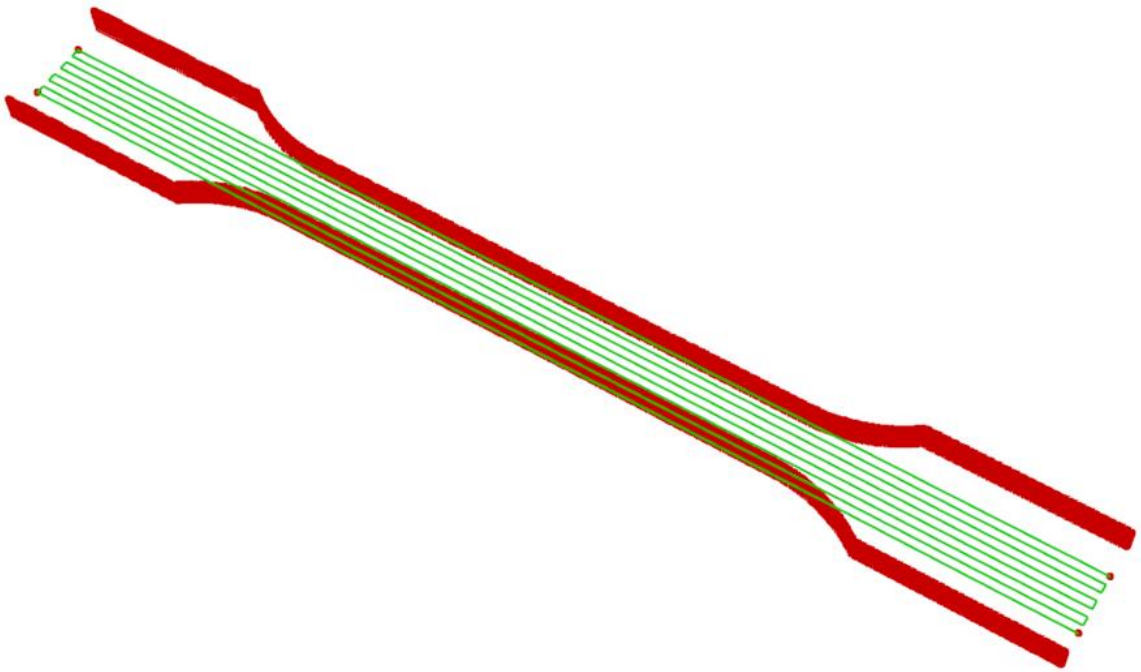

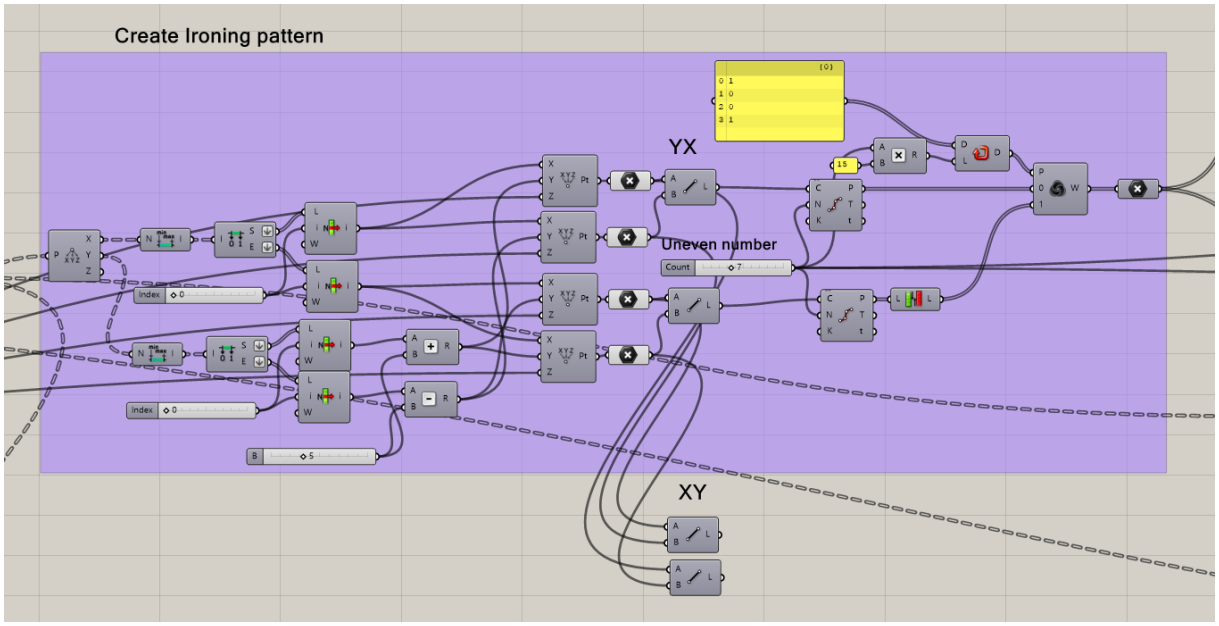

By using the Linear Array component this base shape could be duplicated with a Z-offset of 0.2mm or a multiplication of 0.2mm. This is done to make sure the iron lines are placed on top of each printed layer with a layer thickness of 0.2mm.

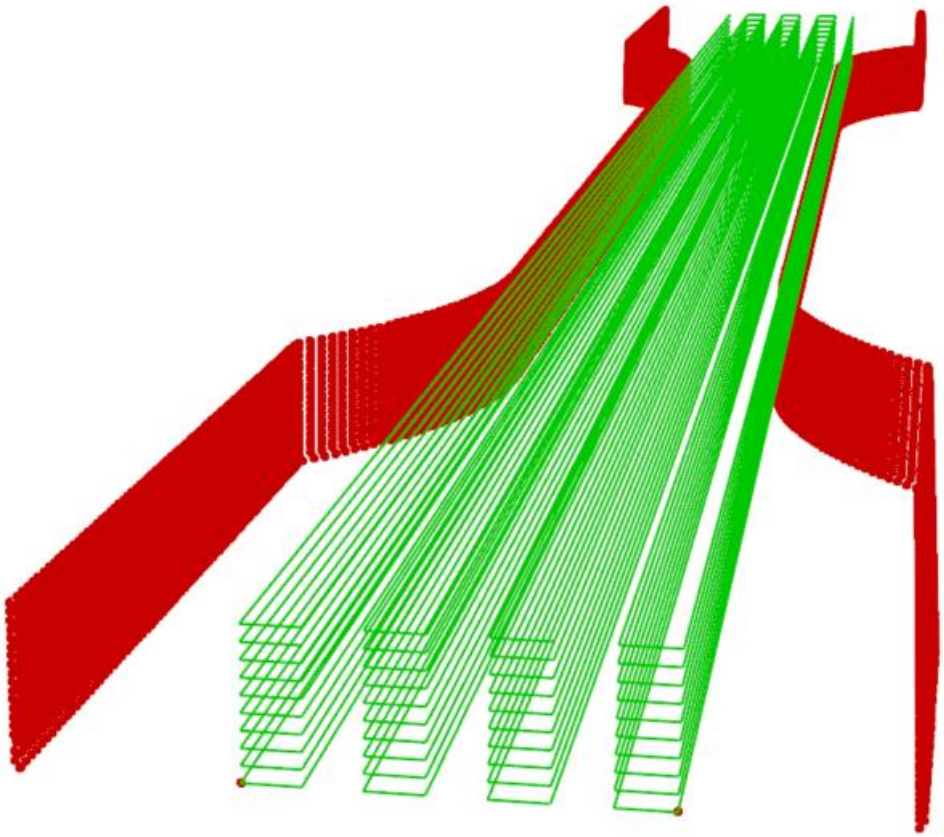

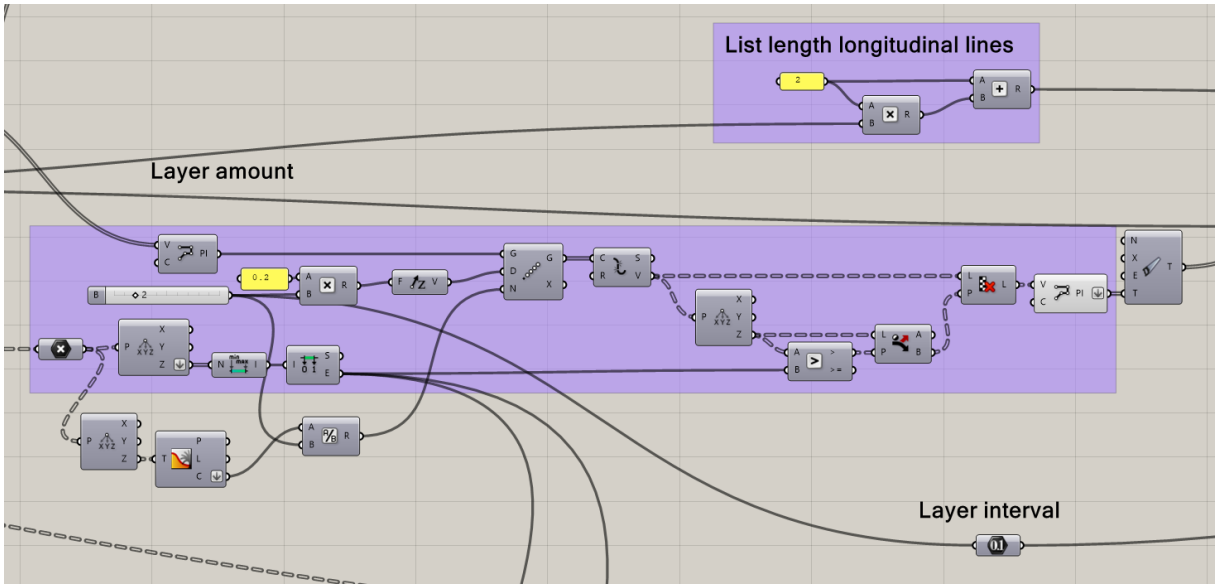

After having generated the ironing lines and their respective list of points, their layer information had to be matched with the original G-CODE. This meant that the branches of the iron points list had to be mapped on the branch structure of the input G-CODE. By doing so ensuring that the Iron nozzle would Iron the 3D print at the correct height and time.

With the correct points, in the correct order and with the same branch structure of the input G-CODE the points can now be transformed into G-CODE.

Appendix 4

To check whether the results of the tensile tests are believable and in the same ball park as previous conducted research several papers have been investigated. Although exact settings often vary in these papers, it does give an indication whether the results are in line with previous research and whether the results are significant. The range of peak stresses in previous conducted research goes from 25MPa until 55MPa.

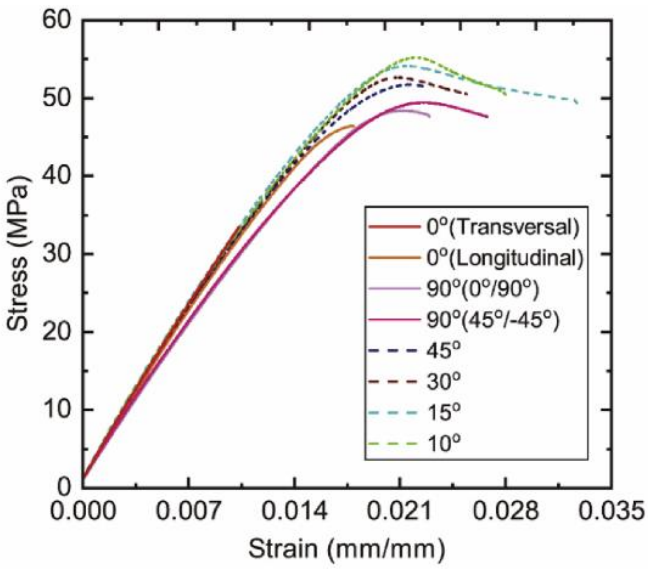

Fig. 3. Stress-strain curve of tensile tests.

A layer thickness tlayer ¼ 0:1mm is chosen, the printing speed is 30 mm/s constantly during the whole printing process. The temperature of nozzle and heat bed are set to 200 C and 60 C, respectively (Sun et al., 2019). Regular PLA was used in various infill orientations.

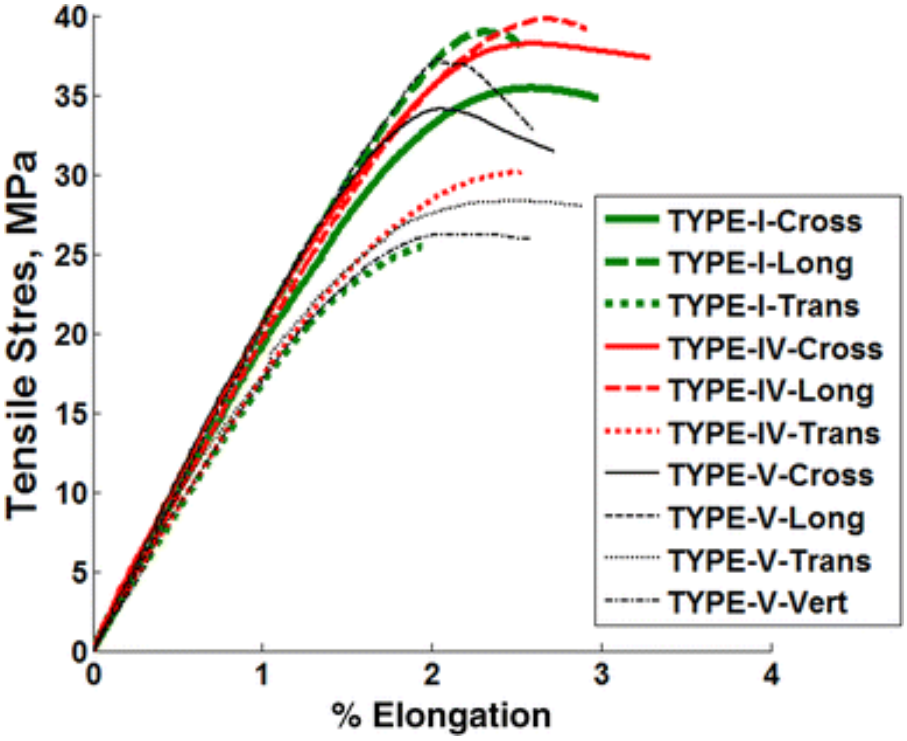

For this research ABS was used with varying infill orientations (Torrado & Roberson, 2016c).

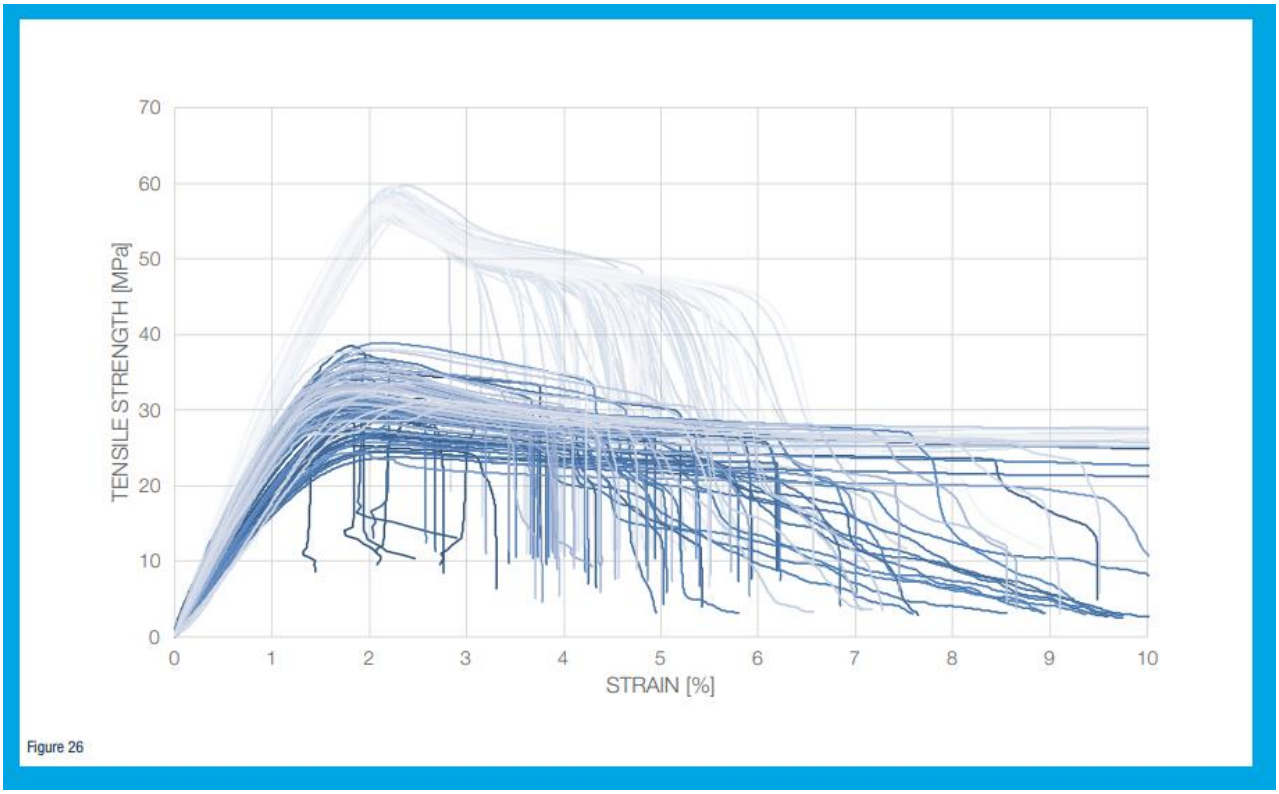

Figure 26

Regular PLA was used with 100% infill, alternating every layer at 90 degrees, with a 45/-45 degree angle relative to the pulling direction. In this graph the dark blue (highlighted) lines are the 3D printed PLA samples, ignore the semi translucent lines (Floor, 2018). Other settings like print temperature, layer height, print speed, fill density vary.

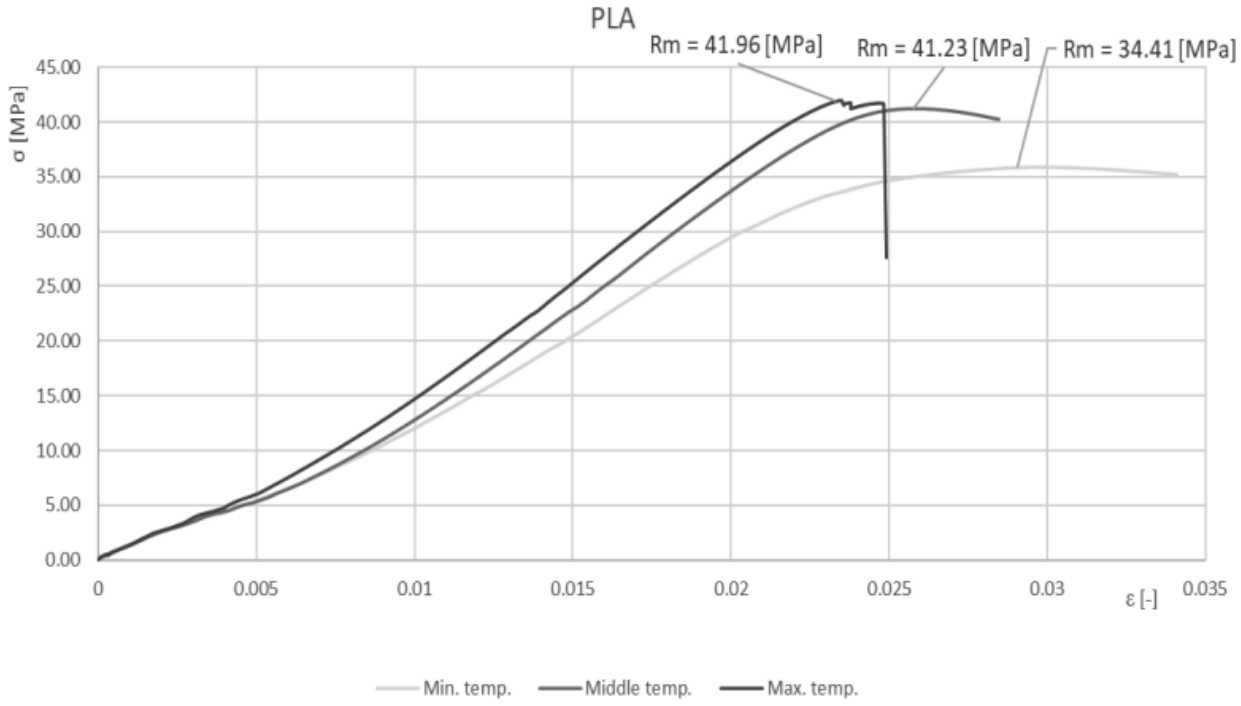

(Pernica et al., 2021a) Regular PLA was used with 100% infill in longitudinal direction. 3 different print temperatures were tested: 190°C ± 5°C, 210°C ± 5°C and 230°C ± 5°C. The Nozzle diameter was 0.4 mm and layer height 0.2 mm.

Appendix 5

Regular PLA V1 (Iron speed 7mm/s)

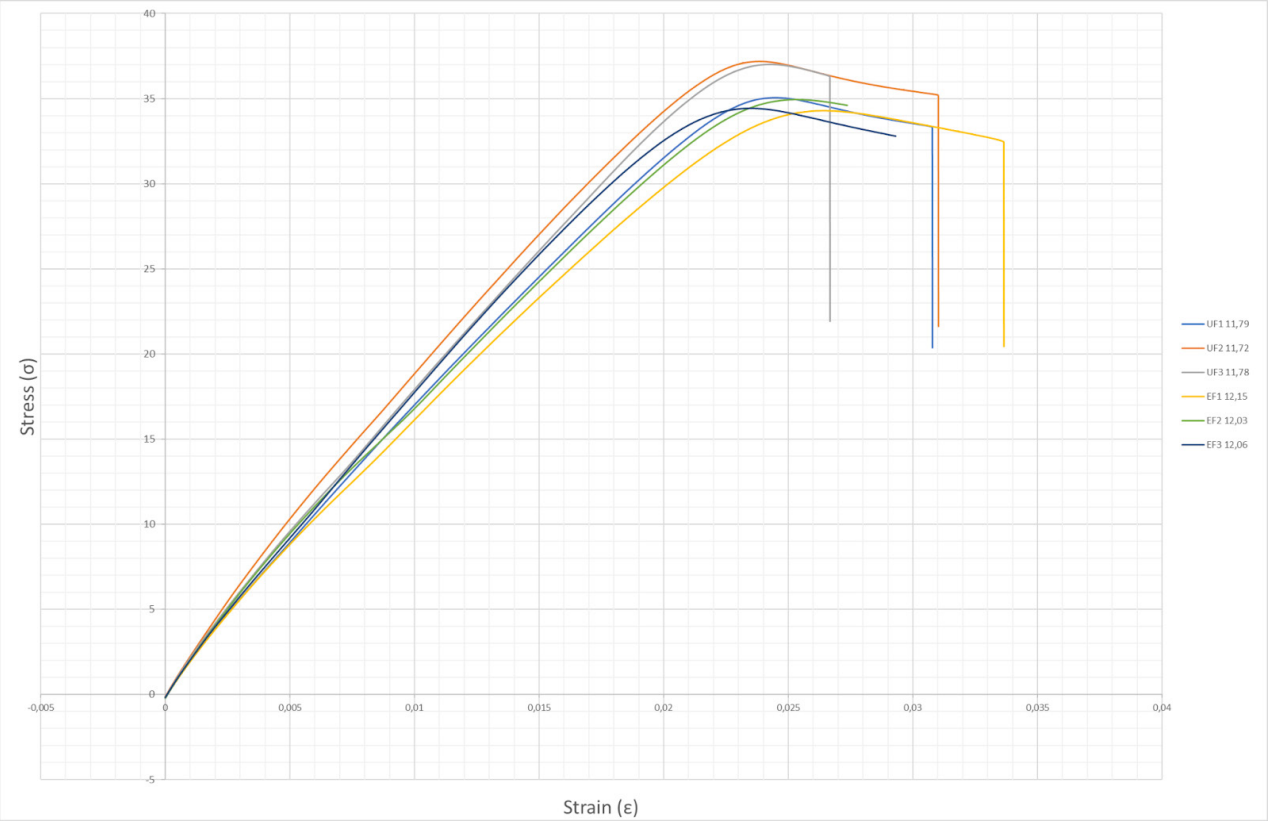

	Maximum	Test speed	Pre-load	Specimen	h	b	A_0	Peak detec	Date/Cloc	$L_{0\,CH}$
	mm	mm/min	N		mm	mm	mm^2	N		mm
UF1 11,79	3	1	0.1	1	4.2	10.6	44.52	1560.774	45541.46	118.1805
UF2 11,72	3	1	0.1	2	4	10.7	42.8	1591.605	45541.46	118.1079
UF3 11,78	3	1	0.1	3	4	10.55	42.2	1561.706	45541.47	118.1483
EF1 12,15	3	1	0.1	4	4.3	11	47.3	1621.792	45541.47	118.2261
EF2 12,03	3	1	0.1	5	4.3	10.7	46.01	1608.297	45541.48	118.2035
EF3 12,06	3	1	0.1	6	4.2	10.9	45.78	1576.156	45541.48	118.2085

With regular PLA no real significant difference between the curves can be observed. There is however, quite a significant difference between the weights of the samples. The enforced samples all weigh quite a bit more than the unenforced ones. This is probably due to the higher wait temperature of the print nozzle whilst the ironing takes place. Because of this, filament leaks out of the print nozzle which results in more filament being extruded whilst starting a new layer. With a unenforced sample, the print nozzle never has to wait, which makes the print flow more consistent.

Another difference between the samples was their intersection area, which turned out higher for the ironed samples. This is probably due a calibration error between the printing nozzle and ironing nozzle. The ironing nozzle ironed too close to the samples' edge, which caused this edge to be rougher. Because of this the caliper measured a larger width and height for the ironed samples.

Regular PLA V2 (Varying iron speeds)

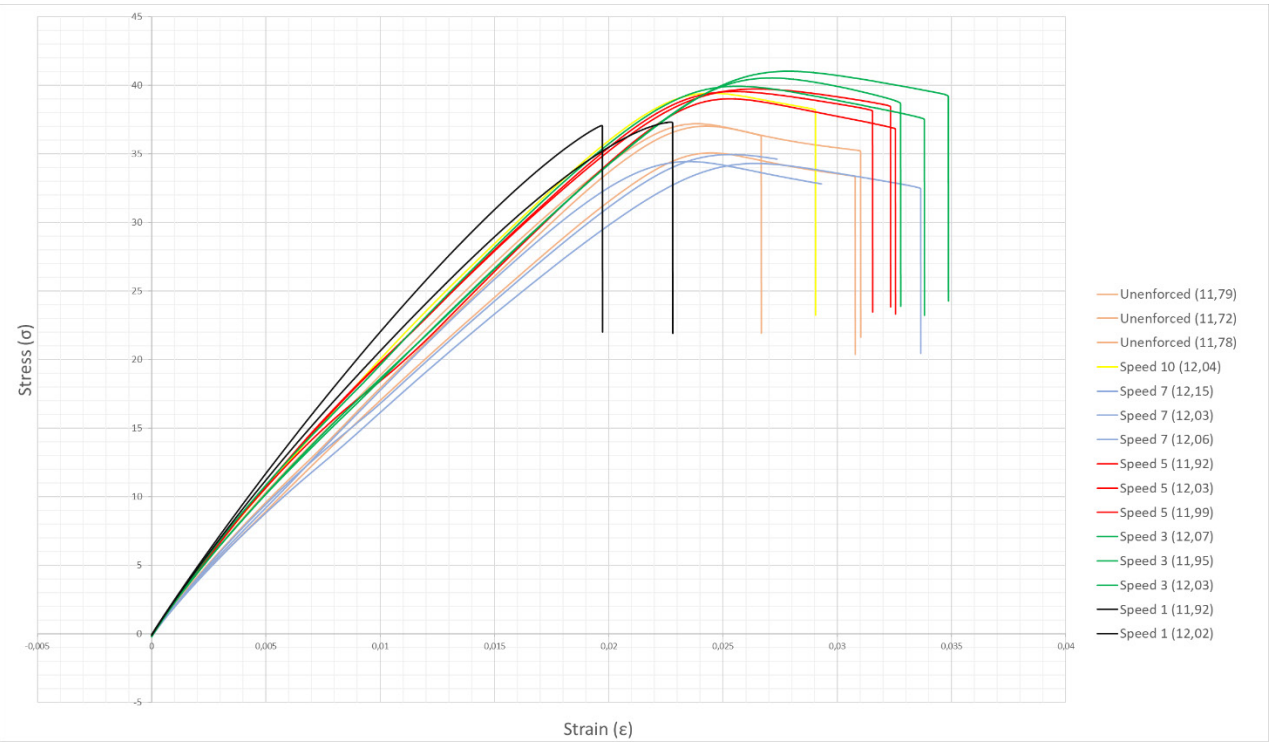

GRAPH shows the effect of ironing speeds on the mechanical properties of a 3D print. The samples with the orange/brown curve are not ironed and the other samples are all ironed with the same configuration: E2L-8L. However, their iron speeds vary. The blue samples were ironed with a speed of 7mm/s. These are the same samples as in Regular PLA V1. The other curves are all ironed with different speeds, ranging from 10mm/s to 1mm/s.

An interesting finding was that all ironed samples showed an improved peak stress except for the iron speed of 7mm/s. The 3mm/s iron speed samples showed an increase in peak stress of around 12% compared to the non-ironed samples. This would seem logical as slower iron speeds transfer more heat to the material, causing it to blend better together. However, the sample with an iron speed of 10mm/s would then be illogical. Since this samples was only tested ones, it could be an outlier. To exclude this further research needs to be done. It could also be the case that this speed influenced other mechanical properties than layer adhesion, for instance string orientation. By ironing more quickly it could have created strings in the longitudinal direction without modifying the initial layer adhesion too much. With 7mm/s, it could be the case that it worsened initial layer adhesion without improving it by re-heating the material.

Another interesting finding is that the 1mm/s curve shows ironing made the material more brittle compared to un-ironed samples. This can be seen by a steeper curve in the plastic region. However, the samples broke before they could plastically deform, hinting that the slow iron speeds might have worsened the layer adhesion, rather than improving it.

Varying iron speeds 10mm/s to 1mm/s

Appendix 6

Settings used for the tensile tests.

LW-PLA (printer2)

TempPrintNozzle=200

TempIroningNozzle=300

BedTemperature=60

WaitTempPrintNozzle=190

SamplingLength=1

LowSpeed=1

HighSpeed=60

XOffset=-18

ZOffset=0

RetractionLength=15

RetractionSpeed=1500

HeatingTime=5

Setting	Profile	Current	Unit
Layer Height	0.2		mm
Initial Layer Height	0.2		mm
Enable Travel Accelera...	True		
Enable Travel Jerk	True		
Generate Support	False	False	

Setting	Profile	Current	Unit
Wall Line Count	0		
Wall Ordering	inside_out		
Top Surface Skin Layers	0		
Top Surface Skin Line ...	[270]		
Top/Bottom Thickness	0		mm
Top Layers	0		
Bottom Layers	0		
Top/Bottom Line Direc...	[270]		
Infill Density	100		%
Infill Pattern	lines		
Infill Line Directions	[180]	[90]	
Infill Flow	105		%
Travel Jerk	50.0		mm/s
Support Density	25		%
Support Z Distance	0.25		mm
Brim Line Count	10		
Brim Distance	0		mm

Appendix 7

Silk PLA (Z-offset)

This batch of samples was made to research the effect of a lower z-offset for the ironing nozzle on the mechanical behaviour of a 3D print. The 'default' ironing speed that was used during the initial quick and dirty test (APPENDIX 1) was 10mm/s. With a z-offset of 0.0, which is the default value for the offset, the ironing nozzle barely scraped the surface of the print. With a speed of 10mm/s, which is quite fast, the ironing nozzle did not really have a noticeable effect on the print. To make the ironing effect more prominent the Z-offset was lowered to -0.05mm, which is a quarter of the layer height. By lowering the Z-offset, the ironing nozzle goes deeper through the printed layer resulting in deeper slits within the samples. By doing so strings of filament are created on the sides of these slits. Intuitively it could be hypothesized that this would strengthen the sample, as the strings would be oriented in the longitudinal direction of the pulling direction.

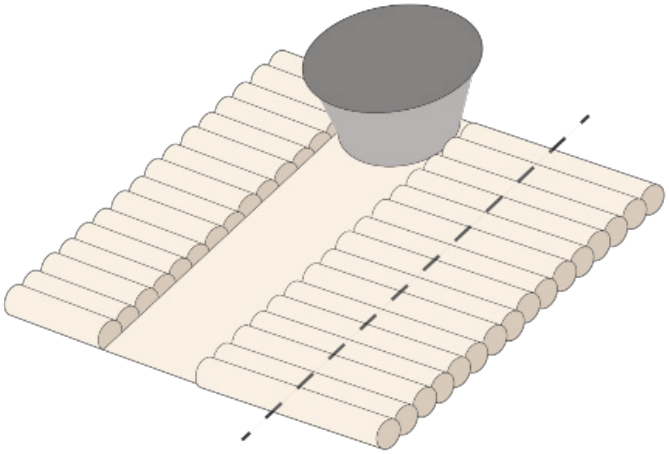

Silk PLA

- 3x unenforced
- 2x E3L-6L
- 1x E2L-6L
- 1x E3L-8L

Figure X: Silk PLA dog bone being ironed with a offset of -0.05mm

Silk PLA results

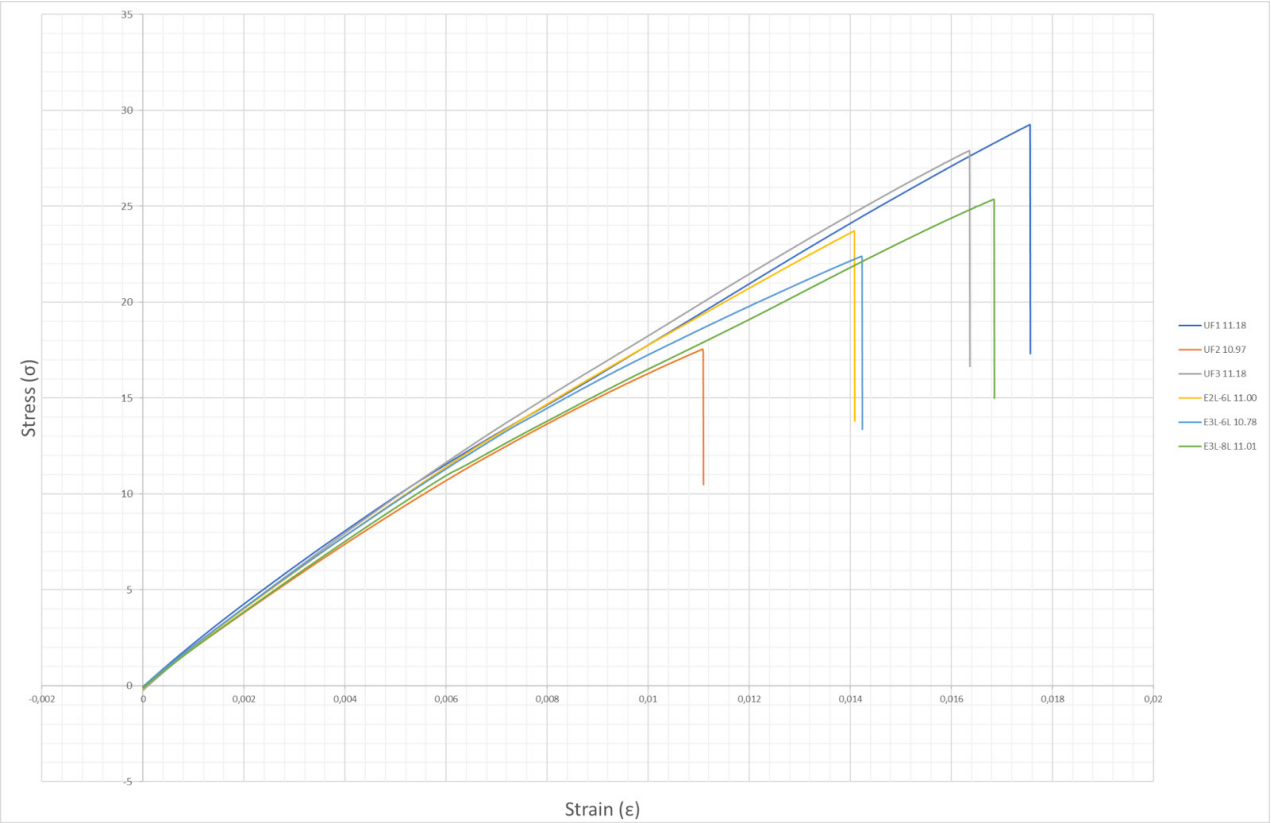

Figure X: Stress strain curve Silk PLA: Unenforced (UF1t/m3) compared to Enforced

	Maximum	Test speed	Pre-load	Specimen	h	b	A_0	Peak detec	Date/Cloc	$L_{0\,CH}$
	mm	mm/min	N		mm	mm	mm^2	N		mm
UF1 11.18	3	1	0.1	1	3.96	10.25	40.59	1187.744	45538.43	118.0908
UF2 10.97	3	1	0.1	2	4.075	10.1	41.1575	722.377	45538.43	118.1899
UF3 11.18	3	1	0.1	3	4.05	10.3	41.715	1163.991	45538.44	118.2077
E2L-6L 11.00	3	1	0.1	4	3.94	10.23	40.3062	955.7045	45538.45	118.1444
E3L-6L 10.78	3	1	0.1	5	3.95	10.23	40.4085	904.8602	45538.46	118.2097
E3L-8L 11.01	3	1	0.1	6	4.07	10.15	41.3105	1047.745	45538.46	118.1337

With this material all samples broke abruptly without showing any plastic deformation. This could be the result due to poor layer adhesion between the printed lines. The samples all showed a clean break line. Under extrusion could be the cause for this poor layer adhesion. Another factor that could have caused this poor layer adhesion are the additives that gives this PLA it's Silk appearance. Thumsorn et al. (2022) experienced worsened layer adhesion due to the PLA containing additives. The sudden breakage of the samples makes the results of this test quite unreliable. Looking at the results no clear conclusion can be drawn on the improvement of the ironed samples. Between the ironed samples however, the 'most' ironed ones performed better than the least ironed one. The differences are quite small though and their respective weights are probably a bigger factor with this improvement, as heavier prints usually result in stronger prints (Floor, 2018).

Foaming PLA

For the second batch of prints foaming PLA was used. Foaming PLA contains TEM's which are membranes within the PLA that expand when exposed to heat. The membranes keep expanding until they break, so ironing foaming PLA too long destroys the material (Pawar et al., 2022). Contrary to the Silk PLA, Foaming PLA did show noticeable results when being ironed with a z-offset of 0.0mm due to

its expanding properties. Therefore, a z-offset of 0.0mm was used for this batch. With foaming PLA, a Z-offset of 0.0 and ironing speed of 10mm/s result in clear ironing lines because of the expanding material. Instead of slits due to the engraving of the ironing nozzle, there are now clearly visible bumped up lines after ironing.

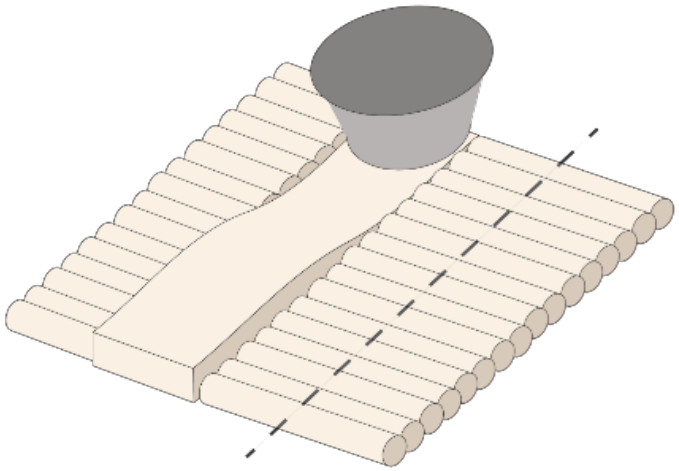

Foaming PLA

- 3x unenforced
- 2x E2L-6L
- 1x E3L-6L
- 1x E3L-8L

Figure X: Foaming PLA dog bone being ironed

Foaming PLA Results

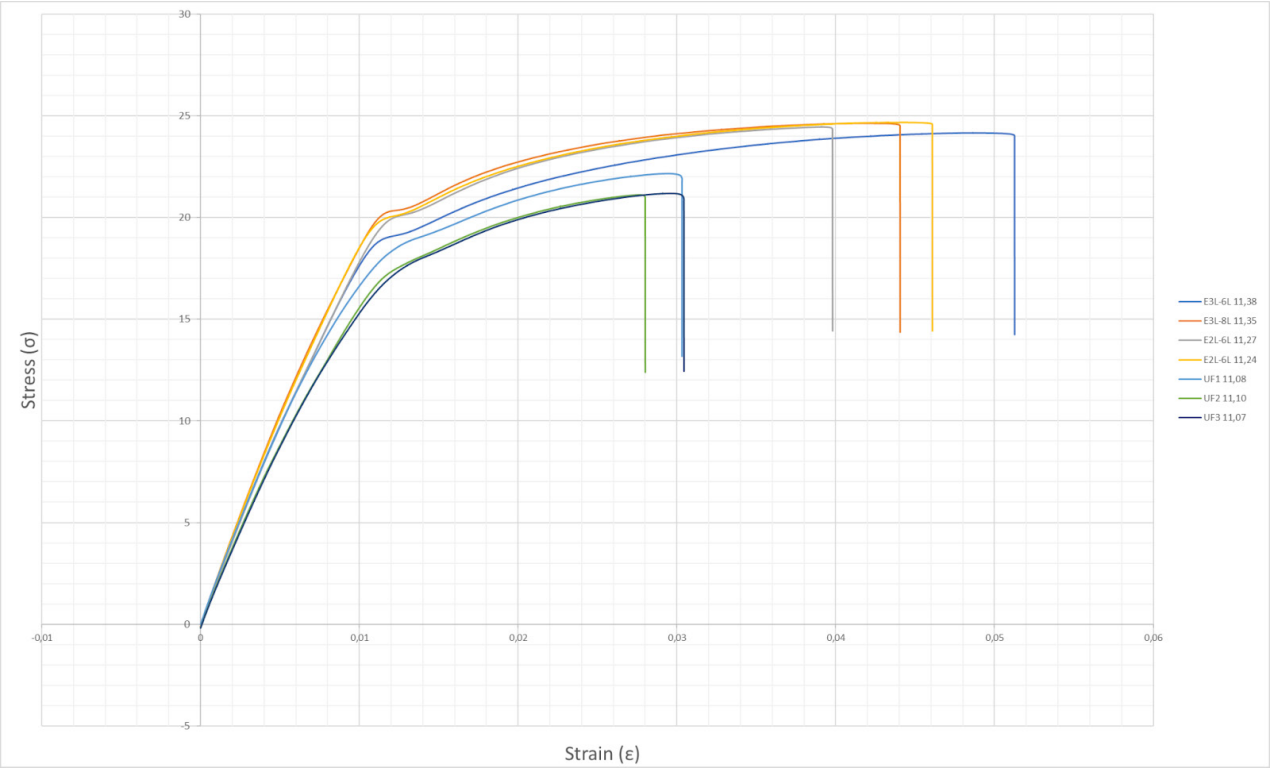

Figure X: Stress strain curve Foaming PLA: Unenforced (UF1t/m3) compared to Enforced

	Maximum	Test speed	Pre-load	Specimen	h	b	A_0	Peak detection	Date/Cloc	$L_{0\,CH}$
	mm	mm/min	N		mm	mm	mm^2	N		mm
E3L-6L 11,38	3	1	0.1	1	4.1	10.26	42.066	1016.955872	45538.49	118.1438
E3L-8L 11,35	3	1	0.1	2	4.1	10.3	42.23	1040.69397	45538.5	118.1124
E2L-6L 11,27	3	1	0.1	3	4.18	10.24	42.8032	1047.505615	45538.51	118.1276
E2L-6L 11,24	3	1	0.1	4	4.1	10.26	42.066	1038.529175	45538.51	118.1038
UF1 11,08	3	1	0.1	5	3.98	10.25	40.795	904.0754395	45538.56	118.0283
UF2 11,10	3	1	0.1	6	4.06	10.22	41.4932	876.2088013	45538.57	118.1668
UF3 11,07	3	1	0.1	7	3.98	10.15	40.397	856.2763062	45538.57	118.1676

As can be seen in the graph all samples with foaming PLA do show plastic deformation. The results show that the ironed samples are more stiff compared to the un-ironed samples. This can be seen by the steepness of their curve in the plastic region. The steeper the curve, the more force is necessary to achieve the same amount of strain. The yield strength, which is the point at which the material begins to deform plastically, is also higher in the ironed samples. Lastly, the peak stress and the amount of elongation are also improved by ironing the samples.

Appendix 8

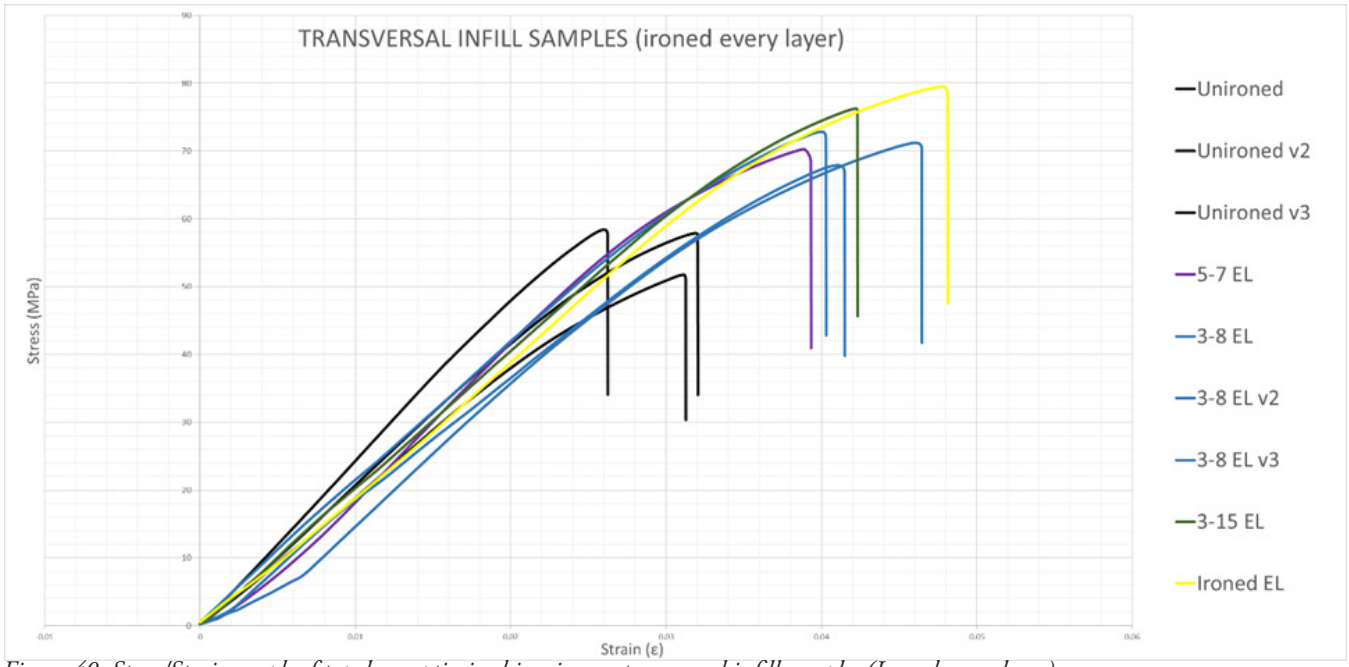

Figure 40: Stress/Strain graph of topology optimized ironing on transversal infill samples (Ironed every layer)

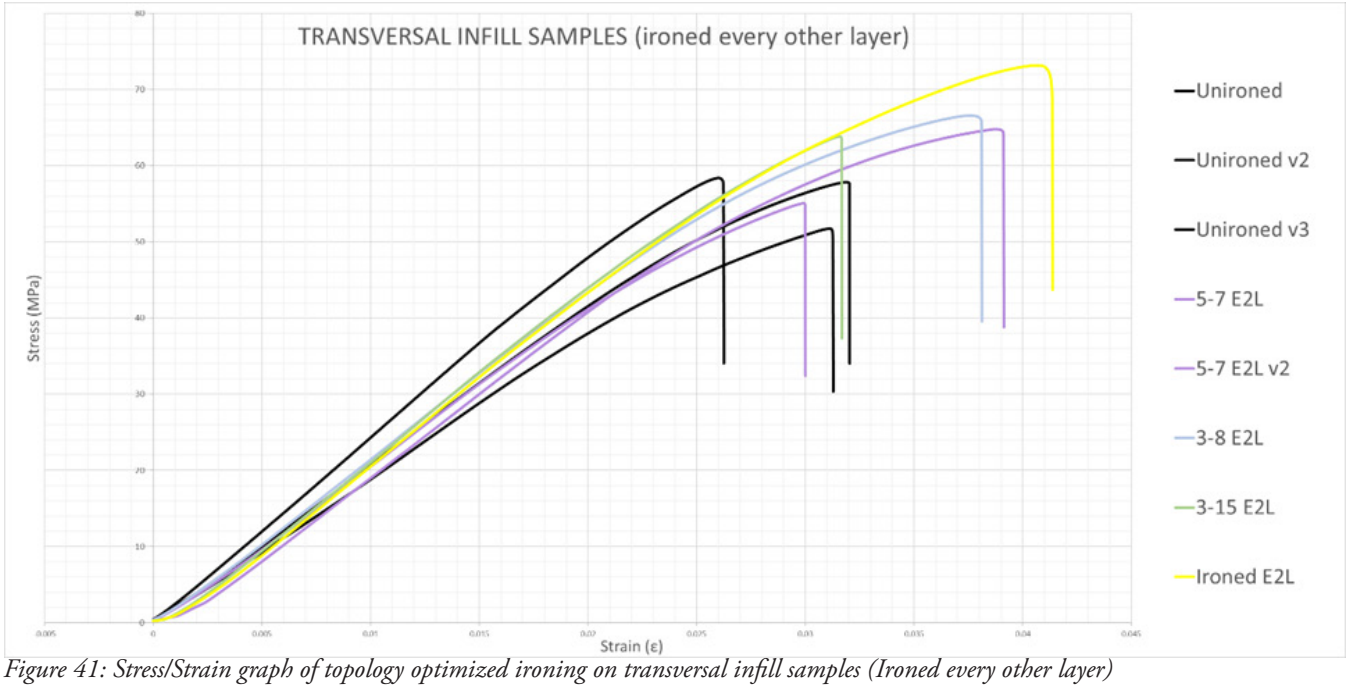

Figure 41: Stress/Strain graph of topology optimized ironing on transversal infill samples (Ironed every other layer)

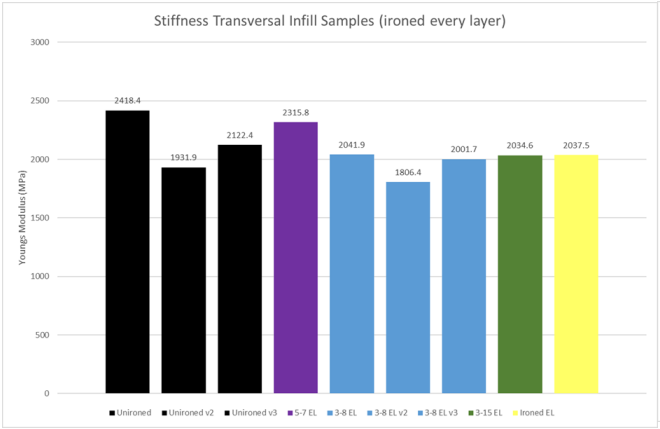

Figure 42: Stiffness of topology optimized samples (transversal)

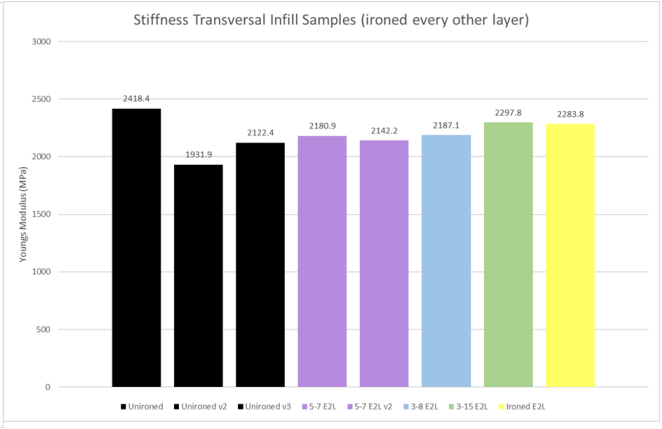

Figure 43: Stiffness of topology optimized samples (transversal)

IDE Master Graduation Project

Project team, procedural checks and Personal Project Brief

In this document the agreements made between student and supervisory team about the student's IDE Master Graduation Project are set out. This document may also include involvement of an external client, however does not cover any legal matters student and client (might) agree upon. Next to that, this document facilitates the required procedural checks:

- Student defines the team, what the student is going to do/deliver and how that will come about
- Chair of the supervisory team signs, to formally approve the project's setup / Project brief
- SSC E&SA (Shared Service Centre, Education & Student Affairs) report on the student's registration and study progress
- IDE's Board of Examiners confirms the proposed supervisory team on their eligibility, and whether the student is allowed to start the Graduation Project

STUDENT DATA & MASTER PROGRAMME

Complete all fields and indicate which master(s) you are in

Family name		IDE master(s)	IPD ✓ Dfl SPD
Initials		2nd non-IDE master	
Given name		Individual programme *(date of approval)*	
Student number		Medisign	
		HPM	

SUPERVISORY TEAM

Fill in he required information of supervisory team members. If applicable, company mentor is added as 2nd mentor

Chair		dept./section	SDE/MD
mentor		dept./section	SDE/MD
2nd mentor			
client:			
city:		country:	
optional comments			

! Ensure a heterogeneous team. In case you wish to include team members from the same section, explain why.

! Chair should request the IDE Board of Examiners for approval when a non-IDE mentor is proposed. Include CV and motivation letter.

! 2nd mentor only applies when a client is involved.

APPROVAL OF CHAIR on PROJECT PROPOSAL / PROJECT BRIEF -> to be filled in by the Chair of the supervisory team

Sign for approval (Chair)

Name _____ Date _____ Signature _____

CHECK ON STUDY PROGRESS

To be filled in by SSC E&SA (Shared Service Centre, Education & Student Affairs), after approval of the project brief by the chair. The study progress will be checked for a 2nd time just before the green light meeting.

Master electives no. of EC accumulated in total _____ EC

Of which, taking conditional requirements into account, can be part of the exam programme _____ EC

	YES	all 1st year master courses passed
	NO	missing 1st year courses

Comments:

Sign for approval (SSC E&SA)

Name _____ Date _____ Signature _____

APPROVAL OF BOARD OF EXAMINERS IDE on SUPERVISORY TEAM -> to be checked and filled in by IDE's Board of Examiners

Does the composition of the Supervisory Team comply with regulations?

YES		Supervisory Team approved
NO		Supervisory Team not approved

Comments:

Based on study progress, students is ...

	ALLOWED to start the graduation project
	NOT allowed to start the graduation project

Comments:

Sign for approval (BoEx)

Name _____ Date _____ Signature _____

Personal Project Brief – IDE Master Graduation Project

Name student _____ Student number _____

PROJECT TITLE, INTRODUCTION, PROBLEM DEFINITION and ASSIGNMENT

Complete all fields, keep information clear, specific and concise

Project title Exploring novel design applications of velocity-controlled ironing within internal structures of 3D prints.

Please state the title of your graduation project (above). Keep the title compact and simple. Do not use abbreviations. The remainder of this document allows you to define and clarify your graduation project.

Introduction

Describe the context of your project here; What is the domain in which your project takes place? Who are the main stakeholders and what interests are at stake? Describe the opportunities (and limitations) in this domain to better serve the stakeholder interests. (max 250 words)

This project aims to discover new applications for velocity-controlled ironing within 3D printed parts. By ironing the extrusion material post-printing with a separate ironing nozzle, the properties of the material can be altered. With foaming filaments for example, the amount of foaming can be influenced. This can result in differences within properties, such as translucency, shade, gloss and texture. Because a separate ironing nozzle is used, the speed of the ironing can be controlled, allowing for local material property variation.

Previous research has investigated potential applications of this technique for the external surfaces of 3D prints. However, possible applications for the inner structures have not yet been explored. This project aims to extend the knowledge of velocity-controlled ironing by exploring the effects and possibilities of this technique on the internal structures of 3D prints.The main stakeholders for this project would be my chair and mentor, who are very much involved in digital fabrication research.

→ *space available for images / figures on next page*

Personal Project Brief – IDE Master Graduation Project

Problem Definition

What problem do you want to solve in the context described in the introduction, and within the available time frame of 100 working days? (= Master Graduation Project of 30 EC). What opportunities do you see to create added value for the described stakeholders? Substantiate your choice.
(max 200 words)

Using a separate nozzle to locally modify 3D print material properties is quite a new technique which leaves a lot of topics to be discovered. Previous research has looked into possible novel applications for this technique, only on the outer layer of a 3D print.

Now that we look into the inside of 3D printed parts a lot of new questions arise. What kind of material properties would be interesting to modify within a 3D context? What materials, used in the previous research, demonstrate this change in properties when being ironed? What are possible applications that could utilize these local variations of material properties? How can the integrity of the print structure be maintained whilst its properties are altered?

Furthermore, the tool that currently is used to control the ironing is tailored towards ironing the outer layer of 3D prints. Therefore the research will also involve further development of the tool to successfully iron inner parts of 3D prints.

Assignment

This is the most important part of the project brief because it will give a clear direction of what you are heading for. Formulate an assignment to yourself regarding what you expect to deliver as result at the end of your project. (1 sentence) As you graduate as an industrial design engineer, your assignment will start with a verb (Design/Investigate/Validate/Create), and you may use the green text format:

Exploring novel design applications of velocity-controlled ironing within internal structures of 3D prints.

Then explain your project approach to carrying out your graduation project and what research and design methods you plan to use to generate your design solution (max 150 words)

The first phase of the project involves studying the available literature to understand the technology and working principles behind ironing and the effects it has on different materials. In this phase I also have to familiarize myself with the ironing workflow and learn how to make and manipulate GCode. The next phase will involve extensive research on the different effects of ironing on different materials. This phase will include extensive prototyping and experimentation with different materials and print settings. To somewhat narrow down the scope, only materials that are familiar to my supervisors and their research will be investigated. After having gathered insides on what material properties can be modified and how different print parameters produce different outcomes, an initial estimation needs to be made on what promising material and/or material property should be selected to be investigated further. Following this selection, further explorative research should be done in topics that are specific to that material/properties. The end goal of the project should be one or several ‘demonstrator(s)’ that showcase the interesting property modification within the inner part of 3D prints, alongside an updated version of the ‘tool’ that is used to iron the print.

Project planning and key moments

*To make visible how you plan to spend your time, you must make a planning for the full project. You are advised to use a Gantt chart format to show the different phases of your project, deliverables you have in mind, meetings and in-between deadlines. Keep in mind that all activities should fit within the given run time of 100 working days. Your planning should include a **kick-off meeting**, **mid-term evaluation meeting**, **green light meeting** and **graduation ceremony**. Please indicate periods of part-time activities and/or periods of not spending time on your graduation project, if any (for instance because of holidays or parallel course activities).*

Make sure to attach the full plan to this project brief.
The four key moment dates must be filled in below

Kick off meeting	15 Jul 2024
Mid-term evaluation	12 Sep 2024
Green light meeting	21 Nov 2024
Graduation ceremony	29 Dec 2024

In exceptional cases (part of) the Graduation Project may need to be scheduled part-time. Indicate here if such applies to your project

Part of project scheduled part-time	
For how many project weeks	
Number of project days per week	

Comments:

Motivation and personal ambitions

Explain why you wish to start this project, what competencies you want to prove or develop (e.g. competencies acquired in your MSc programme, electives, extra-curricular activities or other).

Optionally, describe whether you have some personal learning ambitions which you explicitly want to address in this project, on top of the learning objectives of the Graduation Project itself. You might think of e.g. acquiring in depth knowledge on a specific subject, broadening your competencies or experimenting with a specific tool or methodology. Personal learning ambitions are limited to a maximum number of five.
(200 words max)

Throughout my studies, I have been interested in innovative conceptual design. I love researching new materials and manufacturing techniques, and exploring and designing suitable, valuable applications for them. For me, it is more enjoyable to design a new conceptual product that showcases a new technology or material, rather than a finalized, market-ready product.

In the Minor Advanced Prototyping, I worked on a project that involved exploring the behavior of a shrinkable fabric when laminated with other fabrics. The challenge was to manipulate the shrinkage so that the fabric would take on a desired 3D shape. Exploring this new material and researching ways to control its behavior to give it a valuable purpose was very enjoyable for me.

With my proposed graduation topic, I see many similarities, which gives me confidence that I will find this research project very interesting.